The Development of a Device for the Investigation of Dorsiflexion range of the Ankle with a Capacity to Measure Pathology, Recovery and Pharmacological Benefit

by

Jan Botha

Thesis presented in partial fulfilment of the requirements for the degree of Master of Science in Engineering at the University of Stellenbosch

Thesis Supervisor

RT Dobson

December 2005

Department of Mechanical Engineering
University of Stellenbosch

Declaration

I, the undersigned, hereby declare that the work contained in this thesis is my own original work and I have not previously in its entirety of in part submitted it at any university for a degree.

……. ……...

Signature Date

Abstract

Various ways exist whereby balance abilities of the individual can be assessed. However, most of these are subjective methods. This thesis strives to demonstrate the effectiveness of a new device, the Dorsiflexometer that can be used to objectively assess one's balance abilities. The Dorsiflexometer was constructed and mathematically modelled using appropriate simplifying assumptions. After its construction, the Dorsiflexometer was tested using two experimental set-ups to obtain raw data. Both these set-ups consisted of the two tiltable platforms equipped with three load cells each, the bridge amplifiers and the personal computer (PC). The only difference in the two experimental set-ups is in the type of test that was performed as well as the bridge amplifiers used. Numerous parameters, such as the radius of movement and the Lyapunov number can be extracted from the raw data. A computer program was written to analyse the raw data and present the results in a user-friendly manner. A new parameter, the Sway Index, was used to obtain a single balance value for the tested individual. This parameter proved useful in quantifying balance.

An advanced patent search was carried out before the device was constructed. This was necessary to provisionally patent the device – official application number: 2003/6702.

Samevatting

Verskeie metodes word deur medici gebruik om te bepaal hoe ‘goed’ of ‘sleg’ ’n persoon se balansvermoëns is. Die meeste van hierdie metodes is egter van subjektiewe aard. Hierdie tesis se doel is om te bewys dat ’n nuwe voorgestelde meetapparaat, ’n Dorsiflexometer, vir die uitsluitlike doel van kwantifisering van balansvermoëns van die individu met oorgawe gebruik kan word. Hierdie apparaat is ontwerp, gebou, wiskundig gemodelleer (alhoewel hierdie model baie eenvoudig is) en getoets. ’n Aansienlike getal parameters kan gesolidifiseer word uit die rou data, onder andere ’n Lyapunov nommer en die radius van beweging. Daar is op ’n paar besluit en ’n rekenaarprogram is geskryf om hierdie parameters te bereken en op gebruikersvriendelike wyse weer te gee. Een van hierdie parameters, die Wieg-Indeks (Sway Index), is ’n nuwe parameter waarmee ’n enkele balanswaarde vir die getoetste individu bereken word. Hierdie parameter gee ’n goeie aanduiding van ‘goeie’ en ‘minder goeie’ balans.

’n Gevorderde patentenavorsing is uitgevoer voordat die apparaat gebou is. Dit is gedoen om die apparaat voorlopig te patenteer – aansoeknommer 2003/6702.

Acknowledgements

The author would like to express his gratitude towards Dr. Driver-Jowitt, Dr. P Viviers, and Mr RT Dobson for their role in the project. Acorn Industries are also thanked for their financial support as well as involvement in other areas of the project. Concerning the legal aspects of the project, a word of thanks goes out to Mr G Verhoef.

Completing this project would have been impossible had it not been for the various equipment and advice (by Dr T Terblance in particular) offered by the Mechanical Department of Stellenbosch.

Furthermore, the author would like to thank his family and friends (especially Miss Y Wiese) for their support throughout this project.

Dedicated to Ferdinand Postma Botha

Contents

Nomenclature

A	Constant	N / rad
a	Acceleration	m / s^2
C	Constant	
D	Damping constant	kg / s
F	Force	N
f	Frequency	Hz
g	Gravitational Acceleration	m / s^2
I	Moment of Inertia	m^4
K	Constant	
k	Constant	
L	Length	m
m	Mass	kg
M	Moment	Nm
R	Reaction Force	N
R^2	Correlation Coefficient	
r	Radius	m
SNR	Signal-to-Noise Ratio	dB
T	Time	s
V	Voltage	volt

Greek symbols

β	Angle	rad
δ	Platform Tilt Angle	rad
ε	Strain	
ϕ	Sway Angle	rad
$\dot{\phi}$	Sway Angular Velocity	rad / s
$\ddot{\phi}$	Sway Angular Acceleration	rad / s^2
λ	Lyapunov Number (defined in Appendix A – p. A-18)	
π	Pi	
τ	Torque	Nm
Δ	Change in	
Σ	Summation	
σ_s	Footplate Sensitivity	N / Volt

Subscripts

B	Heel
C	Toe
c	Complementary
CofG	Centre of Gravity
D	Foot
E	Tibia
i	Counter
L	Left
n	Noise
O	Around Point O
p	Particular
r	Right
s	Signal
tot	Total

Superscripts

‾	Distance to Centroid
n	Final Number / New

Abbreviations

AD	After Dorsiflexion
BD	Before Dorsiflexion
BOS	Base of Support
CNS	Central Nervous System
COG	of Gravity
COM	of Mass
COP	of Pressure
DC	Direct Current
DD	During Dorsiflexion
DIR	Direction
GND	Ground
IP	Intellectual Property
LA	Back Footplate of Left Platform
LL	Left Footplate of Left Platform

LN	Lyapunov Number (Defined by Equation A.22)
LoS	Limits of Stability
LR	Right Footplate of Right Platforms
PC	Personal Computer
PNS	Peripheral Nervous System
PWM	Pulse Width Modulator
RA	Back Footplate of Right Platform
RL	Left Footplate of Right Platform
RR	Right Footplate of Right Platform
SI	Sway Index (Defined by Equation A.21)
s/s	Samples per Second
TM	Total Movement
TO_1*	Number assigned to test (Test subject no. 1 with eyes closed)
OO_3*	Number assigned to test (Test subject no. 3 with eyes open)
t_r	Rise-time
VL	Position of Normal Component of Resultant Force on Left Platform
VR	Position of Normal Component of Resultant Force on Right Platform
V_{tot}	Position of Normal Component of Resultant Force on Both Platforms

* These numbers are used to distinguish between test subjects as well as the type of test. Afrikaans abbreviations are used, therefore TO denote an eyes closed (‘toe oë’) test and therefore OO is an eyes open (‘oop oë’) test.

List of Tables

List of Figures

1 Introduction

The aim of this thesis is to investigate the viability of a device to quantify human balance capabilities. This idea came from an orthopaedic surgeon by the name of Dr Driver-Jowitt, and entails the manufacturing of a machine able to measure a human's balanced dorsiflexion range. Data on a 'normal' dorsiflexion range is inconclusive and has not being studied and tested in depth.

From Dr Driver-Jowitt's initial proposition, the idea expanded into the following: The Development of a Device for the Investigation of Dorsiflexion range of the Ankle with a Capacity to Measure Pathology, Recovery and Pharmacological benefits. Therefore the proposed device should be able to detect slight balance impairment in a test subject. Instead of just testing a subject's balanced dorsiflexion range, the overall balance of a person can be tested by making use of simple dorsiflexed perturbation, hence the name Dorsiflexometer.

There are two main areas where the measurement of balance is a necessity. The first falls among the elderly which amounts to millions of government money every year (Bloem et al., 2003). If it can be predicted that an individual has a high risk of falling, certain preventative steps can be taken. Another area where people are particularly interested in balance capabilities is in sport. This interest is fuelled and sustained by the large amount of money involved in professional sport. Recurring injuries and performance in many fields of physical sport are directly or indirectly influenced by an individual's balance abilities.

The Dorsiflexometer concept is to function as a measuring tool which should have the potential to be marketed. In this regard, it is also necessary to do an in-depth patent search to ascertain what other similar devices already exist. Some devices, similar to the proposed Dorsiflexometer, have been constructed (for example, Mechling 1985 and Lynch et al., 1998), though all these devices use different methods of measuring and quantification and were found to be lacking in certain areas.

The design and manufacture of the Dorsiflexometer should be based on sound mechanical principles, and software has to be written to facilitate testing and analysis of

raw data. Form the tests' raw data, parameters should be identified and used to quantify a person's balance abilities. This will then either verify the potential of such a device, or prove that such a simple device is not adequate for the task at hand.

What should be kept in mind is that the device should be as simple and user-friendly as possible in order to enhance its marketability and usability in practice. Some constraints on this project are money and time. Both these constraints are greatly enhanced by the fact that it is a first step in a relatively new direction. Though this device might not achieve all its goals, it will definitely set the ball rolling toward new ways in quantifying balance capabilities.

This thesis presents the process whereby the Dorsiflexometer was designed, constructed and tested. It also presents the criteria used to overcome the complexity of balancing a subject on a tiltable platform used in the mathematical model presented in Section 3.

2 Literature Study

Mankind has always been concerned with its balance. This can be seen over and over again in young children trying to find out what their balance capabilities are and refining them. It takes an enormous amount of computing by the brain to be able to fulfil only the simplest of tasks (Williams and Lissner, 1992)

An individual's brain needs to be aware of what is going on around it – thus making use of all the sensory inputs it receives from the sensory organs (for example the eyes and semi-circular canals present in the ears). Then it has to know where the body is in relation to its surroundings (for example how far the left hand is from that hot stove) via internal (peripheral) sensors. Now only can the brain start to struggle with the complicated concept of moving any part of the body to a new desired position. In realising this desire, it has to take into account all the forces working in on the body (for example gravity and momentum) and be able to deal with any distractions that may occur before, during or after movement. The brain communicates with the muscles involved and while a certain movement is performed, all the sensory organs keep on sending information to the brain. The brain constantly has to analyse all this information to keep the body from falling or ending up doing what is not desired. It is thus very difficult to explain just how complicated the problem of moving is, but a very big part of it is being able to keep one's balance. Without this, one would not be able to perform any useful task at all.

Since an individual's ability to balance is gradually lost with age, it is relevant to look at falls among the elderly to try and understand the importance of maintaining one's balance (Bloem *et al*., 2003). (The loss of balance is also associated with Parkinson's disease, cerebral palsy and various other conditions.)

Falls among elderly persons create immense social problems because of their association with physical decline, negative impact on the quality of life, and markedly reduced survival. In addition, falls pose high costs to the public health service. For these reasons, falls remain a popular topic for research. Considerable attention has been given on early identification of fallers and prevention strategies for falls or injuries.

From this it is evident that investigating balance abilities is an important research field. Many ways of measuring balance abilities, (including posturography) have been formulated using multidirectional moving platforms and computer models or pivotable platforms with very sophisticated sensors mounted on them. All these techniques try to give answers to the universal question of quantifying an individual's balance abilities.

A good definition for 'balance' is the ability to maintain the body's position over its base of support (Berg et al., 1989). Balance can be further divided into static and dynamic balance – as an indication of whether the base of support is stationary or moving. Postural/Balance control refers to the act of keeping the body's of gravity within the borders of the base of support (BOS). The term *Postural Stability* is defined as the ability to maintain or control the of mass (COM) in relation to the BOS to prevent falls and to complete desired movements. Balance is the process by which postural stability is maintained. The ability to maintain posture, such as balancing in a standing or sitting position, is operationally defined as static balance. The ability to maintain postural control during other movements, such as when reaching for an object or walking along the beach is operationally defined as dynamic balance. Both static control and dynamic postural control are thought to be important and necessary motor abilities (Leonard, 1998).

Because balance is so closely associated with walking (gait) – it takes a young mind a considerable time to learn to fully master the art of letting the body know how to take but a few steps – a lot of studies have been done on gait (Crosbie *et al.*, 1999; Detrembleur *et al.*, 2003; Helbostad and Moe-Nilssen, 2003). This proves very useful, since abnormalities in both gait and balance can be identified quite readily through gait analysis. However, these abnormalities (and especially pathological abnormalities) are not properly quantified as yet.

2.1 History

Using a force platform to access a patient's balance abilities is not a new idea. This technique falls under a broader division called *posturography*. Posturography has existed for several centuries (Baron, 1983). Postural sway, difficult to observe with the naked eye, has been recorded using stationary force platforms equipped with strain

gauges (Terekhov, 1976). The use of force platforms to record sway during simple, quiet standing has not proven to be particularly useful clinically when assessing patients with vestibular disorders.

The field of posturography has recently advanced quite rapidly with the aid of computers – making it possible to do computerised dynamic posturography tests. The platform need not be stationary anymore, but can be made so that it can either move in a horizontal plane, i.e. translate, or rotate out of the horizontal plane, i.e. pitch the subject either forward of backward (Nashner *et al.,* 1982; Nashner *et al.,* 1990). Computerised dynamic posturography has been combined with visual stimuli as a means of determining the relative importance of the various sensory inputs critical for balance, namely vision, somatosensation (sensations coming from the skin which include touch, temperature and pain) and vestibular sensation. When compared with other tests currently available for the assessment of vestibular function, computerised dynamic posturography is unique in that it assesses 'balance' rather than attempting to assess peripheral or central vestibular function more directly (Furman, 1994).

2.2 Reaction Time

Reflexes and Motor Control in humans is realized through the neural system. Axonal conduction of action potentials is a fundamental process in neural activity. Interconnections through synapses with other neurons or muscle fibres, as at the neuromuscular junction, form another component in this activity. For the motor neuron, at the neuromuscular junction, this was an excitation of the muscle fibre. At other locations, this process could be inhibitory. Furthermore, the motoneuron serves as an efferent pathway, away from the Central Nervous System (CNS), while other neurons serve as an afferent pathway, sending sensory information from receptors back to the CNS in the form of feedback. Thus, a set of neurons sending stimulus information to the CNS and receiving information back from the CNS, resulting in an appropriate response, can be considered as a system with a feedback loop. If this response is involuntary, i.e. it does not require a conscious decision, then it is termed a *reflex*. A variety of such reflex pathways form the basis for motor control. For the purpose of this thesis, the necessary information required from this section is to establish approximately

how fast (in milli-seconds) a human being is able to respond to postural perturbation in a reflex-basis.

Since the concern is with postural-reflex reaction times, some sort of standard value needs to be acquired. For this standard, a timing sequence of a stretch reflex (a patellar tap reflex) is calculated (Freivalds, 2004) in Appendix C. The total time is 34 ms. From this example, it is deemed unnecessary to be able to take postural measurements on the force platform exceeding 30 samples per second. This assumption is valid because postural reflexes are much slower than that of a patellar tap (this is usually done to examine a patient's reaction – see Figure 2.1 for the position of the patella). The process involves more brain function and also more muscles and sensors.

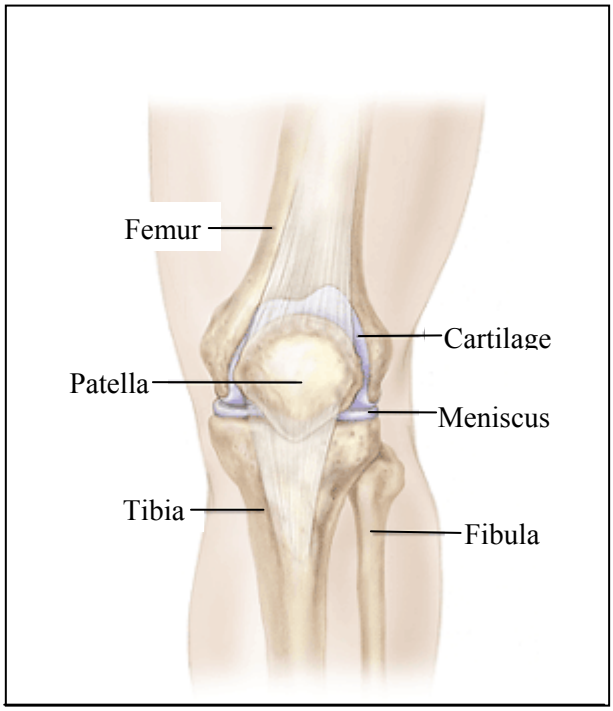

Figure 2.1: Front view of the right knee showing the patella

2.3 Postural Control

Postural control stems from postural stability. One needs to be able to control ones posture in order to maintain a stable state. Postural stability can be defined as the maintenance of an upright posture during quiet stance (standing still). It has been established that during quiet stance, healthy human subjects control their upright

posture by constantly making small movements in different parts of the body (Nashner, 1985). The optimal position during balanced stance – the equilibrium point – requires that a person's COM is maintained within the support frames of the soles. Body sway from left to right, i.e. in the lateral direction, is best compensated for by keeping the feet apart since this introduces a diagonal force against the ground. Furthermore, the shoulders should be directly above the hips and the head and trunk erect (Carr and Shepherd, 1982). Balanced stance also requires an ability to move one's position while standing and to move out of the standing position, all without using the arms for support. During quiet stance, no conscious activation of muscles by the nervous system is required (Enoka, 1994) whereas postural activity is specific to the different balance tasks.

Three motor systems (reflex, automatic and voluntary in Table 2.1) control the process of gaining postural stability after the body's equilibrium position is upset (Schmidt & Lee 1999).

Table 2.1: Motor systems used in balance movement control (Nashner, 2001)

System property	**Motor System**		
	Reflex	**Automatic**	**Voluntary**
Pathways	Spinal	Brainstem/Subcortical	Cortical
Activation	External stimulus	External stimulus	External stimulus/Self-generator
Response	Local to point of stumulus and stereotyped	Coordinated and stereotyped	Unlimited variety
Role in balance	Muscle force regulation	Resist disturbances	Purposeful movements
Latency (in legs)	Fixed 35-45 [ms]	Fixed, medium-latency (95 [ms]) or long-latency (120 [ms])	Variable (150 [ms])

After perturbation, the first motor system to take action is a spinally mediated reflex – also called a stretch reflex – and consists of rapid muscle movement in order to regain postural stability (Nashner, 2001; Rothwell, 1994). Tendon and muscle proprioception, which detects any movement (especially rapid movement), provide the afferent input resulting in muscle action. This muscle action is coordinated in the sense that selected muscles contract over the body. These reflexes contribute directly to balance recovery (Nashner, 2001). When falling, the first response is an automatic response/reaction, which occurs as medium-latency muscle responses. These actions affect all the neck, trunk and leg muscles and are conveyed through vestibulospinal reflexes (Nashner

2001). Co-occurring with these responses, are long-latency responses affecting the antagonist muscles (Diener and Dichgans 1986). Automatic responses/reactions are adaptable and dependant on the specific context of the balance demands. As an example, it was shown that coordination patterns can change depending on recent experience and the reliability of the support base (Nashner 2001). Automatic responses can be thought of as overlearned reflexes that rapidly respond by resisting any disturbances to posture (Diener and Dichgans 1986).

Voluntary movements, in contrast to reflex and automatic reactions, are based on the humans' conscious attention and may vary considerably from situation to situation and from one specimen to another (Nashner, 2001). These voluntary movements result in postural adjustments and these displace the position of the of gravity (COG) of the body. As an example, consider a human hyperextending his/her thorax (bending backwards) from the anatomical position. The COG moves backward with this movement. Postural adjustments and voluntary movements appear to be part of the same motor programme in self-placed movements (Lee *et al.*, 1987). Figure 2.2 (Rothwell, 1994) illustrates postural adjustment.

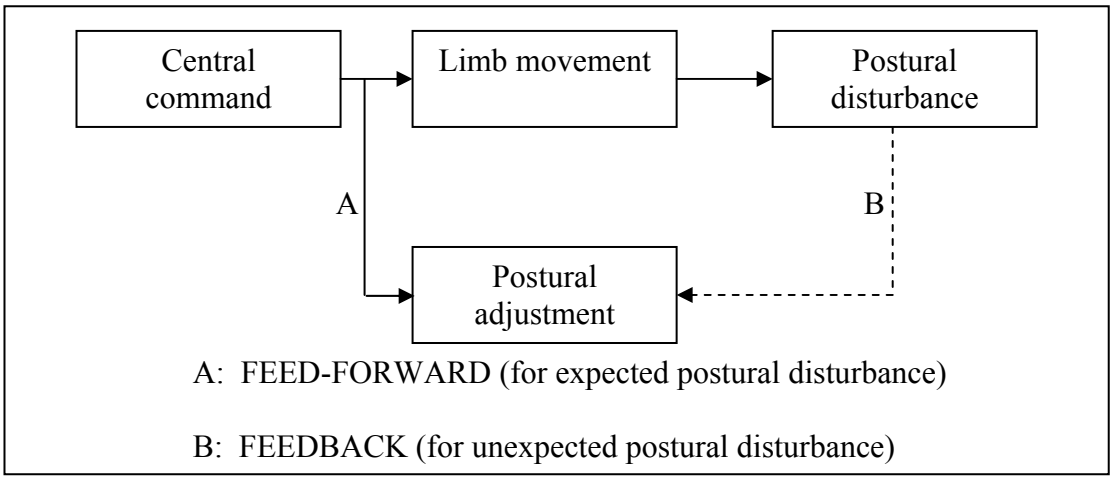

Figure 2.2: Feed-forward and feedback for postural adjustment (Rothwell, 1994)

Healthy adults use three preferred movement strategy models in controlling their postural stability: the ankle, hip and stepping strategies. In the first, the ankle strategy, the body is regarded as a stiff, inverted pendulum and postural adjustments are made mainly in the ankle joint (Nashner 1985). This strategy introduce plantar and dorsiflexion of the ankle. To define all the movements of the lower limbs of the human body refer to Figure 2.3.

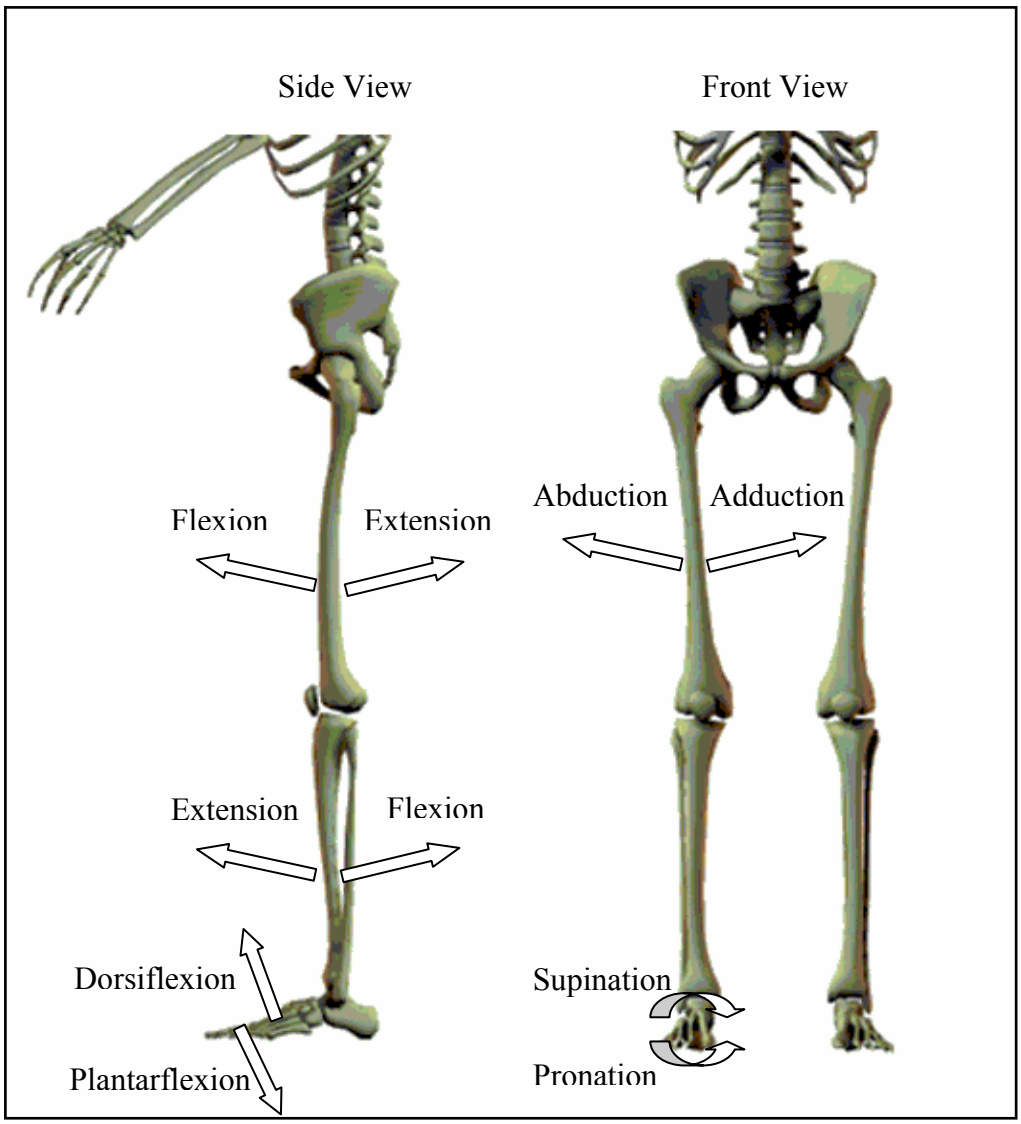

Figure 2.3: Definition of the movements of the lower limbs

In the second preferred strategy, the hip strategy, the hip joints are the primary inducers of resulting postural control (Horak and Nashner, 1986). The third preferred strategy to maintain balanced stance, involve taking steps. This strategy is mainly used in more difficult conditions. This last strategy can be seen when, for example, one is required to stand on one leg with both eyes closed. The human brain, when balancing or exercising postural control, uses a combination of these three strategies mentioned as well as temporal relations, which are influenced by the subject's recent experience (Horak and Nashner, 1986). Because of this, it is possible for people to adjust their postural programme during a 'balance' test or from one such test to the next (Woollacott *et al*., 1988).

2.3.1 Postural Control Systems

To keep the COG within the base of support of the soles, corrective movements have to be made by the subject. For these movements to succeed, very good coordination is needed between all the systems involved in sensing the unbalance and then executing these movements. These systems are the sensory, skeletal and CNS. Table 2.2 shows all the parts of the postural control system which will be discussed in detail.

Table 2.2: Postural control systems (Era, 1997)

Sensory system	Skeletal system	CNS
Vestibular system located in the inner ear (semicircular canals, otholiths, maculae's)	Muscles of the upper and lower extremities	Stretch reflex
Vision (retina)	Trunk muscles	Long-loop reflexes
Proprioceptive system (muscle spindle-type I and II, Golgi tendon organ, joint receptors)	Neck muscles	Pre-programmed reactions (Learned skills) Synergistic action
Cutaneous receptors		

2.3.1.1 Sensory Systems

The function of the sensory systems is to provide enough information regarding the body's own state, its relation to its surroundings and of its surroundings. This information is 'sensed' by the sensory receptors, which 'sends' the information to the CNS via afferent pathways. These sensory receptors sense physical phenomena (for example heat, light pressure, sound, etc.) and convert them into small electrical impulses that are then relayed to the CNS, where they are interpreted. Table 2.2 depicts the main types of sensory receptors used in postural control. A short description of each of the important sensory systems follows.

(i) Vestibular System

It has been known for some time that the vestibular system may contribute to body orientation perception and therefore contribute to postural control. But some studies have shown that this system does not play an important role in the perception of sway during normal quiet stance (Fitzpatrick and McCloskey, 1994). The sensory parts of the vestibular system consist of the semicircular canals and the otholiths. The semicircular

canals respond very sensitively to velocity changes of movement at frequencies between 0.2 Hz and 10 Hz. Therefore, they are active during the beginning and end of movement. The otholiths, on the other hand, operate at lower frequencies of less than 5 Hz and therefore provide linear acceleration information (Toppila and Pyykkö, 2000). The vestibular nuclei in the brainstem receive information from the semicircular canals, the otholiths and other sensory sources. The main goal of the vestibulo-spinal reflexes is to stabilise the head and body (Baloh *et al.*, 1993).

(ii) Visual System

The eye collects visual information and sends it to two main locations in the brain. This information is used for two main purposes, namely for object identification and for movement control (Schmidt, 1991). The ambient system uses visual information to exercise movement control and has also been shown to strongly affect stability as well as balance (Lee and Aronson, 1974).

Though vision is very important for postural control, it can be compensated for by other sensor information (Brandt *et al.*, 1986), of which the most important is the contribution of the semicircular canals located in the labyrinth of the inner ear. Vision influences postural control by 'recording' a relative image shift on the retina and it also triggers the muscle activation necessary for postural corrections (Brandt *et al.*, 1986). Exactly how effective vision is in postural control depends on a number of things, including object distances (Brandt et al, 1986), visual contrast (Leibowithz *et al.*, 1979), room illumination and visual acuity (Paulus *et al.*, 1984). Vision's contribution to posture control is the best when the visual distance is less than 2 m (Brandt et al, 1986). Visual cues play a bigger part in postural control of elderly people than in younger persons (Pyykkö *et al*., 1988).

(iii) Proprio- and Exteroceptive Systems

Proprioceptive receptors located in muscles, tendons and joints (Jäntti, 1993) and exteroceptive receptors located in the cutaneous and subcutaneous tissue (Johansson and Vallbo, 1980) send information related to body position as the somatosensory system. Proprioceptive receptors give information about limb position, distension of the respective muscles and about the body. While exteroceptive information is derived from various types of pressoreceptors on the sole of the foot such as Meissner corpuscles, and Pacinian corpuscles (Latesh, 1998). Relative movement and position of body parts

are sensed by receptors in joint capsules, though their role in postural control is not fully understood as yet. Muscle spindles give information about changes in muscle tension and muscle length. Pressoreceptors sense body sway and mechanoreceptors determine acceleration and pressure changes as well as the site and velocity of an indentation of the skin (Magnusson *et al.,* 1990).

Some very important inputs are produced by proprioception during stance for postural control purposes. Some of these inputs include proprioception of the ankle joint, neck muscles and the eye's position in the head. The ankle joints rotate about their axis when the COG moves while the neck muscles' proprioceptive receptors give information concerning head movement relative to the trunk. Finally, it has been suggested that the eye muscles reflect the eye's position relative to the head (Spirduso, 1995). All these movements are 'sensed' by proprioceptive receptors that send the information to the CNS.

2.3.1.2 Skeletal and Muscle System

To provide postural control during bodily movements, the calf muscles are activated first (Nashner, 1983). Other "prime postural muscles" are activated thereafter following, in order of, the neck muscles, the hamstring muscles, the soleus and the supraspinalis muscles (Johansson and Magnusson, 1991). Certain other muscles also participate in balancing the body position by either producing voluntary movements or reflective movements of which the latter has differing latency/response times (Nashner 1983). Whenever muscles are stretched or contracted, the proprioceptive receptors within the muscles and their tendons sends the change in muscle length as a signal to the "central mechanism of the postural control system" (Spirduso, 1995).

Coordinated muscle action is required to exercise postural control (Johansson and Magnusson, 1991), for example to produce sufficient muscular contraction (Era *et al.,* 1996). The role of the ankle, knee and hip joints played in postural control is very important. According to the passive stiffness control model, ankle stiffness stabilises the unstable mechanical system during quiet stance (Winter *et al.,* 1998). Though this has been disputed since other researchers "showed" that balanced stance is the active mechanism of postural stabilisation (Morasso and Schieppati 1999), where the muscle and foot receptors play an essential role (Morasso and Schieppati 1999).

2.3.1.3 Central Nervous System (CNS)

The CNS consists of the brain and the spinal cord. Clusters of cell bodies in the CNS are called nuclei, whereas the far fewer collections of cell bodies that lie along the nerves in the peripheral nervous system (PNS) are called ganglia (Marieb, 2001). The CNS plays a very important role in posture control. Spinal reflexes trigger a change in stance or posture as a first response in postural control (Allum and Keshner, 1986). This response is also the fastest, whereas the voluntary movements needed for postural control is planned within the brain itself. Output commands are sent through the pyramidal and extrapyramidal systems to the targeted muscles. The pyramidal cells transmit information to the spinal motoneurons and interneurons that control voluntary movements and the segmental reflexes needed (Jäntti 1993).

The basal ganglia and the nuclear groups take part in the facilitation and planning of both voluntary and reflex movement during postural control. The cerebellum and its connections are responsible for the coordination and smoothing of the reflex movements and the regulation of voluntary movement.

2.3.1.4 Integration of the Components of the Postural Control System

Continual sensor information needs to be integrated in the CNS to exercise proper postural control. Sensory input sources are the visual, vestibular and proprioceptive and exteroceptive systems. Though the information from all these systems is not necessary for non-complicated circumstances, it has been suggested that only one of these three systems' information is necessary as a source in these circumstances (Rothwell, 1994). Postural adjustments may be adequate even without peripheral feedback – and has been demonstrated by Forget and Lamarre (1990).

Stretch reflexes are triggered by afferent impulses from the spinal cord whereas neural connections mediate more complicated motor responses in higher levels of the CNS. A very important pre-condition for proper balancing is the ability to select the appropriate responses, modifying these responses according to sensory inputs and to produce the needed muscular contractions (Era *et al.,* 1996). Past experience determines context-dependent responses utilising all available sensory input and leading to pre-programmed motor responses.

2.3.2 Balance Assessment

In order to obtain appropriate information on balance capabilities during standing, various balance tests have been developed (Berg *et al.,* 1989) and many different measurements have been presented (Juntunen *et al.,* 1897; Wing *et al.,* 1995; Era *et al.,* 1996). However, desired goals and results usually determine a suitable method. As yet, there exist no single balance test or assessment technique that is a true and accurate indicator of the overall integrity of the balance control system (Winter *et al.,* 1990).

Coordinated movements of the body and taking advantage of the interaction of external and internal forces results in balanced stance. These movements are accomplished by the neuro-muscolu-skeletal system (Medved 2001). Three distinct subsets of physical variables need to be addressed when measuring standing balance in a laboratory environment (Kejonen, 2002):

- kinematics (e.g. motion analysis) is concerned with details of the movement itself rather than forces (Winter 1990),
- kinetic data (e.g. platform measurements) present the forces and the moments of forces that are developed during movements, and
- bioelectric changes (e.g. electromyography) are associated with skeletal muscle activity (Medved 2001).

These three methods may be used either separately or in combination to perform balance measurements – depending on the purpose and aim of the experiments (Gatev *et al.,* 1999). Care should be taken to ensure time-synchronisation of the data (Winter, 1990) and selection of measuring time and stance conditions is of the essence. Typical duration of platform measurements, for example, is 20 to 30 seconds (Kejonen P, 2002), though longer (Scott and Dzendolet, 1972) and shorter (Era and Heikkinen, 1895) periods of time have been used previously. A very important factor in choosing a relevant measuring time is the fact that it should neither be to short, therefore producing inaccurate results, nor too long, thereby inducing fatigue in the subject. A clear decrement in balance times was found in the Romberg test among subjects between 60 and 90 years of age (Iverson *et al.,* 1990).

Many variations in measuring posture have been used regarding the position of the feet, for example where the feet may be together, with the heels touching or the heel touching the toe (Harrison *et al.,* 1994). However, standing on two legs is the easiest and therefore the safest position to use when testing subjects with balance-related problems.

2.4 Mechanical sensors

The previous section dealt with the biological sensors used by the human for balancing purposes. This section will primarily concern itself with mechanical sensors that are used in posturography. These mechanical sensors appear in the form of load cells or, more specifically, strain gauge load cells.

Strain is the amount of deformation of a body due to an applied force. More specifically, strain ε is defined as the fractional change in length as shown in Figure 2.4.

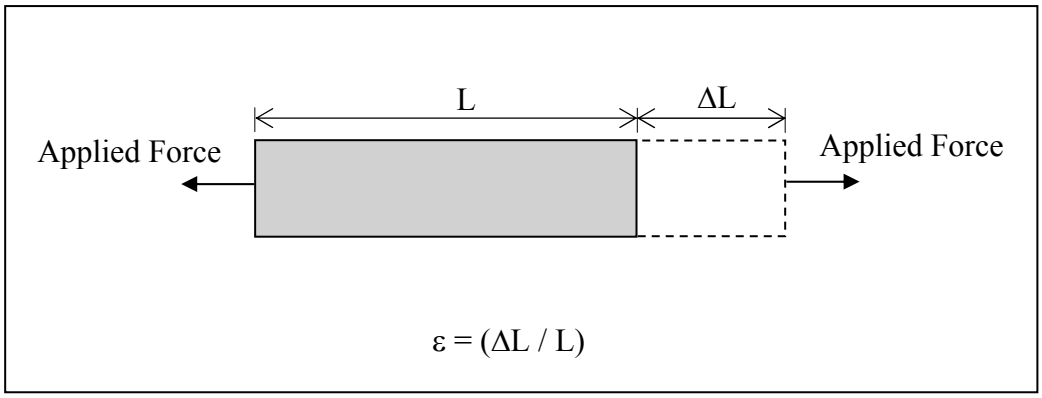

Figure 2.4: Definition of strain

While several methods exist for measuring strain, the most common is with a strain gauge – a device whose electrical resistance varies in proportion to the amount of strain it is subjected to.

The strain gauge load cell is thus a unit for converting applied force into an electrical output by virtue of the internal strain gauge installation. This strain gauge's increasing or decreasing resistance is amplified by using, usually, a Wheatstone Bridge shown in Figure 2.5. This is necessary since the change in resistance is usually very small – therefore strain gauges are almost always used in a bridge configuration with a voltage

excitation source. The Wheatstone bridge consists of four resistive arms with a input voltage and other resistors necessary for temperature compensation.

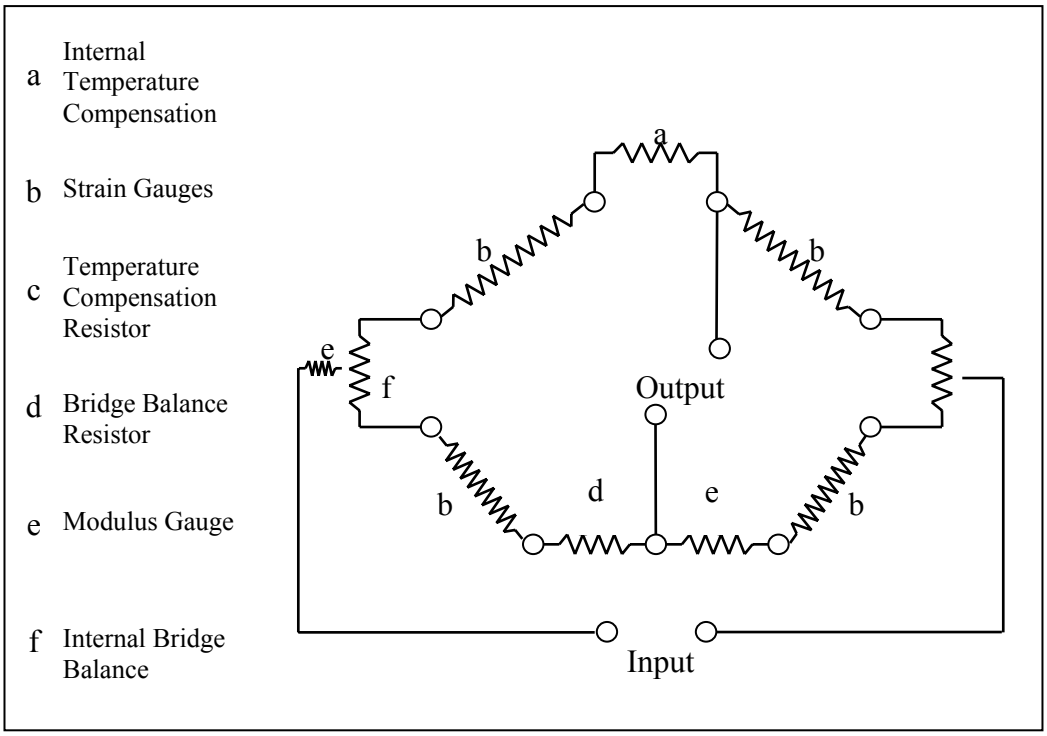

Figure 2.5: Wheatstone bridge used in a typical load cell

The most widely used strain gauge is the metallic strain gauge. This gauge consists of fine wire or metallic foil arranged in a grid pattern. The grid maximises the amount of metallic wire of foil subjected to the strain in the parallel direction (Figure 2.6). The cross-sectional area of the grid is minimised for reduced Poisson effect. The grid is bonded to a thin backing, called the carrier, which is attached directly to the metal subjected to the strain. Therefore the strain experienced by the metal is transferred directly to the strain gauge, which responds with a linear change in electrical resistance.

The electrical output is connected to different types of measuring instruments (e.g. for weight indication, recording and control).

The load cells are very small and have a simple construction. Load cells have extremely good linearity and high response performance to make them a suitable measuring tool for the dynamic load measurement necessary in posturography.

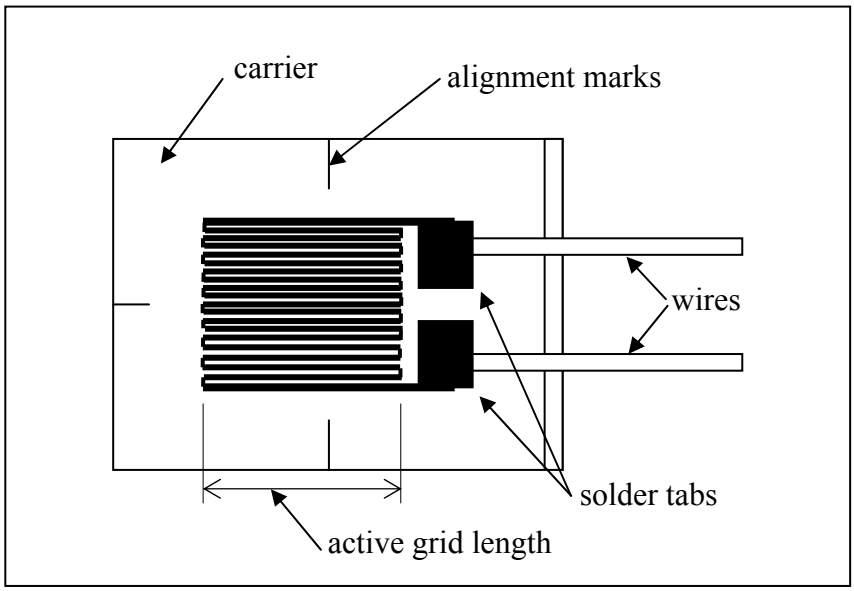

Figure 2.6: Bonded metallic strain gauge

2.5 Devices used for balance assessment

In this section, short descriptions of some of the available devices used for balance assessment are given. Biokineticists use a device that consists of a platform with a half-sphere attached to the bottom of the platform. The patient is then required to try and keep his/her balance by not letting the edges of the platform touch the ground. The biokineticist observes the proceedings and makes a conclusion about the patient's balance ability based on the number of times the edge touched the ground in a specified time. There are various other commercially available devices for measuring gait and balance performance (see Appendix B). Most of these are aimed at improving athletes' performances in various disciplines.

One company in particular, (namely NeuroCom® International Inc.) is involved with balance in humans and markets a number of devices for testing and evaluating balance and balance disorders. They use the data collected for orthopaedic rehabilitation as well as to improve an athlete's performance. Of the various devices used by NeuroCom®, there is one in which the so-called Motor Control Test (MCT) is conducted. This test assesses the ability of the automatic motor system to quickly recover following an unexpected external disturbance and is done with a device consisting of a platform that translates in the sagittal plane.

NeuroCom® also has a *Basic Balance Master® System* (Figure 2.7) which provides objective assessment of the sensory and voluntary motor control of human balance. This system also includes visual biofeedback. Another device by NeuroCom® is called the EquiTest® System (Figure 2.7) which is used to evaluate balance and postural stability under dynamic test conditions.

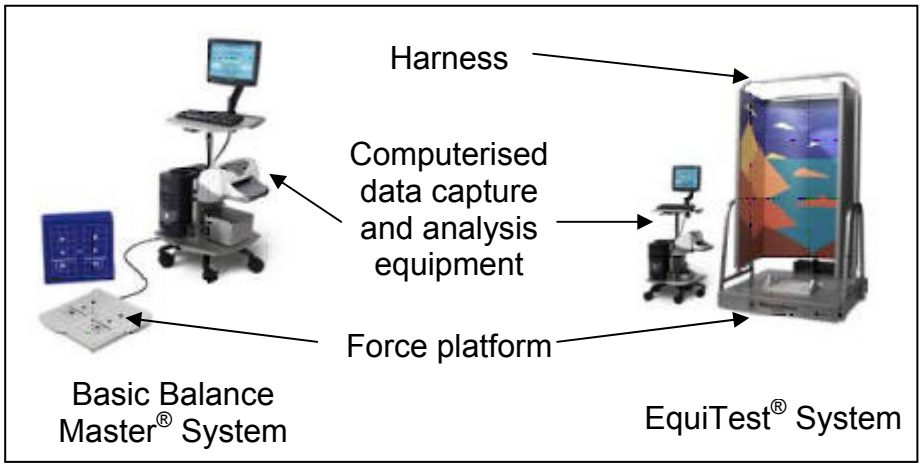

Figure 2.7: Devices used by NeuroCom ® to assess balance capabilities

Another device is one made by FallTrak (www.medtrakonline.com). This device claims to assess both static and dynamic balance performance. The device's diagnostic component is an infrared/video system that provides two or four-channel videonystagmography. The therapeutic component of the device is a computer-assisted visual vestibular proprioceptive balance assessment and training device that allows for balance assessment. It is claimed to identify specific deficits during the test phase.

Micromedical Technologies market a machine called a "Balance Check" (Figure 2.8a). The "Balance Check" utilises the modified Clinical Test for the Sensory Interaction of balance and the Limits of Stability (LoS) Test and claims to objectively quantify a patient's balance capabilities. The Balance Check testing protocol can be used as a screening tool to infer fall risk. This machine also includes a harness to prevent falls during testing.

Micromedical Technologies also has a "Balance Quest" machine (Figure 2.8b). This device consists of a dynamic platform that floats on a spring suspension allowing

dynamic motion in the 6 degrees of freedom of movement. The COP (Centre of pressure) is then measured as a function of all the directions.

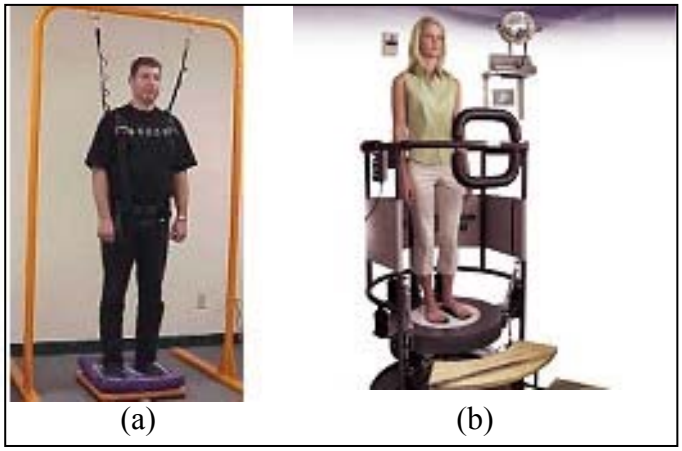

Figure 2.8: Micromedical Technologies' (a) "Balance Check" (b) "Balance Quest"

2.6 Devices used for balance assessment

A patent search on posturography devices was done in order to find other similar devices and in order to patent the proposed device (as discussed in chapter 4). The device was provisionally patented in 2003 (official South African application no. 2003/6702). The detailed result of the patent search is given in Appendix B and E.

From the patent search, at least two devices with a similar function were discovered. The first is one by Mechling (US patent number 4,548,289). This device claims to objectively analyse human balance reactions involving a pivotable platform and a damping device. Another is one by Lynch (US patent number 5,820,096) called an adjustable kinetic stabilisation instrument. This device's purpose is mainly to assist physiotherapists to help improve a person's sense of kinaesthesia. Others include a stabilometer, a variable resistance tiltboard for evaluation of balance reaction and an apparatus for movement coordination analysis. Where the Dorsiflexometer exceeds these devices is the fact that it is simple in design (therefore results can be readily interpreted by doctors and scientists) and that it can be used on any individual who is able to stand. Therefore tests can be done irrespective of age and agility.

3 Mathematical Modelling

A general physical description of an applicable mathematical model (see Figure 3.1) is as follows: The actual leg (modelled here as a rod) is pin-joined to the foot (supported by the platform) with all the body's mass concentrated at the top of the leg. The leg and foot are connected by a piston (ED) that creates the necessary torque (ankle torque) around point A to keep the mass from falling over. Figure 3.1 indicates the motion of balanced dorsiflexion. Figure 3.1 (c) depicts a dorsiflexed ankle, while in Figure 3.1 (a) no dorsiflexion of the ankle is present.

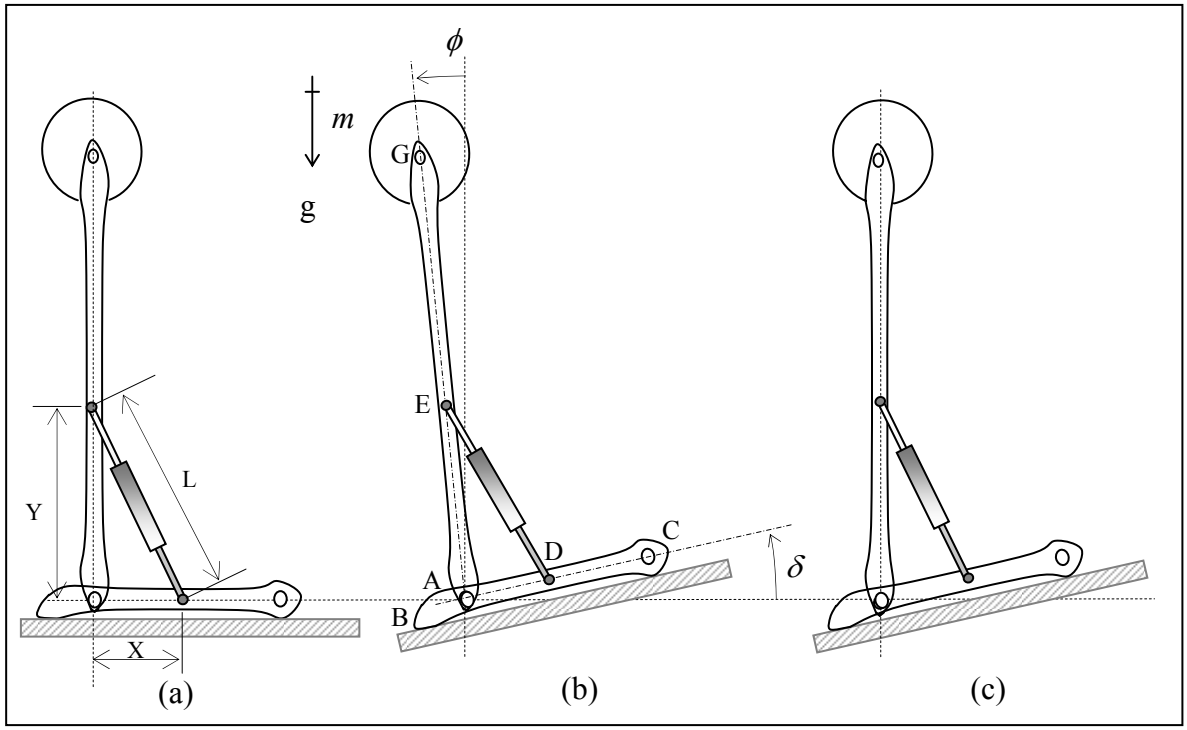

Figure 3.1: Balancing during dorsiflexion: (a) no dorsiflexion, (b) perturbation of the platform, (c) dorsiflexed ankle

Figure 3.1 indicates the supposed method/sequence of events required for balancing, when assuming the test subject is using the ankle joint as the main method of maintaining balance during perturbation on a support platform, and consists of three parts. The first part of this sequence is the body in equilibrium with the platforms – though it has 'normal sway' resulting in a small angle $\phi(t)$ (angle between the vertical axis and the body's vertical axis) being introduced (Figure 3.1 (a)). The second part is when the platforms tilt (angle δ) and the body is not in equilibrium any more – angle $\phi(t)$ increases significantly (Figure 3.1 (b)). The last part is when the body regains

equilibrium by shortening piston ED, thereby reducing angle the $\phi(t)$ to within normal sway boundaries (Figure 3.1 (c)).

3.1 Mathematical Model

Assuming two dimensions in a vertical plane (dorsiflexion in the sagittal plane) and exploring the model further, the general physical description can be elaborated by considering a person's mass concentrated at the end of a slender (without mass) rod that is able to rotate about a fixed horizontal axis without friction. To prevent the rod (person) from falling over from an upright vertical position, as a result of a small angular perturbation, a "righting" torque, τ, is required. This torque is induced by the double acting piston ED (shown in Figure 3.1). To simplify the model further the person's ankle joint is made to coincide exactly with the axis of rotation of the platform as shown in Figure 3.2. Figure 3.1 shows the piston ED (of length, *L*) positioned from a distance *Y* along the length of the leg to a distance *X* on the foot. This piston can exert a force in both directions to create the torque, τ, necessary to keep the mass as close to coinciding with the y-axis as possible.

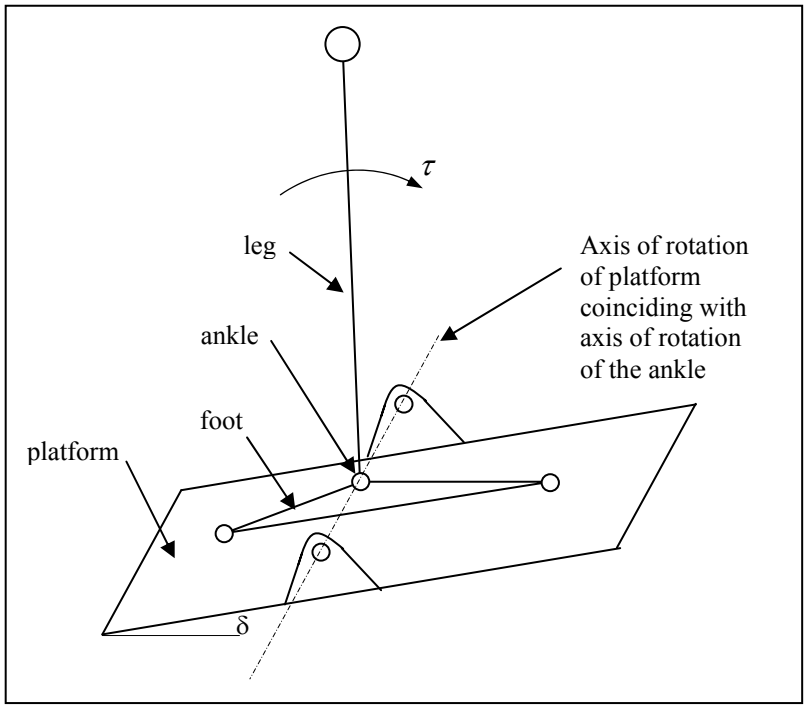

Figure 3.2: Three dimensional presentation of the model (piston ED omitted)

The free-body diagram of a person during dorsiflexion is shown in Figure 3.3. The torque around the ankle joint is realised through the piston ED. This piston is replaced

by two forces working in on point E and D (these forces are considered as internal forces to the system as presented in Figure 3.3) and have the same magnitude except that one of these forces works in the opposite direction than the other. Note that the foot is modelled as a triangular linkage element (triangle OBC) and the rest of the body as linkage element GO with the mass concentrated at G a length *r* from point O. This method of modelling has been used by, for example, Pai *et al,* 2000 and Pietro and Morasso, 1999.

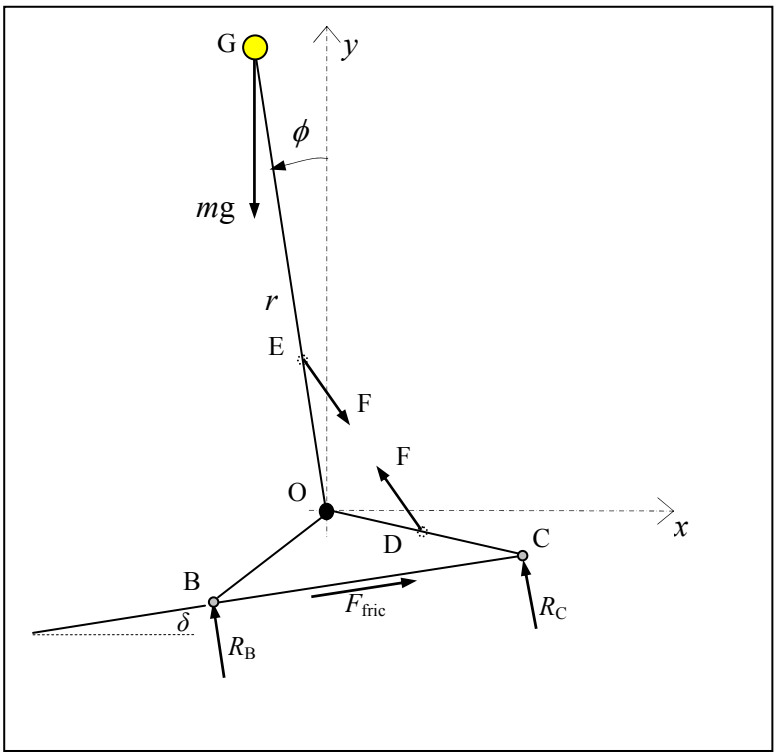

Figure 3.3: Free-body diagram of a person during dorsiflexion

δ is the angle of rotation of the platform around the hinge point, O. This hinge point/axis is multi-purpose – implying that both the ankle(s) and the platform rotate about this axis as shown in Figure 3.2. This angle, *δ,* and a function for the force F are the only inputs to the system. In Figure 3.3 the reaction forces R_B, R_C and F_{fric} are shown. R_B and R_C are the reaction forces normal to the platform of the front and the rear of the foot respectively.

The free-body diagram (Figure 3.3) is split into the linkage element GO and the triangular linkage element BOC, thereby creating two free-body diagrams – refer to Figures 3.4 and 3.7. The first of these two diagrams represent the pendulum-part of the system. It represents the mass concentrated at G with the rod rotating frictionless about point O. Figure 3.4 depicts all the relevant angles and distances. The force, F, is

split into its components F_{PP} (component perpendicular to rod GO) and F_{PL} (component parallel to rod GO).

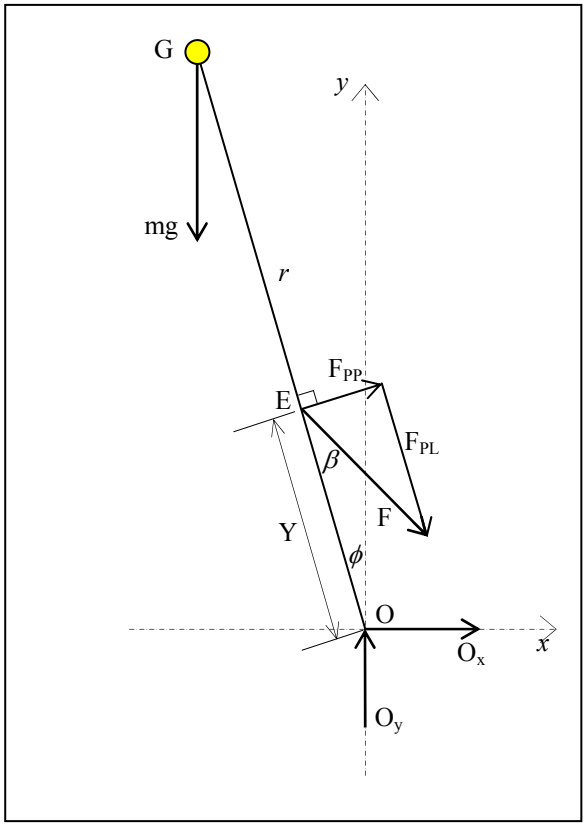

Figure 3.4: Pendulum-part of the free-body diagram

The mathematical equation of motion is obtained by equating the moments around point O to the angular momentum:

$$\sum M_O = I_O \ddot{\phi} \tag{3.1}$$

Depicting anti-clockwise as the positive direction:

$$rmg \sin\phi - YF_{PP} = I_O \ddot{\phi} \tag{3.2}$$

where

$$I_O = mr^2 \tag{3.3}$$

The equation of motion for this part of the model is thus:

$$\ddot{\phi} - \frac{g}{r}\sin\phi + \frac{YF_{PP}}{mr^2} = 0 \tag{3.4}$$

Equation (4.3) governs the inverted pendulum part of the model. However, this part of the model interacts with the foot part (linkage element BOC). Since we are interested in finding the forces R_B and R_C respectively, it is necessary to derive further equations of equilibrium relating to the foot part of the model. Figure 3.5 indicates all the relevant angles as well as distances X, Y and L necessary to obtain these equations.

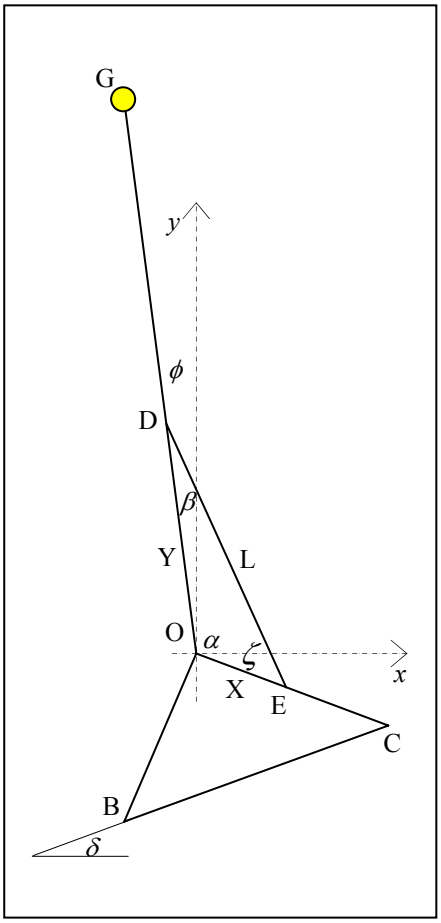

Figure 3.5: Figure defining the angles in the model

From Figure 3.5, α is calculated in terms of ϕ and δ (refer to Figure 3.6 for dimensions of the triangular foot) keeping in mind that all these angles are a function of time:

$$\alpha = \frac{\pi}{2} + \phi + \tan\left(\frac{a}{c}\right) - \delta \tag{3.5}$$

Using the sin-rule, other angles are related as follows:

$$\frac{\sin\beta}{X} = \frac{\sin\alpha}{L} \qquad \text{and} \qquad \frac{\sin\xi}{Y} = \frac{\sin\alpha}{L}$$

where $L = \sqrt{X^2 + Y^2 - 2XY\cos\alpha}$ (3.6)

The equilibrium equations for the inverted pendulum part of the model are obtained by summing the forces in both the x- and y-direction and equating it to zero (from Figure 3.4):

$$(\uparrow)\sum F_y = O_y - mg - F_{PL}\cos\phi + F_{PP}\sin\phi = 0 \tag{3.7}$$

$$(\rightarrow)\sum F_x = O_x + F_{PP}\cos\phi + F_{PL}\sin\phi = 0 \tag{3.8}$$

where

$$F = \frac{F_{PP}}{\sin\beta} \tag{3.9}$$

$$F_{PL} = F\cos\beta \tag{3.10}$$

Equations (3.9) and (3.10) are used to determine F and F_{PL} when F_{PP} are known. This perpendicular force, F_{PP}, is solved by using the differential Equation (3.4). From Equations (3.7) and (3.8) the forces O_x and O_y can be determined. These forces connect the two bodies of the model.

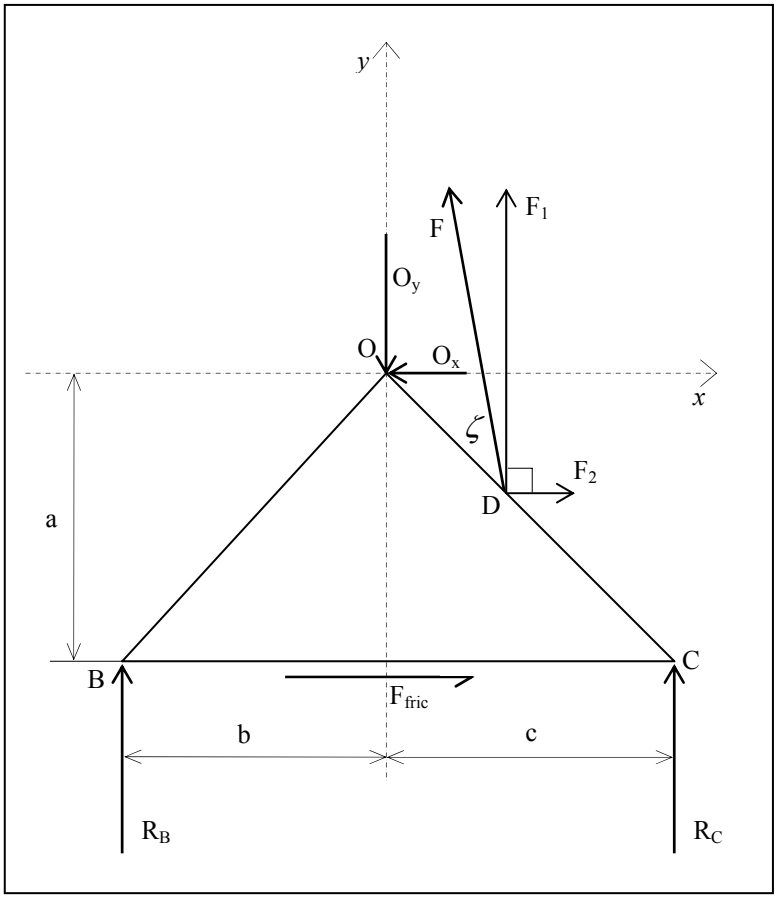

Figure 3.6: Indicating the dimensions of the foot-part of the model

From Figure 3.6, the following relations are used to define forces F_1 and F_2:

$$F_1 = F\sin\left(\zeta + \tan^{-1}\left(\frac{a}{c}\right)\right)$$
$$F_2 = F\cos\left(\zeta + \tan^{-1}\left(\frac{a}{c}\right)\right) \tag{3.11}$$

Figure 3.6 depicts the distances and forces of the foot-part of the model without any perturbation (δ = 0), while that of Figure 3.7 is the free-body diagram with perturbation included.

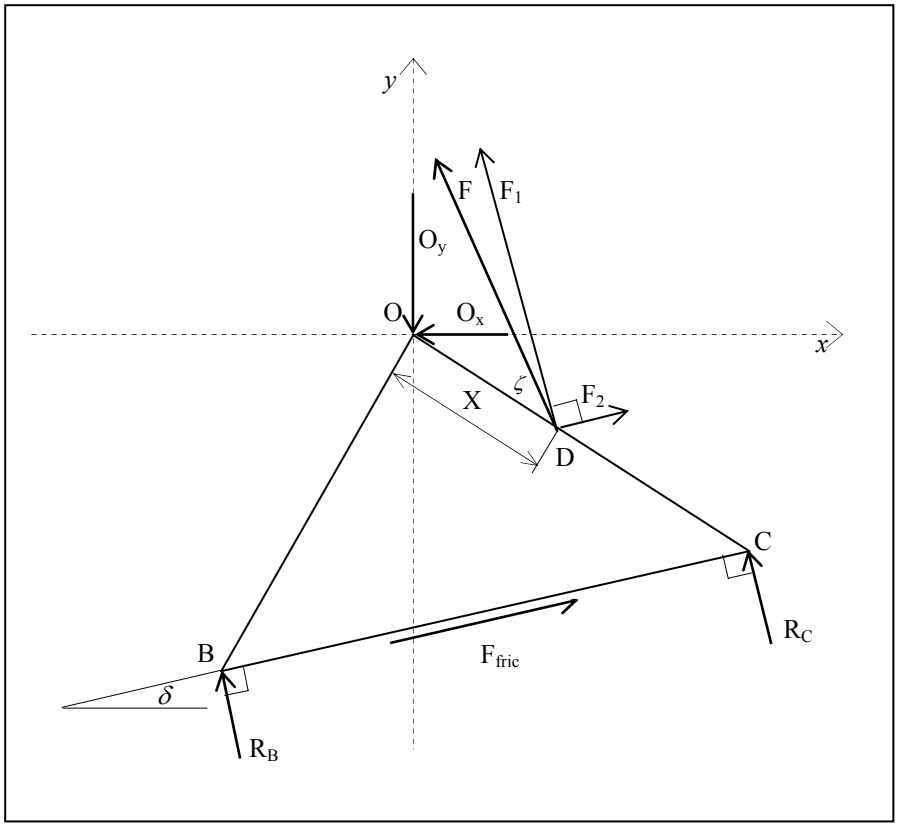

Figure 3.7: Free-body diagram of the foot-part of the model

From Figure 3.7 the equilibrium equations derived:

$$(\uparrow)\sum F_y = -O_y + R_B\cos\delta + R_C\cos\delta + F_{fric}\sin\delta + F_1\cos\delta - F_2\sin\delta = 0 \tag{3.12}$$

$$(\rightarrow)\sum F_x = -O_x - R_B\sin\delta - R_C\sin\delta + F_{fric}\cos\delta - F_1\sin\delta - F_2\cos\delta = 0 \tag{3.13}$$

$$(\curvearrowleft)\sum M_O = (b)R_B - (c)R_C - (a)F_{fric} - (X)F\sin\zeta = 0 \tag{3.14}$$

The three unknown variables are R_B, R_C and F_{fric}. These are solved simultaneously – refer to Appendix G. Finally, the resultant force, R, exerted on the platform is calculated by using yet another equilibrium equation (Figure 3.8).

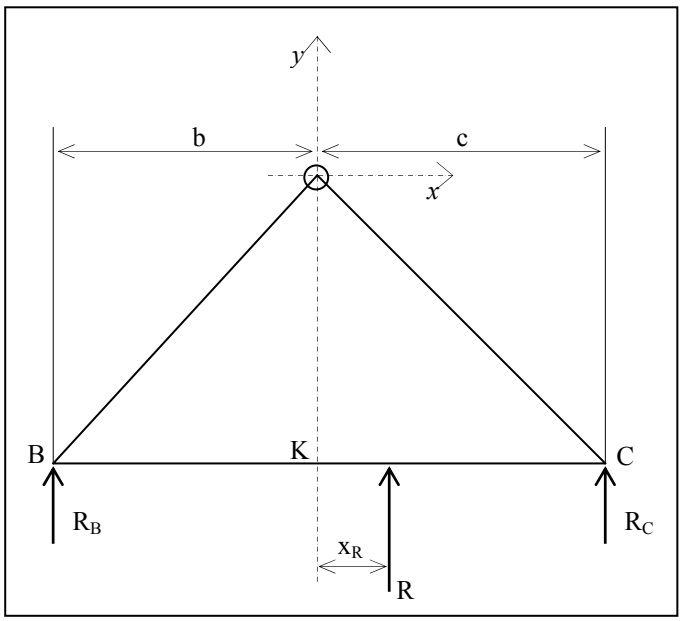

Figure 3.8: Foot-part of the model indicating R and x_R

The two forces, R_B and R_C are replaced by one single force, R some distance, x_R, from point K. This point, K, is in line with the axis of rotation, O, and perpendicular to the platform. The forces working in on point O are omitted from the figure and the calculation because they are not relevant here. Thus, the equation is:

$$\sum M_K = (b)R_B - (c)R_C = (R_B + R_C)x_R = Rx_R \tag{3.15}$$

And therefore,

$$x_R = \frac{(b)R_B - (c)R_C}{(R_B + R_C)} \tag{3.16}$$

3.2 Numerical Solution

3.2.1 Theory

Since an explicit method is used, the second order differential equation, Equation (3.4), has to be solved by calculating small time steps. Equation (3.4) can be written as:

$$\sum M_O = rmg\sin\phi - YF = I_O\ddot{\phi} \tag{3.18}$$

$\ddot{\phi}$ is defined for use in the explicit method by using the following relation:

$$\ddot{\phi} = \frac{\dot{\phi}^n - \dot{\phi}}{\Delta t} \tag{3.19}$$

Where $\dot{\phi}^n$ indicates the new value being calculated for the angular velocity whilst $\dot{\phi}$ is the value calculated in the previous time step. Equation (3.19) becomes:

$$\dot{\phi}^n = \dot{\phi} - \frac{\sum M_O \Delta t}{I_O} \tag{3.20}$$

To calculate the angle associated with this $\dot{\phi}^n$-value, the following relation is used:

$$\phi^n = \phi + \dot{\phi}^n \Delta t \tag{3.21}$$

The next time step then uses these new values as old values and then calculates new values from those. The success of this explicit method relies greatly on using small time steps. The numerical solution was realised through programming the above equations in Visual Basic and executing the program. The program logic is presented in Figure 3.9 (refer to Appendix H for more detail on this logic).

One of the input parameters, as stated earlier, is the force F (see Figure 3.3 and 3.4). This force has to be calculated for each time step. It is apparent that the greater the sway angle, ϕ, the greater F has to be to ensure that the sway angle decreases and therefore avoids the pendulum from falling over. However, F is also dependent on the sway angular velocity as well as many other parameters. For a first approximation, F will be related only to the sway angle and the angular velocity of this angle:

$$F = A\dot{\phi} + B\ddot{\phi} \tag{3.22}$$

Whilst for a second better approximation, F will also be related to the acceleration of the platform angle, δ (see Figure 3.3). It was decided to use the perturbation angle's acceleration here instead of just the angle or the angular velocity because the human brain is tremendously quick to adapt to a situation. Therefore, the force in Equation (3.22) becomes:

$$F = A\phi + B\dot{\phi} + C\ddot{\delta} \tag{3.23}$$

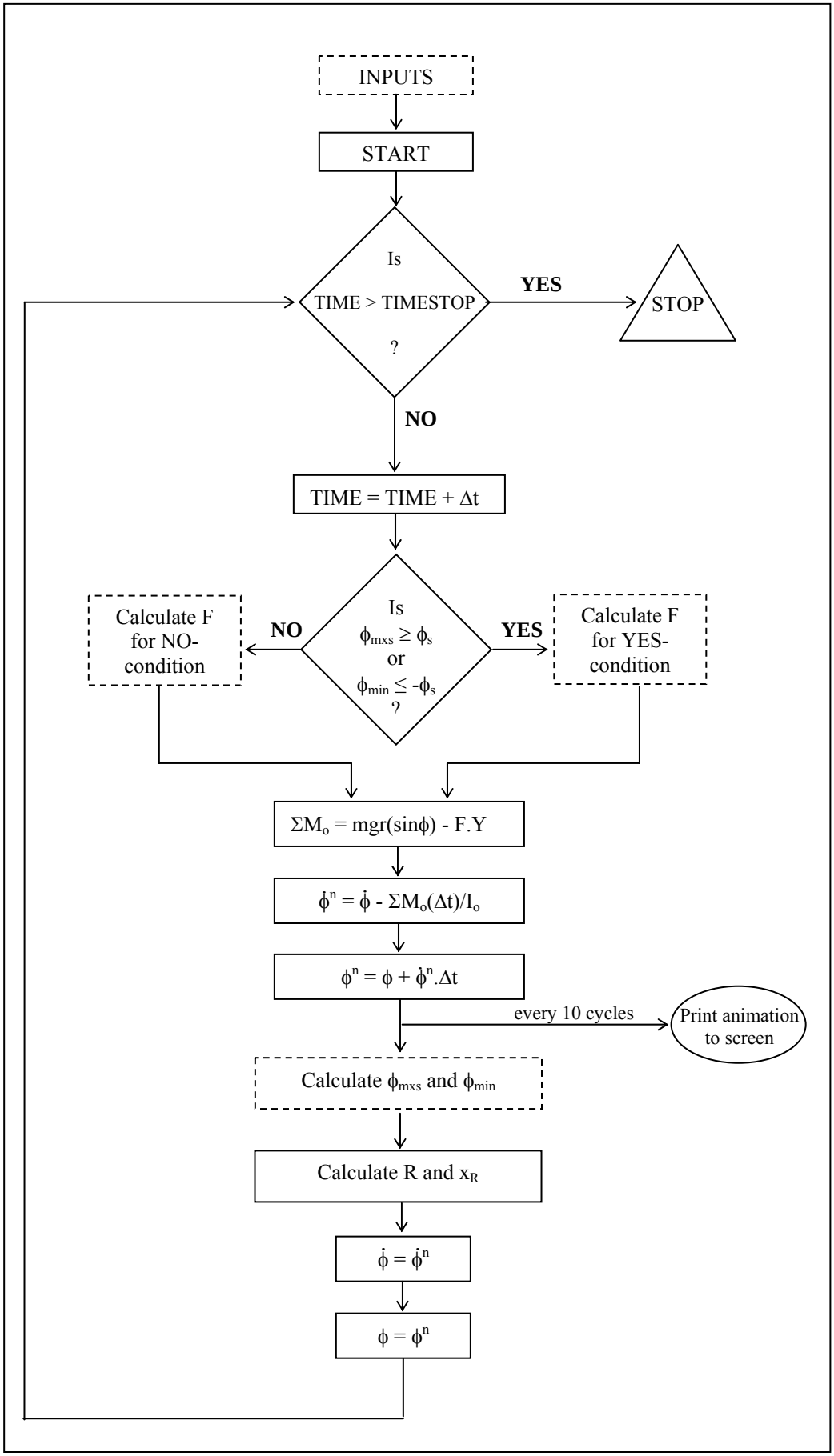

Figure 3.9: Program logic used to solve the mathematical model

Other parameters used in solving the mathematical model are presented in Appendix H, and are defined as the:

- detection angle (ϕ_d): it is the angle, ϕ, which has to be achieved in order for the human to sense that a sway angle exist. If the sway angle is less than ϕ_d, the subject is oblivious to the fact that this angle exists.
- normal sway angle (ϕ_s): this angle defines the magnitude of the maximum angle ϕ that is achieved during normal sway. When ϕ is greater than this angle, the subject would decrease the amplitude of the sway angle until within ϕ_s. If, however, ϕ is smaller than ϕ_s, the subject will increase the sway angle.
- start sway angle (ϕ_{start}): this angle merely states the starting angle ϕ. This angle can be either greater or smaller than ϕ_s, thereby creating different model behaviour.
- starting angular velocity ($\dot{\phi}_{start}$): this angular velocity defines the starting velocity of ϕ. This parameter also causes different starting behaviour of the model.

3.2.2 Results and model verification

Using the Visual Basic program (the program used to obtain the results displayed is on the CD that accompanies this thesis), all the input parameters may be changed and therefore every simulation yields different results. The simulation and parameters were kept to resemble that of the tests done on the Dorsiflexometer.

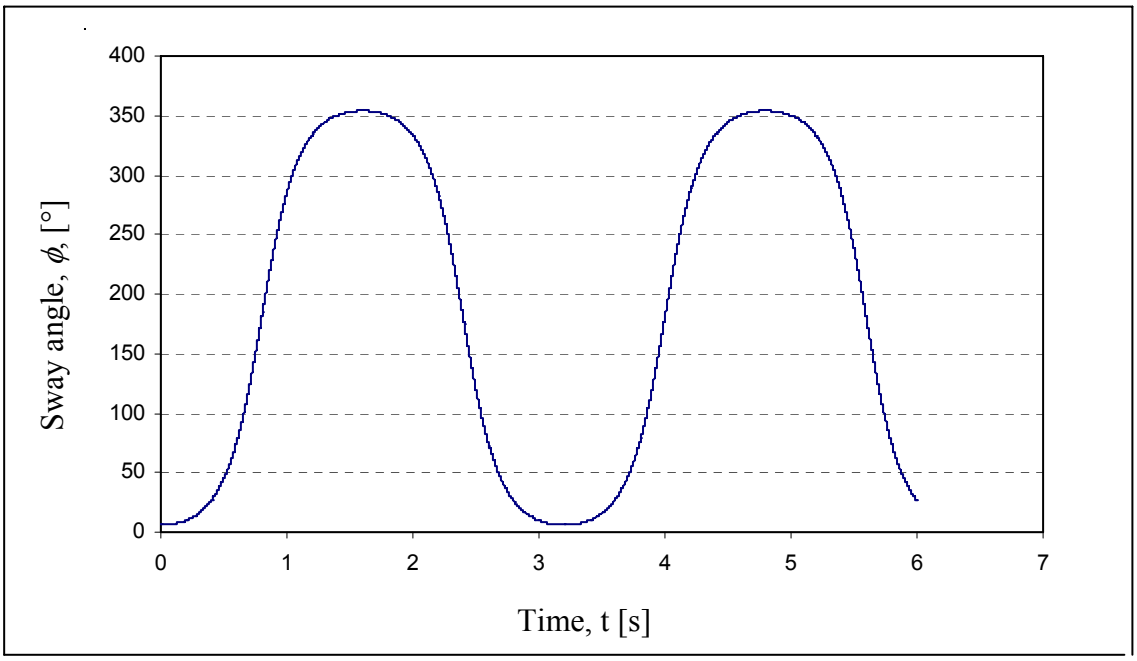

Figure 3.10: Graph depicting the sway angle against time with F = 0

The first simulation run (as shown in Figure 3.10), was without the force F present. The rest of the input parameters were the same as those set out in Table 3.1 (used to obtain the first set of results). The results were exactly that for a free-swinging pendulum, as the following figure verifies, thus serving as a means to verify the soundness of the written program.

Table 3.1: Parameters for the first simulation

parameter	abbreviation	value	unit
time step	Δt	0.0001	s
Mass	m	1	kg
Length	l	1	m
tilt angle's velocity	$\dot{\delta}$	0.7	rad/s
detection angle	ϕ_d	0.15	°
start angular velocity	$\dot{\phi}_{start}$	0	rad/s
start sway angle	ϕ_{start}	0.001	°
normal sway angle	ϕ_s	1	°
Force (Equation 3.22)	F	$1000\phi - 30\dot{\phi}$	N

Table 3.1 presents the input parameters used in obtaining the results shown in Figures 3.11 and 3.12. The force, F, is stipulated according to the first approximation (from Equation (3.22) with appropriate A- and B-values). The values for A and B were obtained from running numerous simulations. The result obtained for the sway angle as a function of time, is as follows:

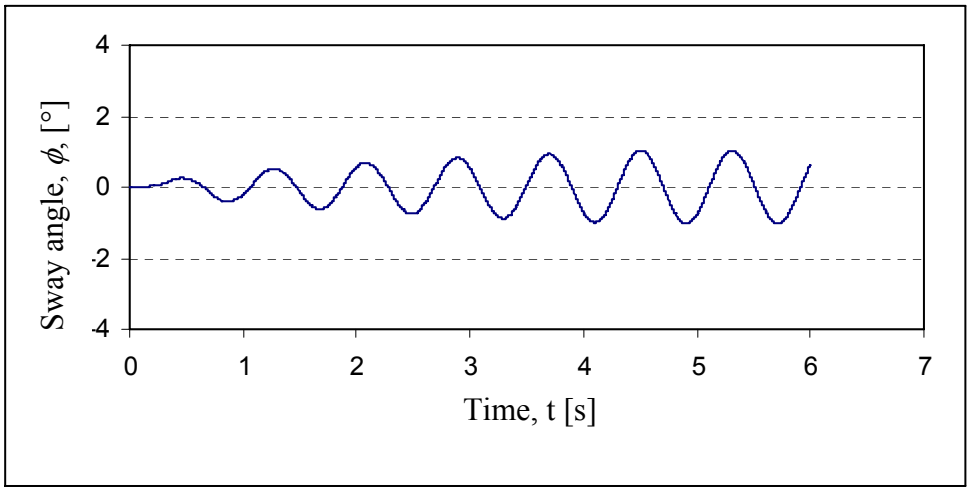

Figure 3.11: Graph depicting the sway angle against time for the parameters stipulated in Table 3.1

The corresponding graph of the distance x_R (see Figure 2.8) as a function of time yields the graph presented in Figure 3.12.

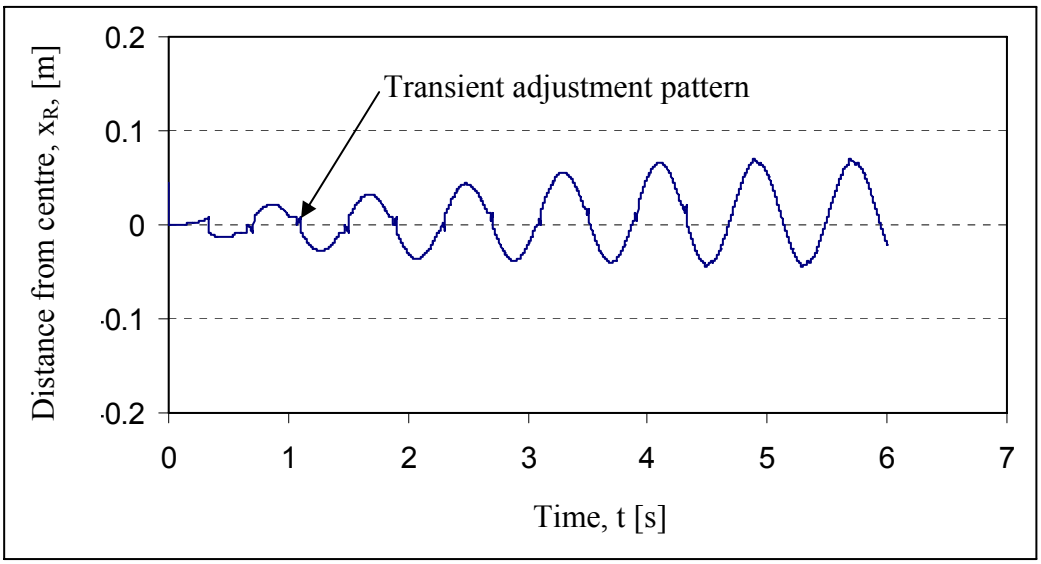

Figure 3.12: Graph showing the normal component of the resultant force's distance from the against time for the parameters stipulated in Table 3.1

In Figure 3.11, the graph clearly indicates that the sway angle increases until it reaches the detection angle. The frequency stays constant throughout the simulation. Figure 3.12 indicates the movement of the position of the normal component of the reaction force on the platform. This distance fluctuates between +0.6 and -0.6 m from the centre and presents the same frequency as that of Figure 3.11. The graph presented in Figure 3.12 indicates a transient adjustment (resulting from the yes/no rule in the mathematical model) every now and then that seems to die away slowly towards the end of this simulation.

As apparent from Figures 3.11 and 3.12, no change is noticeable when perturbation of the platform starts or ends. This is because in force F's first approximation, presented in Equation (3.22), only the sway angle and the sway angle velocity are incorporated. Another parameter was added to include the 'sensing' of the perturbation angle. This resulted in the second approximation given in Equation (3.23). For the second set of simulation results, values for A, B and C used for calculating F, are presented in Table 3.2 along with the other parameters.

Table 3.2: Parameters for the second simulation

parameter	abbreviation	value	Unit
time step	Δt	0.0001	s
mass	m	1	kg
length	l	1	m
tilt angle's velocity	$\dot{\delta}$	0.07	rad/s
detection angle	ϕ_d	0.15	°
start angular velocity	$\dot{\phi}_{start}$	0	rad/s
start sway angle	ϕ_{start}	0.001	°
normal sway angle	ϕ_s	1	°
Force (Equation 3.23)	F	$1000\phi - 30\dot{\phi} - 50\ddot{\delta}$	N

The second simulation's results are presented in Figure 3.13 and 3.14 respectively. Evident in Figure 3.13, is the slight change in the normal pattern at two seconds and at four seconds. At these times, perturbation of the platform starts and ends respectively. Visible in Figure 3.13 is how the sway angle, starting at the specified zero degrees (as presented in Table 3.2) increases to reach the normal-sway boundary, but increase beyond this boundary when perturbation starts and ends. This is more apparent at four seconds, when the sway angle increases to about two degrees – double that of the specified normal sway angle. However, after four seconds, the sway angle decreases steadily again to within the stipulated normal sway boundary.

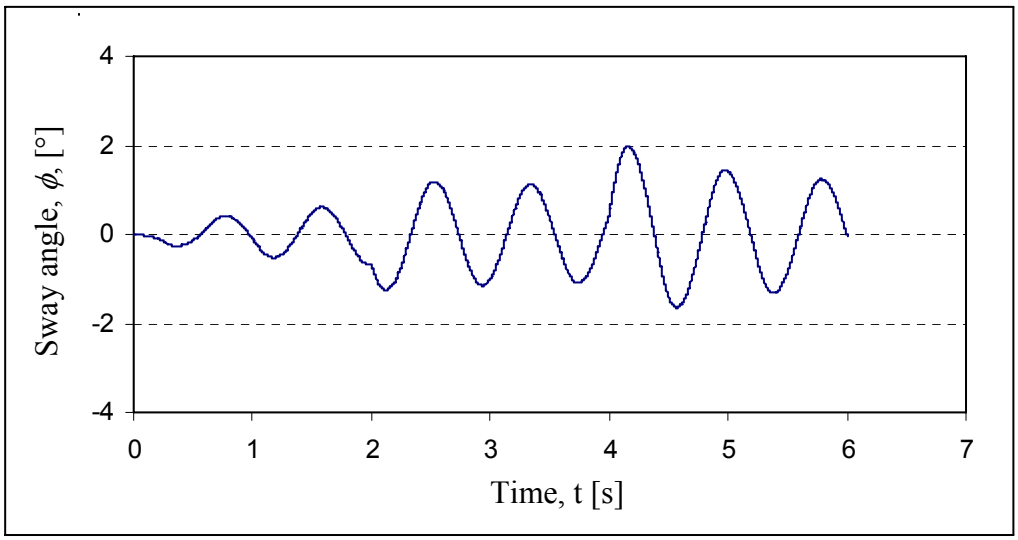

Figure 3.13: Graph depicting the sway angle against time for the parameters stipulated in Table 3.2

Figure 3.14 showing the movement of the normal component's movement, indicates a very clear discontinuity at two and four seconds respectively, reaching an absolute value in excess of 6 m. Because the distance is much more than that of the support base of the feet, the subject would surely have fallen off the platform. This discontinuity happens because the force in Equation (3.25) 'pulls' hard when a change in perturbation angle is apparent, and since the platform and foot is modelled to be fixed to one another, the force can have any magnitude without the pendulum 'falling off' the platform.

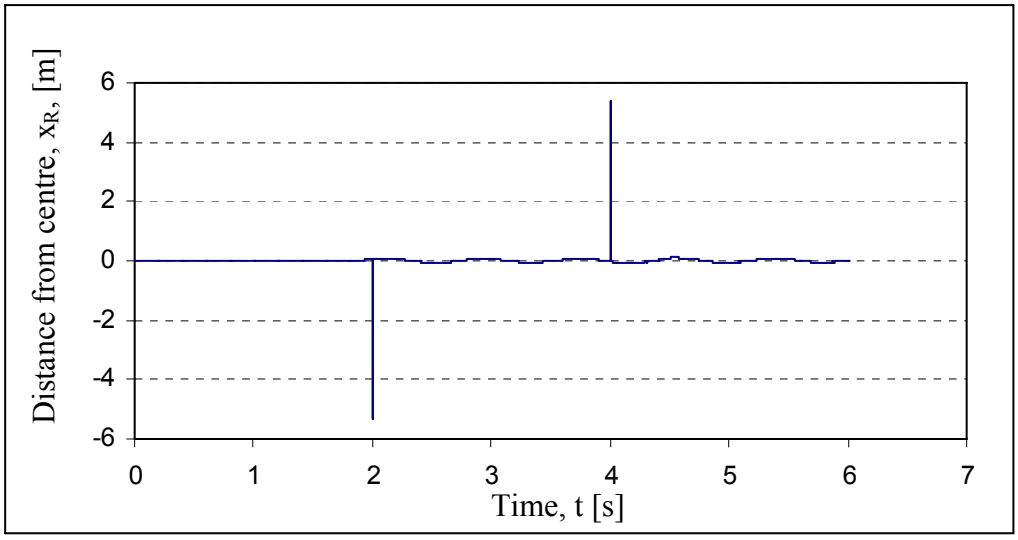

Figure 3.14: Graph showing the normal component of the resultant force's distance from the centre against time for the parameters stipulated in Table 3.2

Figure 3.15 presents a zoomed-in graph of Figure 3.14, indicating the small irregularities as present in Figure 3.12.

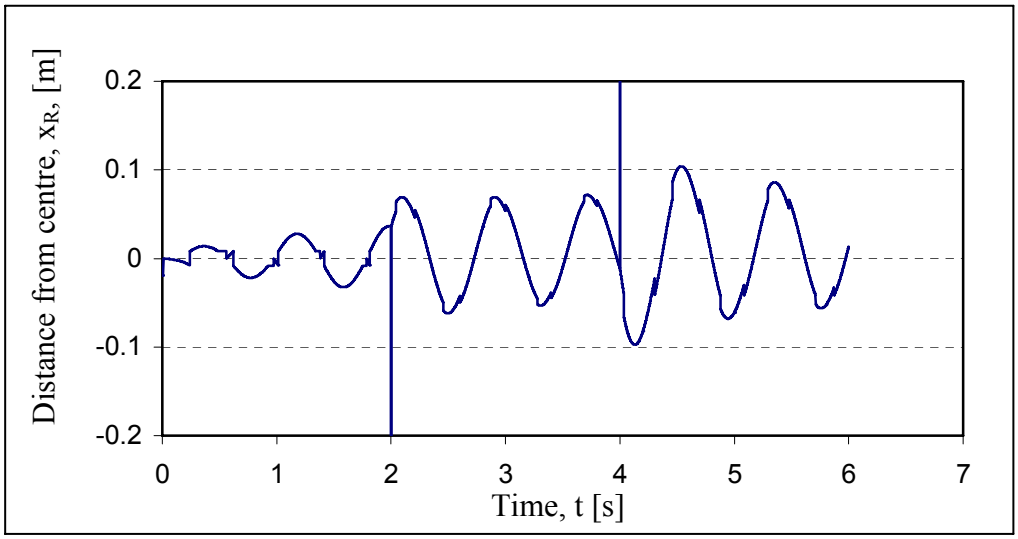

Figure 3.15: Zoomed-in graph of Figure 3.14

As seen from the results obtained in Figure 3.11 and 3.12, the model does not accurately predict how humans respond when subjected to perturbation of their support-platform. There are numerous factors contributing to this fact. Foremost is the simplicity of the model used – consisting of one 'link', the pendulum-part of the model, pin-jointed to the foot-part of the model. Van der Kooij, *et al.*, for example, used a more sophisticated three-link model to predict sensory perturbations on total body sway. Another factor may be that several of the inputs used in this model are not readily known. In the proposed model, a 'detection angle' has been used. It is not known whether such an angle actually exist, but is necessary to define the model's behaviour. Finally, other inputs or parameters had to be chosen. The force, F (the one acting in piston ED – refer to Figure 3.2) does not have a known specific form or relation. Therefore the relation was chosen to react in relation to the off-set / sway angle as well as the angular velocity of the angle. Viewed differently, the force has a 'spring' and a 'damping' component. Since normal sway must always be present, the damping-part of the force does not act when within normal-sway boundaries.

Figure 3.13 resembles a closer comparison to what is expected when a human subject's sway angle is measured during a perturbation test than that of Figure 3.11. This is contributed to the second, more refined, approximation of F. It is important to note that all of the inputs used to obtain the results displayed in this section are changeable and can be varied to obtain different results. The results presented in this chapter are only those for the parameters given in the tables.

The model used in this thesis' purpose is to gain understanding of how the dynamics of human posture works, and judging from Figure 3.13, it has been achieved to some extent.

4 Mechanical Design

The design process of the device constructed for the testing of human subjects, started in 1998 (Botha, 1998). This year a device for measuring the pressure distributions underneath a test subject's feet, when subjected to dorsiflexural perturbation, was constructed. An image of this device is shown in Figure 4.1.

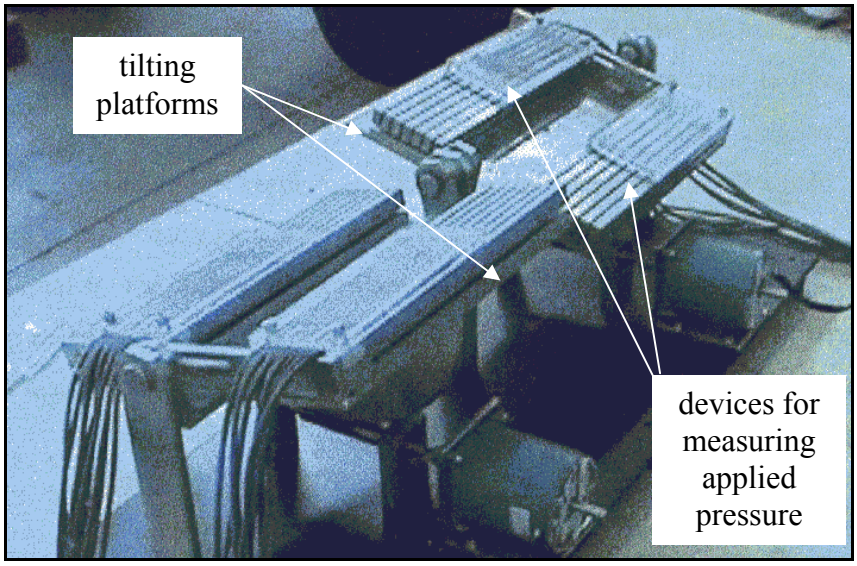

Figure 4.1: Earlier device for measuring pressure during perturbation (Botha, 1998)

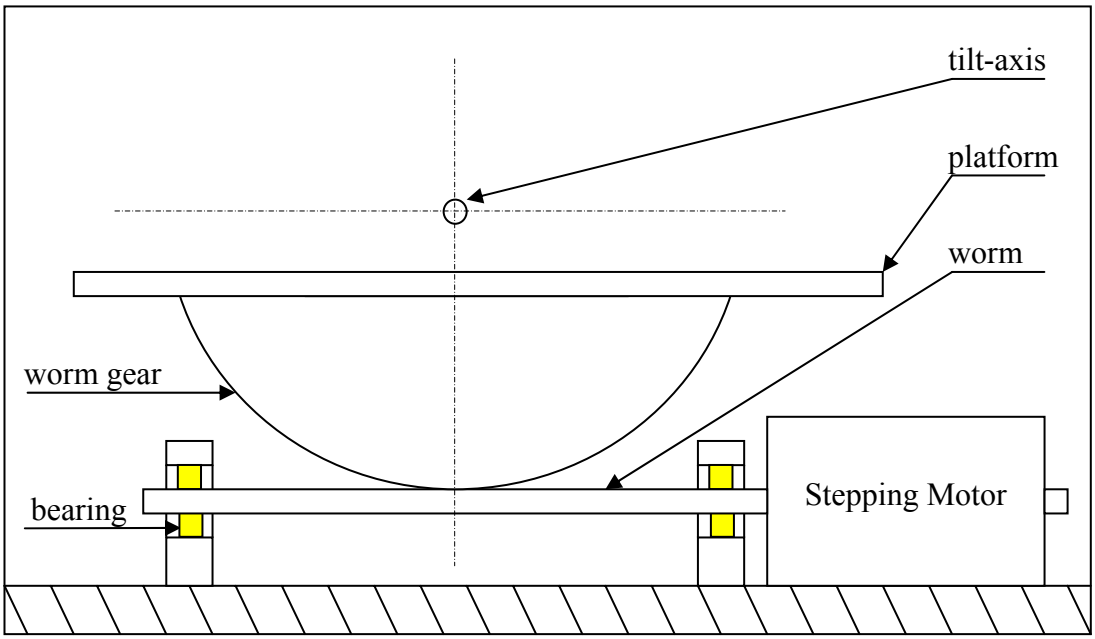

Figure 4.2: Diagram of the tilting mechanism (Botha, 1998)

The tilting platforms are indicated in Figure 4.1. Both platforms were tilted with stepping motors. Figure 4.2 illustrates the tilting mechanism where the worm and the worm gear are shown.

The design specifications for the Dorsiflexometer follow the description of what the device is supposed to do. The following statements clarify the function of the device to be designed and manufactured: *A device needs to be constructed. This device should be able to measure balanced dorsiflexion with the aim to detect balance impairment. This entails constructing two tiltable platforms (one for each foot) able to tilt the subject in the sagittal plane. Each of these platforms must be able to be moved and controlled separately. They should also be equipped with a means to measure the resultant force created by the foot.*

From the above statement, concepts were drawn up. From these concepts, the best concept was chosen (following the comparison of the concepts with regards to the design decision criteria).

4.1 Concepts

Two concepts were decided upon, and both were modelled using the computer program *Pro Engineer* (this is a very powerful software package in which solid modelling techniques are used). Before discussing these concepts, however, the force platform to be used in both these concepts will be described and discussed.

4.1.1 The Force Platform

Each force platform consists of three footplates, each of which is mounted on a load cell. The load cells have a specification of 50 kg. From the three load cells, the direction and magnitude of the resultant force applied can be derived. One such platform will be mounted on each of the tiltable platforms – implying one force platform per foot. A sketch of one such platform is shown in Figure 4.3 and a photograph of both platforms in Figure 4.4.

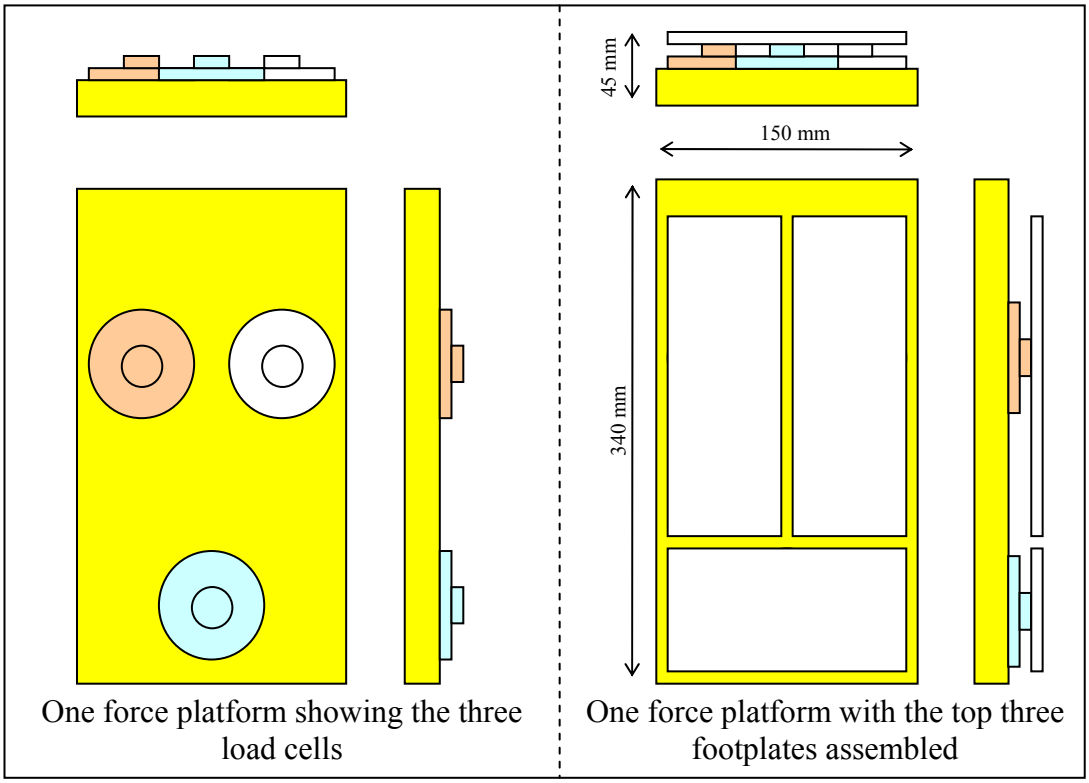

Figure 4.3: A sketch of one force platform

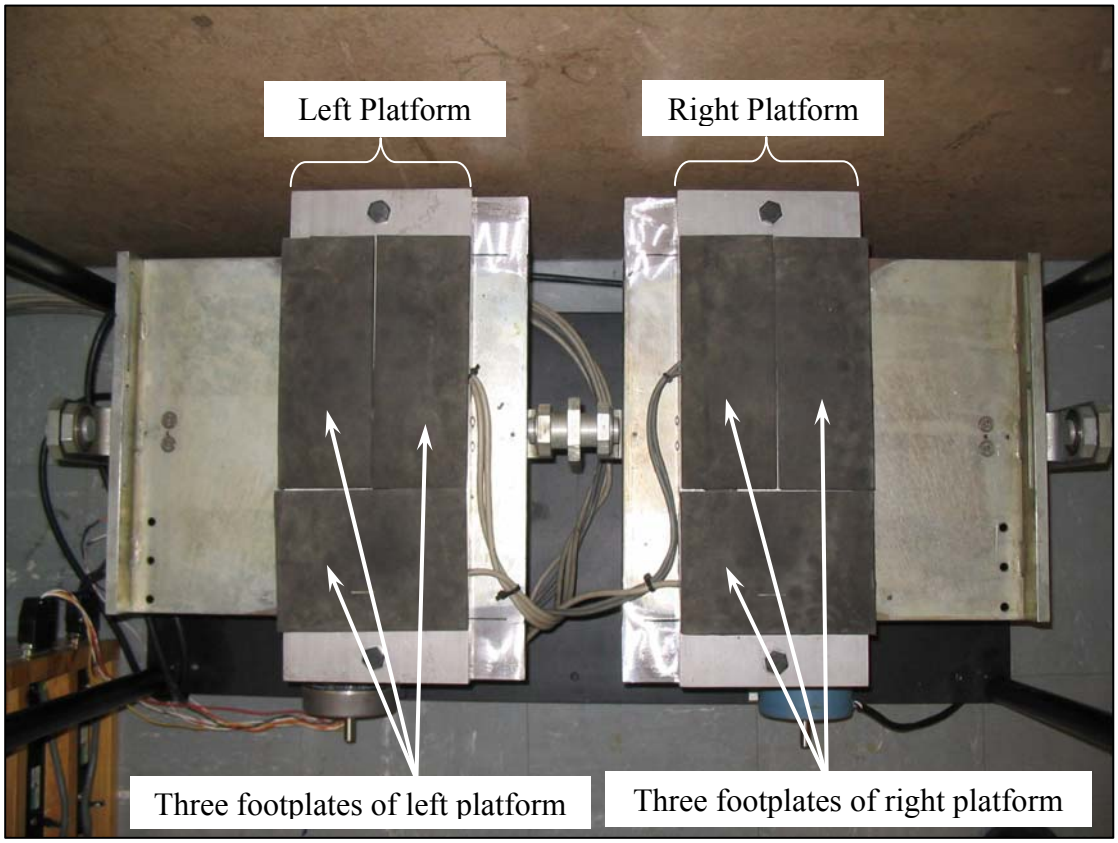

Figure 4.4: A photograph of the force platforms

Figure 4.3 indicates the design of the force platform used. On the left-hand side of Figure 4.3 is a top-, rear- and side-view of the platform with its load cells (the footplates covering the load cells are removed from this view), whereas on the right-hand side of Figure 4.3 the force platform is assembled and therefore includes the footplates. The overall dimensions are also shown here. Figure 4.4 is a view of the two platforms from the top.

4.1.2 Sliding mechanism concept (Concept 1)

The first concept (excluding the motors used to drive the tilting mechanism) is shown in Figure 4.5.

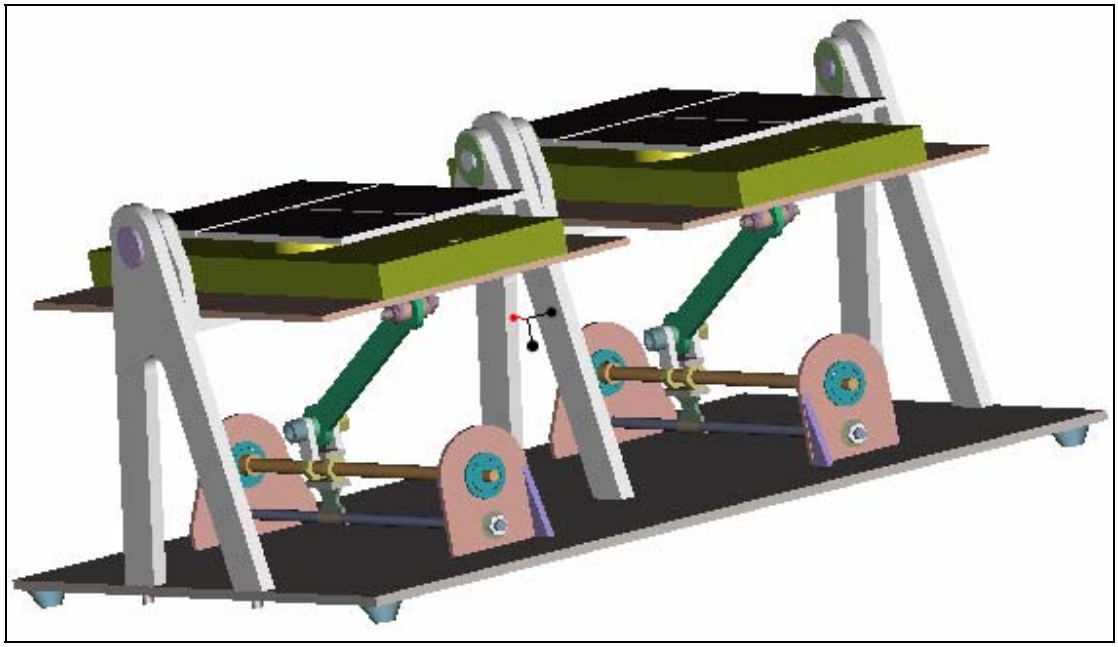

Figure 4.5: Sliding mechanism concept (note, DC-motors not shown)

The tilting mechanism and the force platform are the two parts necessary to fulfil the function of the intended device. The tilting mechanism of this concept is quite simple and involves a rotating threaded shaft. The 'nut', in which the threaded shaft turns, is modified to incorporate the pivoting of the arm. This arm connects the 'nut' to the platform. Therefore, a rotating shaft induces a tilting movement when the shaft rotates. The reason for using a nut-bolt method for creating linear movement from a rotating rod/axle is because the threads of a nut and bolt mesh very well. This, therefore, ensures a configuration that has virtually no play associated with it. A sketch of the essential element of the sliding mechanism concept with its 'nut' is shown in Figure 4.6.

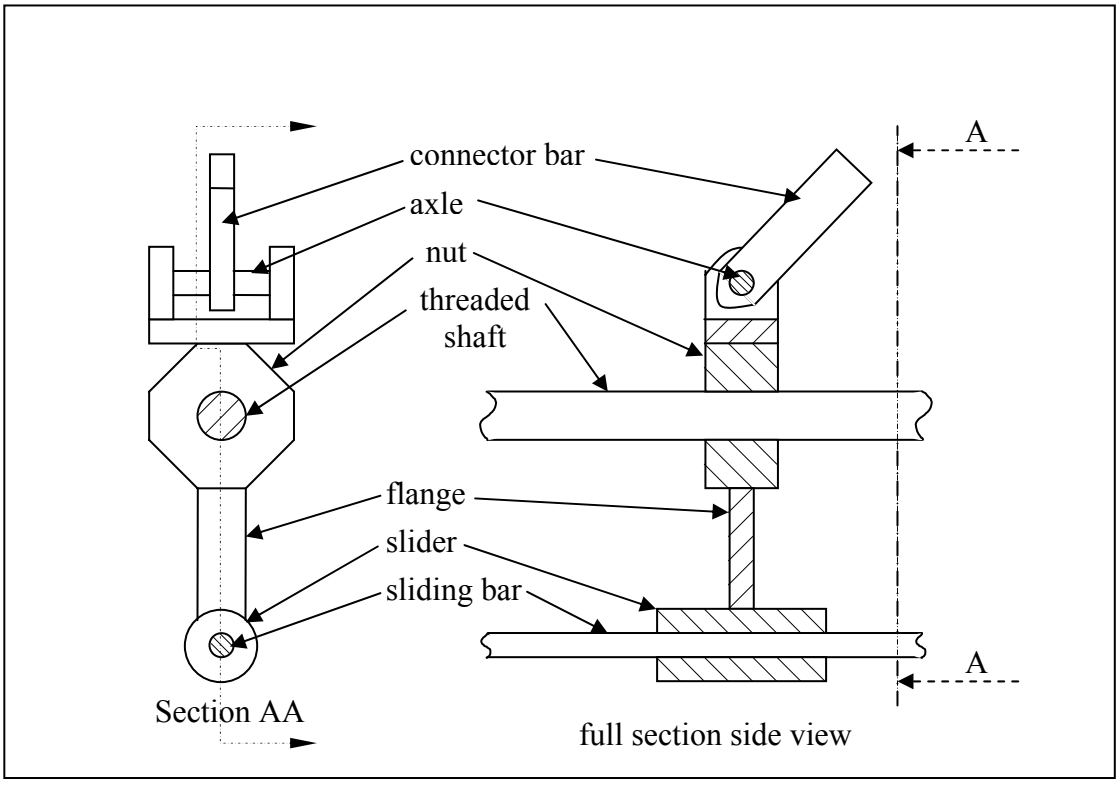

Figure 4.6: Sliding mechanism concept: A diagram of the tilting mechanism (simplified).

This concept makes use of direct current (DC) motors to drive the tilting mechanisms. It was thought that using stepping motors is a bad idea because stepping motors increment in little steps when in use and therefore induce electromagnetic noise in the measuring system. Therefore this concept uses DC-motors (one for each platform). With DC-motors one can easily alter the speed at which they turn, by simply using a pulse width modulator (PWM) controller for each of the motors.

4.1.3 Worm gear concept (Concept 2)

A solid model (created in Pro-Engineer) of this concept is shown in Figure 4.7. This concept incorporates stepping motors, as well as the worm gear configuration (Figure 4.2). The tilting platforms as well as the stepping motors are identified in Figure 4.7. Note that the gears, including the worm gear, are not modelled in detail.

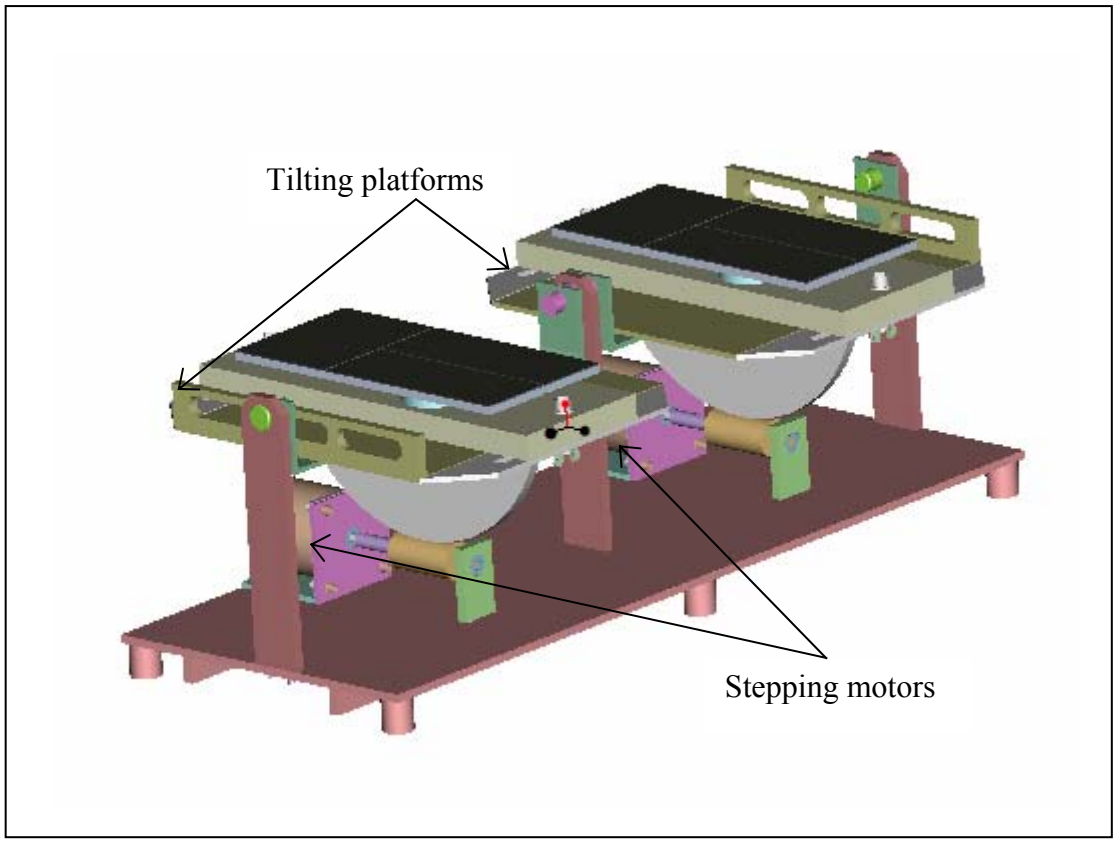

Figure 4.7: Worm gear concept: using stepping motors to drive the platforms

4.2 Final Design

A decision table (Table 4.1) was used to decide between the two concepts. The design criteria included robustness, reliability, ease of manufacture, time and money and motor type.

4.2.1 Design Decision Criteria

Design decision criteria include robustness, reliability, manufacturing, time and money, aesthetics, and the motors to be used. Each of these criteria are discussed shortly followed by the decision table.

- *Robustness*

  Building a robust device has obvious advantages, of which the most important one is that a robust product would not break easily. Because limited time is allocated for conducting tests, it is imperative to have a robust device to reduce the possibility of a breakdown. Looking more closely at the concepts, the sliding mechanism concept (concept 1) could be considered less robust than the worm gear concept (concept 2)

mainly because it has less moving parts and a worm gear configuration is very robust while the threaded shaft tilting mechanism might break more easily.

- *Reliability*

This factor is very important. Considering the two concepts, there might be a slight difference in their reliability. Concept 2 would be more reliable than concept 1 because it is more robust in design. Also, Concept 1 needs speed controlling equipment to control the DC-motor's speed. This equipment may be susceptible to outside electromagnetic interference and therefore cause unreliable operation.

- *Manufacturing*

The ease of manufacture also plays an important role in the decision-making process. Since Concept 2 has a worm gear configuration it will take more time and expertise to manufacture than Concept 1 (which is made from standard material sections joined and welded together).

- *Time and money*

Manufacturing Concept 2 would involve more time and money than Concept 1. However, the tilting mechanism of Concept 2 had already been manufactured (Botha 1998), therefore Concept 2 involves less time and less money to make (for Concept 1 two new DC-motors have to be bought and the tilting mechanism needs to be manufactured).

- *Aesthetics*

Both concepts look very similar. Therefore, there is not much to choose between the two concepts from an aesthetic point of view.

- *Motor type*

Traditionally, stepping motors are used when it is desired to know exactly how many revolutions have been made by the motor shaft – therefore they are used mainly in process control applications. Direct current motors are used in a variety of applications (for example electric windows of cars). But knowing exactly how many revolutions are made with a DC motor, one needs a sensor (for example a tacho-meter). Thus, using DC-motors in control applications is more difficult than using stepper motors because of the extra sensor input that needs to be verified and

checked every time. Since the tilt angle of the platform is needed it is better to use a stepping motor than a DC-motor. The number of revolutions of the motor can be directly related to the angle of the platform. But there is a drawback in using stepper motors. The stepwise incrementation has the undesired result that it will induce noise in the electrical measurements taken from the load cells.

Having evaluated the different criteria, the decision-making table is presented in Table 4.1 (in this table, Concept 1 is the Sliding Mechanism Concept while Concept 2 is the Worm Gear Concept). Concept 2 is seen as the better choice, scoring highest in most of the criteria. Therefore, Concept 2 is chosen as the final design.

Table 4.1: Decision table

Criteria	Weight	Possible Perfect concept	Concept 1	Concept 2
Robustness	10	10	8	10
Reliability	8	10	8	9
Aesthetics	5	10	7	7
Time and money	7	10	6	8
Manufacturing	6	10	7	5
	Total:	**50**	**36**	**39**

4.3 Design Specifications

This section deals with the design specifications applicable to the final design. Each of the design specifications will be discussed briefly. Their importance and threshold performances, to which the final product must conform, are considered.

4.3.1 Signal-to-Noise Ratio

In analog and digital communications, signal-to-noise ratio (SNR) is a measure of signal strength relative to background noise. The ratio is usually measured in decibels (dB). If the incoming signal strength in volts is V_s and the noise level, also in volts, is V_n, then the SNR (in decibels) is given by the formula (Online Encyclopaedia):

$$SNR = 20\log_{10}\left(\frac{V_s}{V_n}\right) \tag{4.1}$$

For the purpose of the Dorsiflexometer, the SNR will be defined slightly differently. F_s and F_n will replace V_s and V_n respectively. F_s and F_n is the magnitude of the amplitude of the signal and noise level, respectively, measured as a force in Newton.

The design specification for the SNR will be set to a signal level of F_s = 20 N a noise level of not more than F_n = 0.01 N. This gives the minimum allowable SNR as:

$$SNR = 20\log_{10}\left(\frac{F_s}{F_n}\right) = 20\log_{10}\left(\frac{20}{0.01}\right) = 66 \qquad (4.2)$$

In the Figure 4.8, hypothetical values (x = y = 0.01 N) are used to illustrate the definition of the signal-to-noise ratio as well as the maximum allowable SNR for the Dorsiflexometer.

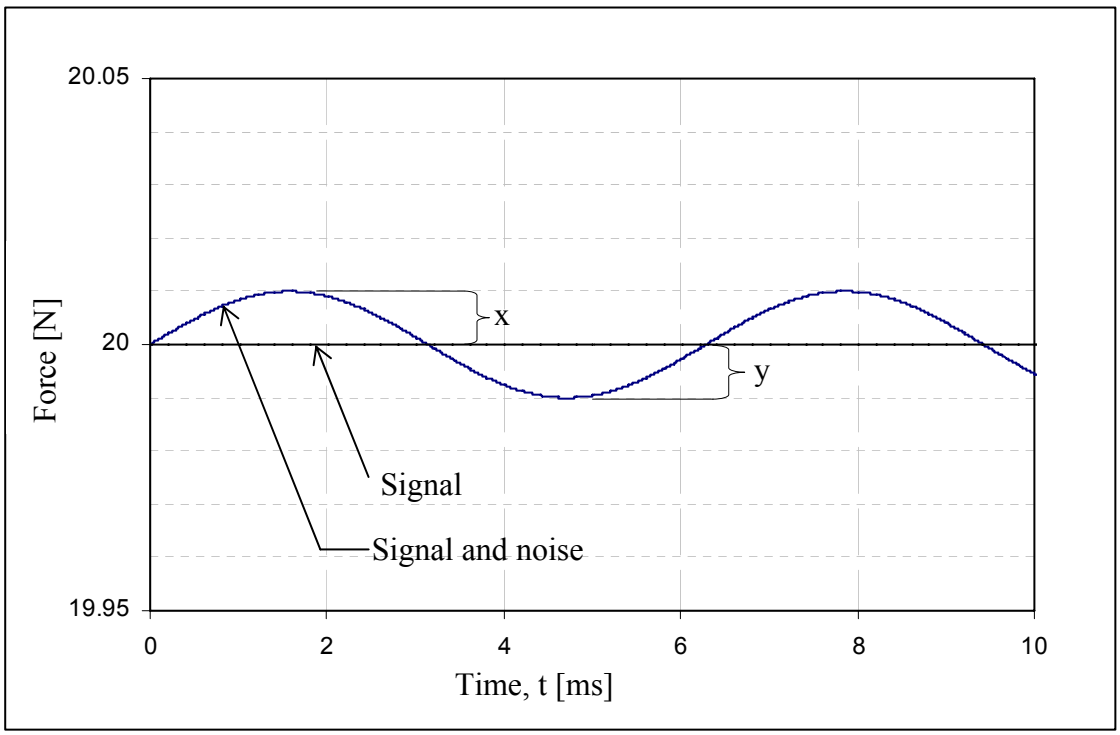

Figure 4.8: Desired maximum SNR for the Dorsiflexometer

In the above figure, the force supported by the platforms is taken as the absolute value (plotted in the graph as the straight line – 20 N in this instance). This value should correspond with the average value of the signal coming from the sensor. The signal measured (after it has been converted to a mass reading) is plotted as the sinusoidal graph in Figure 4.8. The maximum difference (x or y) is then the maximum deviation off the desired result. This value should not be more than 0.1 N (this value was concluded

upon because movement on the force platform is very slight and therefore 20 $\pm \frac{1}{100}$ kg was deemed a fine enough resolution).

4.3.2 Tolerances

Tolerances on the design are most important on the gear mesh. Playing between the gears is to be eliminated as far as possible, since this will inevitably induce an unstable platform and noise-related problems. Other tolerances, for example the railing, are to be kept within acceptable workshop standards.

4.3.3 Reliability

Reliability is one of the results of a robust designing. Therefore, emphasis is placed on robustness yet again. This is due to the fact that a robust product will not break easily. A sub-division of the reliability criterion is that the acquisition of data also needs to be reliable. Repeatability of the test is of utmost importance. The device cannot be successful if reliable repeatability is not achieved.

4.3.4 Computer Programs

Part of designing this product is producing a computer program. This computer program should be user-friendly and understandable results should be displayed.

4.3.5 Sensors

All the sensors used on the Dorsiflesometer should be reliable and rapid. The only sensors used are the load cells, therefore these load cells have to be rapid-acting and reliable.

4.3.6 Safety

The design needs to have a device (or devices) to ensure that the test subjects are at ease when being tested. The adding of a simple railing, is the easiest way to ensure a subject's safety during testing (similar railings are used in commercially available equipment as presented in Section 2.5).

4.3.7 Final design

Features of the final design for the Dorsiflexometer will be discussed briefly.

- *Safety*

A railing was designed, manufactured and bolted to the structure. For the railing to be steadfast, it has to be positioned against a wall. See Figure 4.9.

- *Force platforms*

The force platforms used in the final design are as discussed in paragraph 4.1.1.

- *Tilting mechanism*

The tilting mechanism consists of two stepping motors (with their drivers), the worm gear configuration and the platforms onto which the force platforms are mounted. The platforms are able to tilt a maximum of 22.5° each in the dorsiflex direction (50° in the plantarflex direction). These maximum values are due to physical constraints. The tilting speed can be set on the drivers to either high or low.

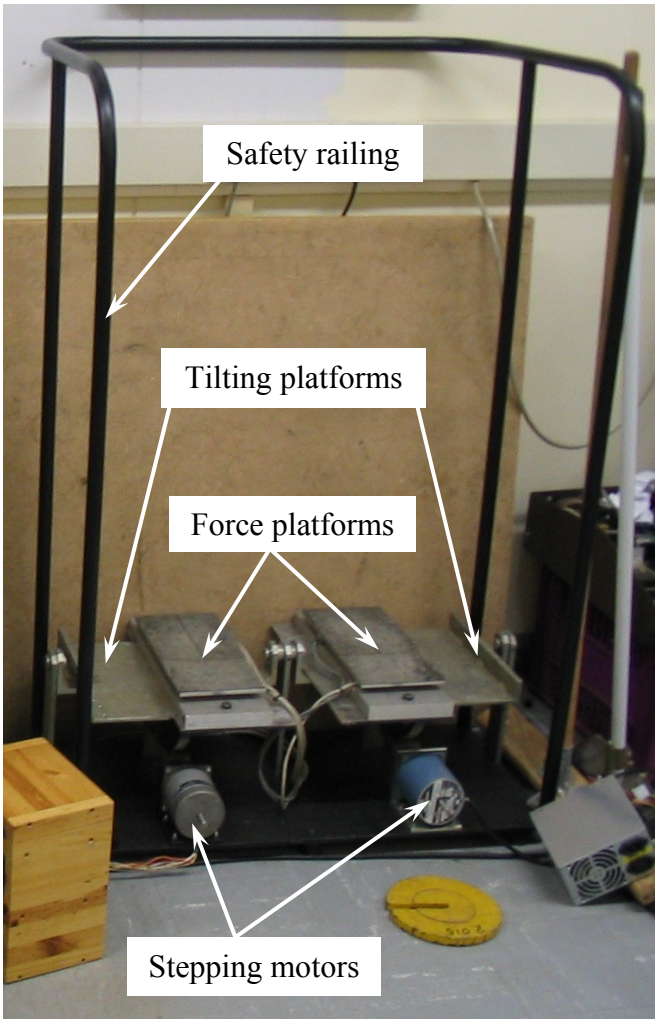

Figure 4.9: A photograph of the final design

5 Experimental Work

Since the Dorsiflexometer's aim is to accurately measure the balance capabilities of a human subject, it has to be calibrated and certain aspects of the machine need to be verified. These aspects include the reliability and performance of hardware (load cells and data acquisition system) and software associated with the Dorsiflexometer – as stated in Section 4.3. This section starts with a look at the experimental set-ups and the physical calibration of the device (this includes calibration of the load cells, the bridge amplifier used and the software package, LabView) and concludes with the experimental procedures and an example of a test result.

5.1 Experimental Set-ups

Two experimental set-ups using different measuring equipment were used. Figures 5.1 and 5.2 show block diagrams of the first and second set-ups respectively.

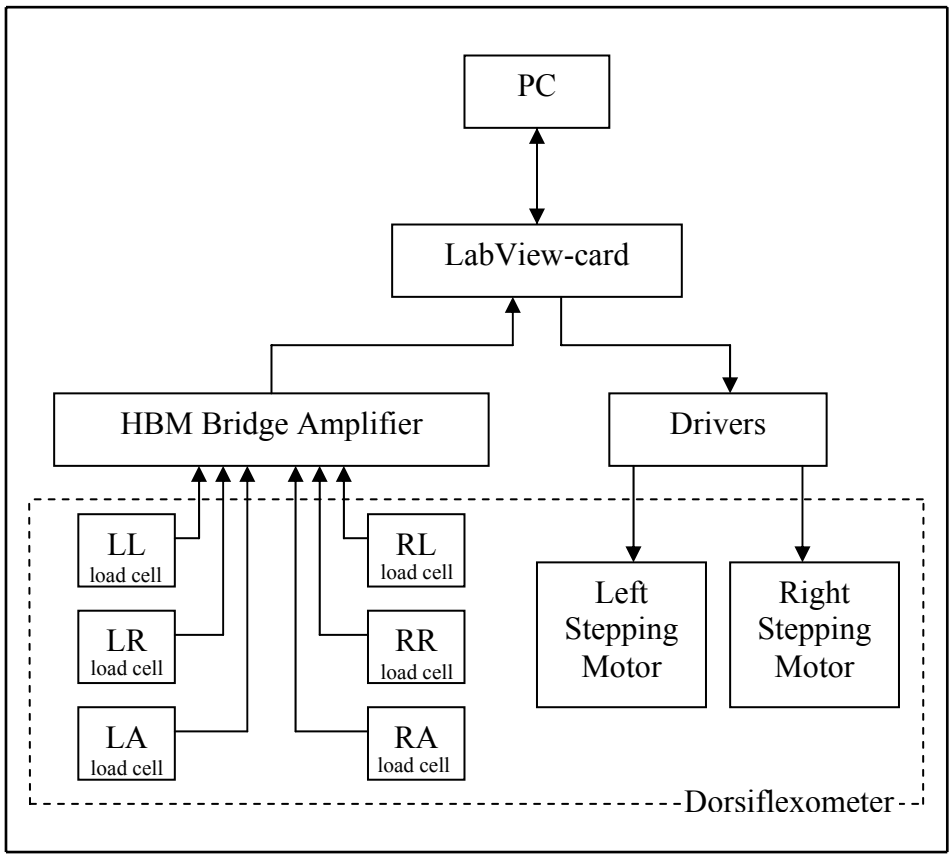

Figure 5.1: Block diagram of experimental set-up 1

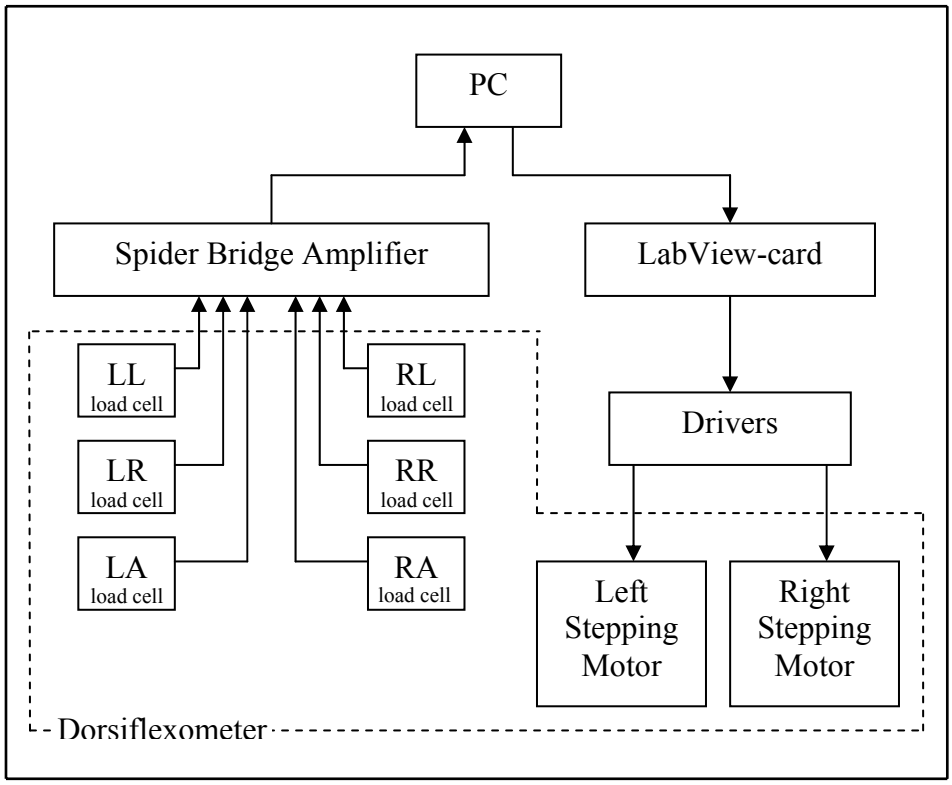

Figure 5.2: Block diagram of experimental set-up 2

For both these set-ups, four distinct parts exist: the Dorsiflexometer, the drivers, the bridge amplifier (HBM Bridge Amplifiers in set-up 1 and the Spider in set-up 2) and the personal computer (PC). A photograph of the experimental set-up 1 is presented in Figure 5.3. The four main parts of the set-up are indicated. Each of the four main parts will be discussed in the following sub-sections. Reasons for the two set-ups used will be discussed in Section 5.3.

5.1.1 The Dorsiflexometer

This is an important part of the experimental set-up (see Figure 5.1, 5.2 and 5.3). This is the device that had to be manufactured and assembled in order to test human subjects. In actual fact, the name, *Dorsiflexometer*, is the name for the entire set-up, but for this section, the name *Dorsiflexometer* will be used for that part of the experimental set-up indicated by Figure 5.3 as the Dorsiflexometer. The Dorsiflexometer consists of the safety railing, two force platforms, two tiltable platforms and two stepper motors.

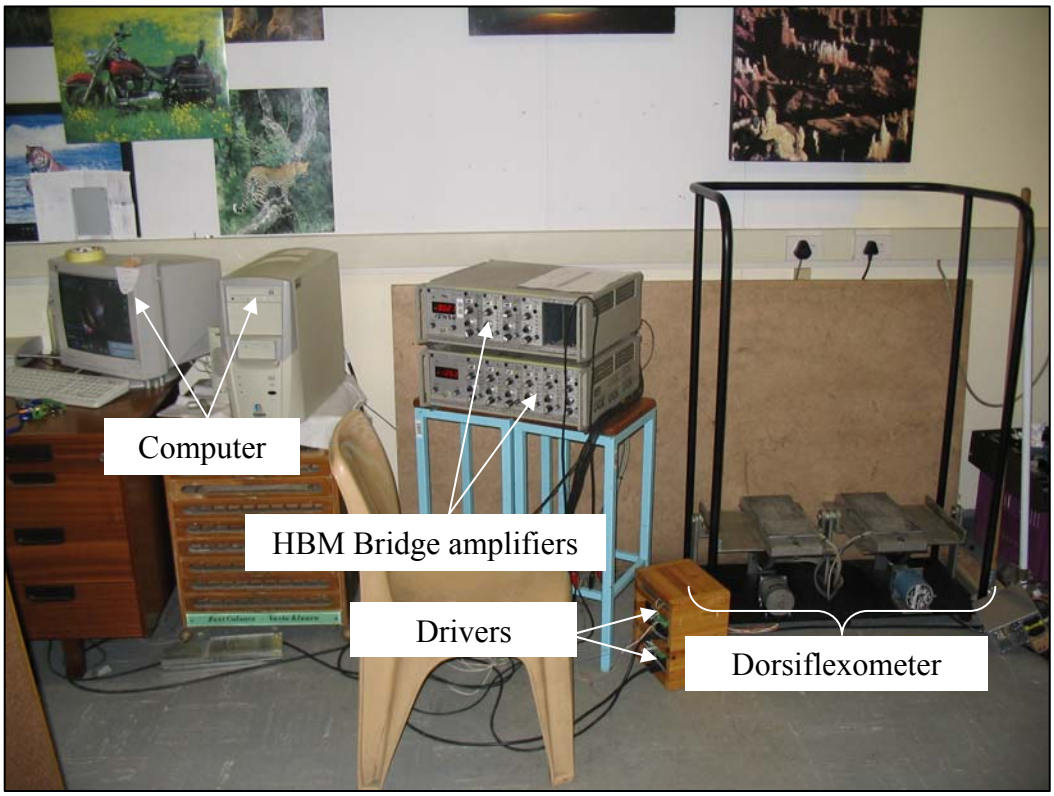

Figure 5.3: Photograph of experimental set-up 1

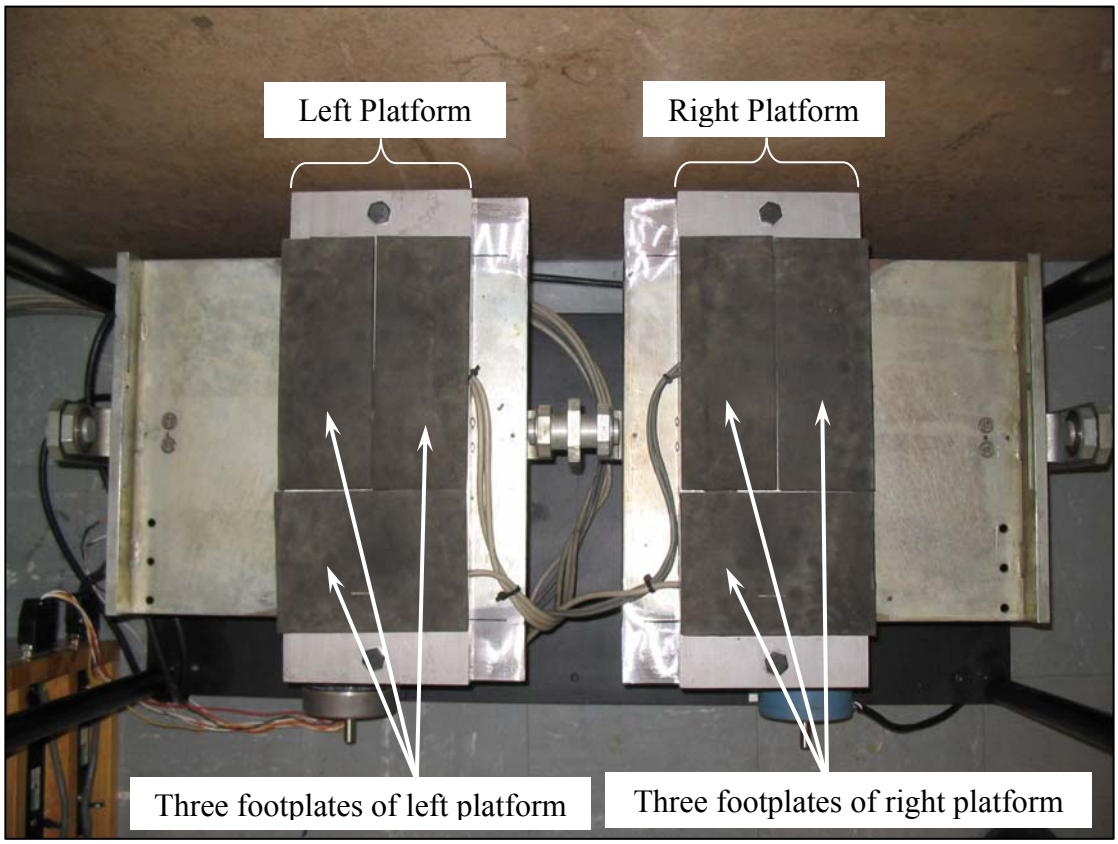

Figure 5.4: The three footplates of each force platform (Figure 4.4 repeated for convenience)

Each of the two platforms is equipped with three separate footplates, each mounted on a load cell. These load cells are the sensory part of the experimental set-up.

5.1.2 The Drivers

The drivers are used to drive the stepping motors on the Dorsiflexometer. These drivers respond to signals coming from the LabView-card connected to the PC. The signals coming form the LabView-card are digital signals (1 = 5 V and 0 = 0 V). The drivers (model PK2 Packaged Stepper Drive from Parker Hannifin Corporation) work on 12 V signals. Therefore, a small PC-board had to be prepared to convert the 5 V signal to a 12 V signal. This was done according to the following diagram (Figure 5.5).

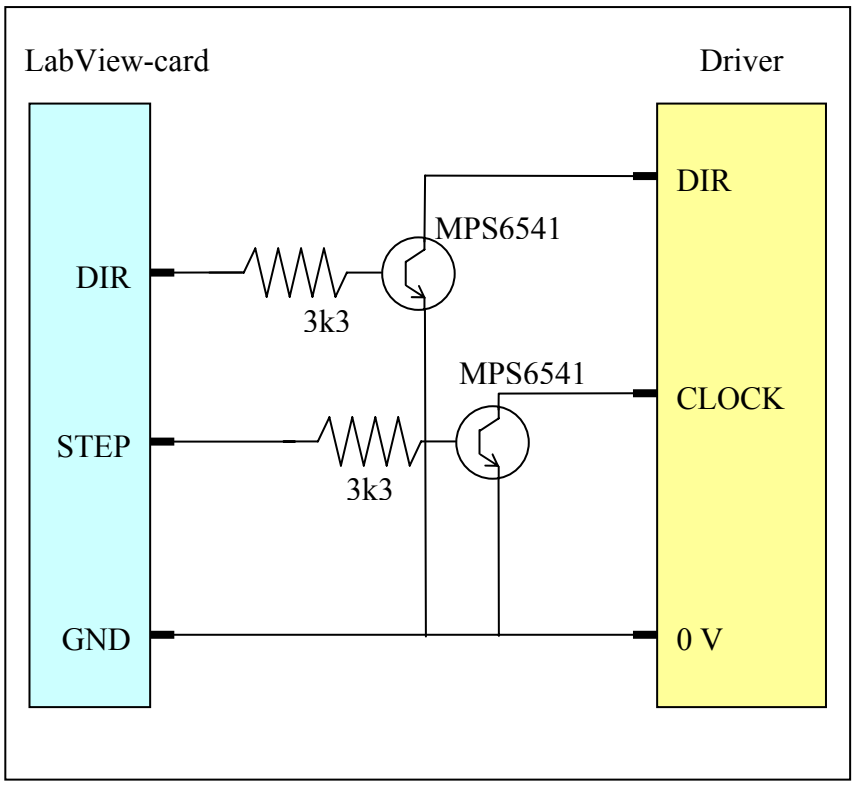

Figure 5.5: Diagram showing the wiring of the driver to the LabView-card

In order to calculate the angular velocities ($\dot{\delta}$) of the platforms when tilting on the 'slow' setting, the angular displacement, during two seconds of tilting, of both platforms were measured experimentally. Table 5.1 shows the calculated angular velocities of the platforms. These angular velocities were used during the experiment. Note that the two angular velocities of the platforms are different. This is deemed not a problem, since the function of the platforms is only to perturb the subject so that the subject undergoes a balanced dorsiflex motion.

Table 5.1: Measured angular velocities of the platforms

Platform	δ [degrees]	δ [rad]	Time [s]	$\dot{\delta}$ [rad/s]
Left	9.7	0.1693	2	0.08465
Right	7.6	0.1326	2	0.0663

5.1.3 Bridge Amplifiers

Two HBM Bridge Amplifiers were used in the initial experimental set-up (see Figure 5.1 and Figure 5.3). Another bridge amplifier (the Spider) was used during later testing in experimental set-up 2. This was done to eliminate some of the HBM Bridge Amplifiers' associated problems. These problems include drifting, manual zeroing before every test and not being sensitive enough. These factors will be discussed in more detail in Section 5.3 (Data Acquisition Systems).

5.1.4 Personal Computer

In both experimental set-ups, the PC serves as the means to store data acquired from the bridge amplifier as well as to send data (in both experimental set-ups, this is realises with digital signals to drive the stepping motor drivers). Data is sent by means of a LabView-card and collects data by using the LabView-card (set-up 1) or the Spider (set-up 2). The data acquired is stored for analytical purposes.

LabView is a graphical programming language that uses icons to create applications. It makes use of dataflow programming (National Instruments). In LabView, the user builds a user interface by using a set of tools and objects. The user interface is known as the front panel. Code can then be added using graphical representations of functions to control the front panel objects. The block diagram contains this code.

5.2 Calibration

Two types of calibration procedures were undertaken: a static and a dynamic calibration. The static calibration is necessary in order to know what force is being

applied to the force platform. The dynamic calibration is necessary to determine how fast the load cells respond to a suddenly applied load.

5.2.1 Static Calibration

The static calibration involved three main steps, namely zeroing the footplates, taking readings of the forces with different masses and obtaining the calibration curves. In the first step, the software program recorded 100 samples at 40 000 samples per second with no mass on the specific footplate. This data was stored and used to obtain the mean and standard deviation of the samples.

The static sensitivity (N/Volt) of each of the load cells was determined by placing five known masses on each of the six footplates and measuring the amplifier voltage. The voltage was read using LabView by taking the average of 100 samples that were sampled at 40 000 samples per second. Figure 5.6 presents the calibration curve for one such footplate.

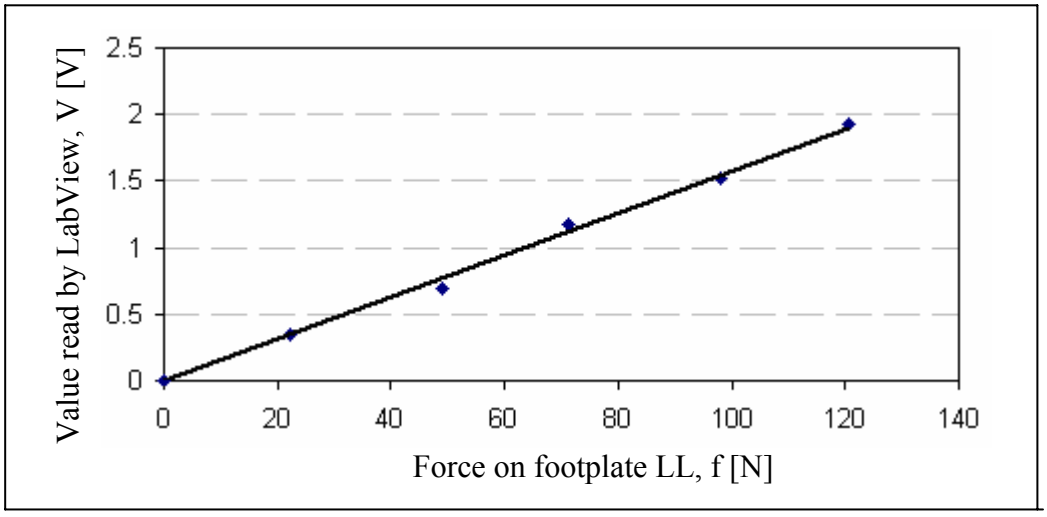

Figure 5.6: Calibration curve for the LL-load cell

From Figure 5.6, the sensitivity of footplate LL is given by the value 63.29 N/Volt with a R^2-value of 0.9961. Therefore, to determine the force applied to this specific platform, the voltage value read by LabView should be multiplied by 63.29. All the load cell sensitivities, σ_s, are given in Table 5.2. (It is evident that a lower σ_s-value denotes a more sensitive load cell.)

Table 5.2: Footplate sensitivities

Load Cell	σ_s	R^2
LL	63.29	0.9961
LR	40.65	0.9578
LA	46.95	0.9998
RL	47.17	0.9957
RR	57.47	0.9964
RA	47.39	0.9992

5.2.2 Dynamic Calibration

In the dynamic calibration process, the dynamic response time of the platforms were checked. The faster sampling takes place, the faster the dynamic response of the machine needs to be. The way in which dynamic testing was done, was by dropping a 0.125 kg mass from a height of 50 mm above the platform and measuring the platform's response – see Figure 5.7. The rise time, t_r, is the important parameter here. For the Dorsiflexometer to achieve its goals, this rise time needs to be as small as possible. In this test done, t_r is within a few milliseconds. It is difficult to determine this value exactly since it is directly dependant on the sampling rate. In this little experiment, the sampling rate was 100 samples per second. Therefore, the rise time of the sensor is less than 10 ms. This value is deemed within appropriate boundaries (refer to Appendix C).

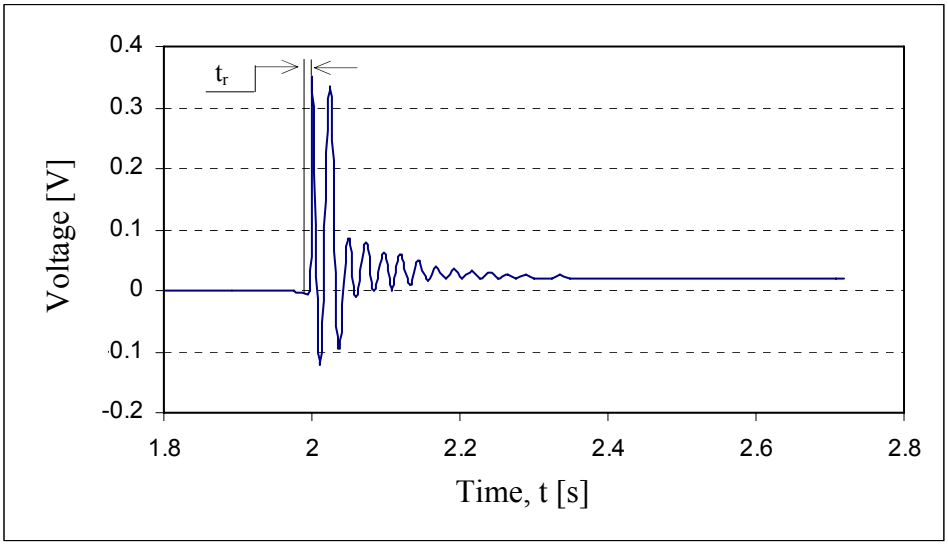

Figure 5.7: Dynamic response of loadcell LL.

Also visible in Figure 5.7 is the 300 ms it takes for the load cell to settle after the mass was dropped. This delay is not desirable, though there is not much to be done to this

problem since the only solution is to incorporate very expensive load cells – which also only reduce that delay time to 75 ms (Online Website).

5.3 Data Acquisition Systems

Two data acquisition systems were used, as shown in Figures 5.1 and 5.2. For the first set of tests, the two HBM Bridge Amplifiers were used to amplify the load cell signals that were then measured with LabView (set-up 1). Interest arose as to how much noise was associated with this set-up. This led to the HP Datalogger being used for comparison. Finally, the Spider Bridge Amplifier was used for data capturing for a second set of tests, hence set-up 2. These data acquisition systems will be described and compared in the following subsections. All the graphs presented in Section 5.3 are for zero mass on Platform LL (the left platform's top left footplate).

5.3.1 Computer Card (LabView and HBM Bridge Amplifiers)

Figures 5.8 to 5.10 are the results of using set-up 1 (given in Figure 5.1) with LabView measuring at 30 000, 1 000 and 10 samples/s respectively. Noise is very apparent in Figure 5.8. The SNR sampling at 30 000 samples/s is 25.1 and not within specification (see Section 4.3.1 for specification).

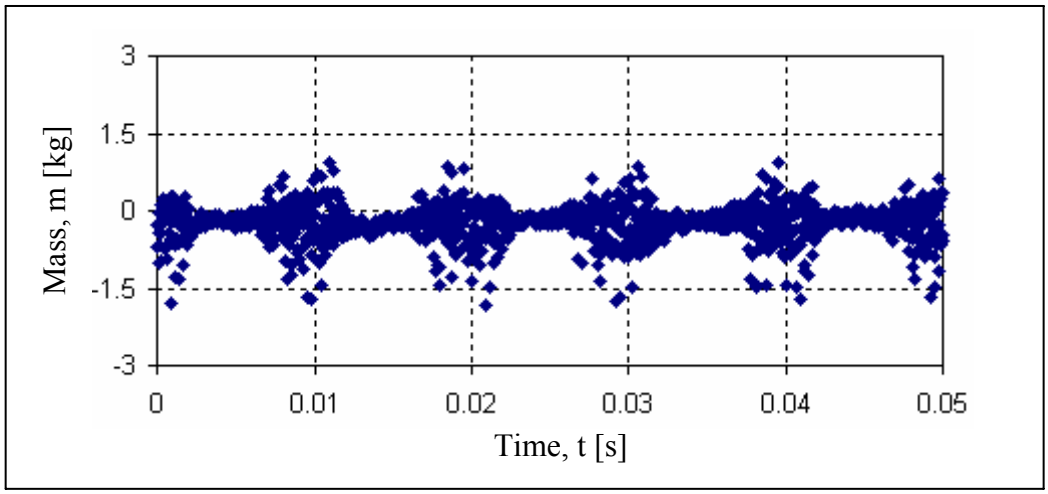

Figure 5.8: Platform LL with no mass supported (LabView at 30 000 samples/s)

The graph presented in Figure 5.9 is for 1 000 samples/s and indicates the same SNR as that of Figure 5.8. Figure 5.10 is for 10 samples/s and the resulting SNR ≈ 38.1. From this it is concluded that decreasing the sampling rate does not proportionally decrease the noise in set-up 1.

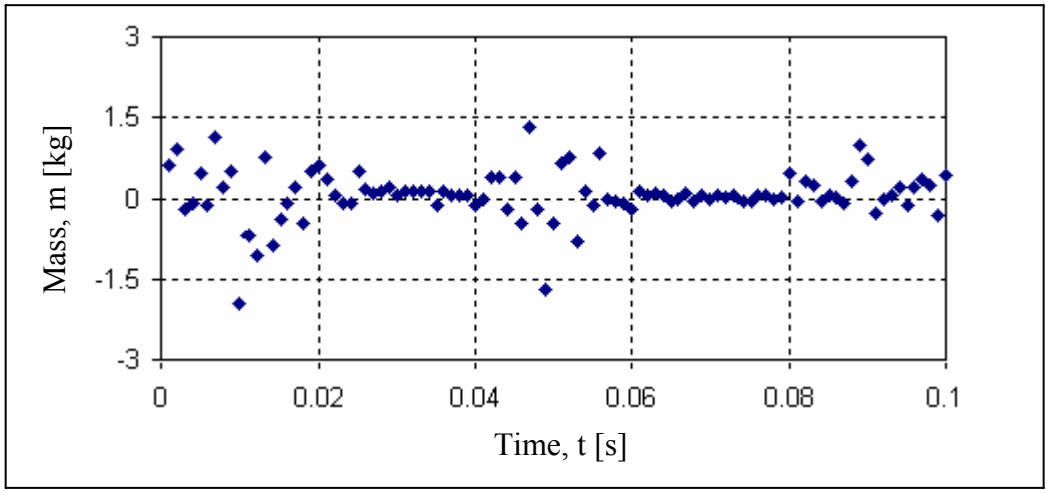

Figure 5.9: Platform LL with no mass supported (LabView at 1 000 samples/s)

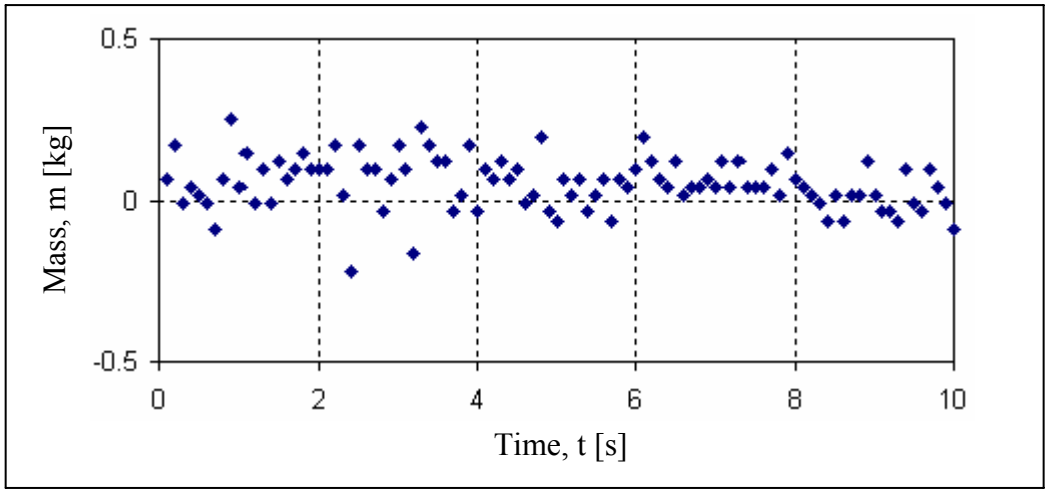

Figure 5.10: Platform LL with no mass supported (LabView at 10 samples/s)

To reduce the noise, an averaging technique was used in analysing the data. This technique works with the mean of either 10 or 100 sampled data points. Therefore the number of points to be used in analysing the data ('useful' data points) is reduced by either 10 or 100. An average of 100 samples for every 'useful' data point for the same data as that presented in Figure 5.8 is shown in Figure 5.11. Using this method, the 'noise' in the calculated 'useful' data points is reduced to a SNR ≈ 46 (still not within specification).

A problem with using this averaging technique is a reduction in the quantity of 'useful' data points (especially when using the mean of 100 sampled points to produce one point).

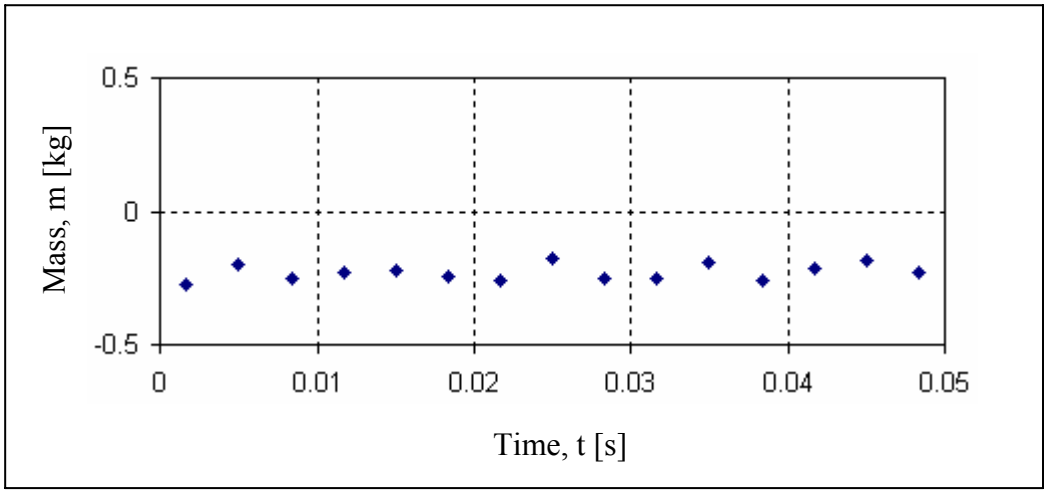

Figure 5.11: Platform LL with no mass supported (average of 100 samples per point for LabView at 30 000 samples/s)

5.3.2 Datalogger (HP)

In an effort to establish the source of the noise, a HP Datalogger was used instead of the two HBM Bridge Amplifiers and the LabView-card. The HP Datalogger's maximum sampling rate is only six samples/s. Therefore, it was not a suitable alternative for the HBM Bridge Amplifiers-LabView-combination. Figure 5.12 gives the values measured with the HP Datalogger (SNR ≈ 68). This is within specification.

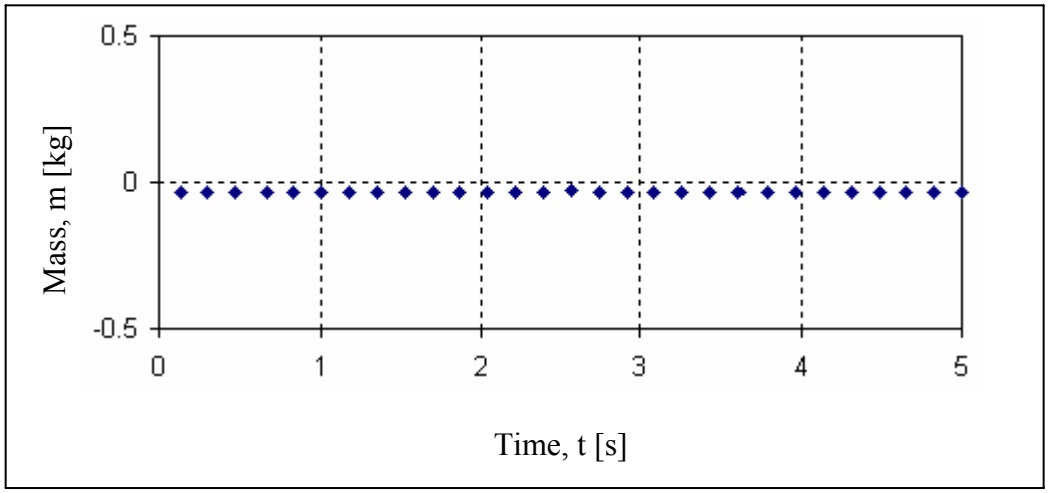

Figure 5.12: Platform LL with no mass supported (HP Datalogger at 6 samples/s)

5.3.3 Spider

For the second set of tests, a Spider Bridge Amplifier replaced the two HBM Bridge Amplifiers and the LabView-card (set-up 2 given in Figure 5.2). The Spider was

connected directly to the PC (using a Catman software program) and therefore LabView was not necessary for measuring the amplified signals – though still important since it sends the appropriate signals to the two stepping motors. Resulting graphs are presented in Figures 5.13 and 5.14.

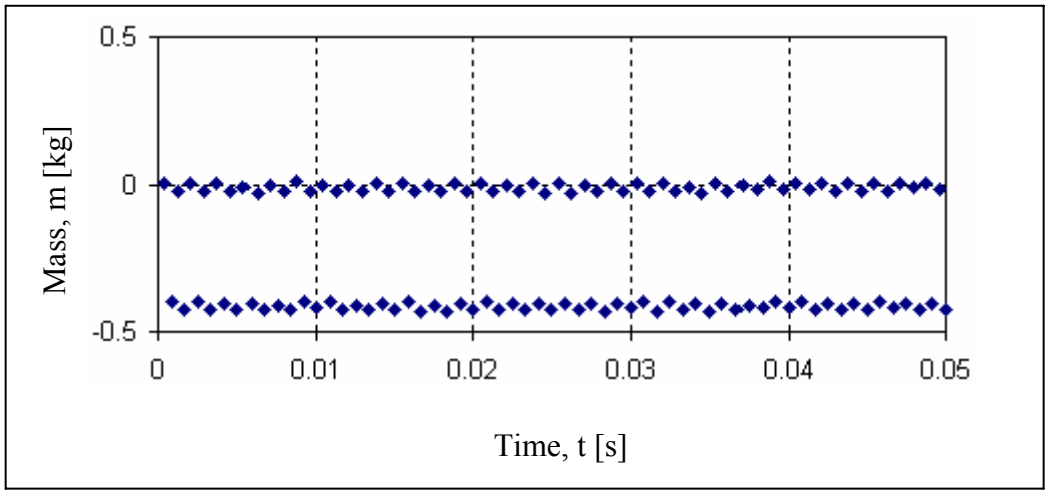

Figure 5.13: Platform LL with no mass supported (Spider at 2 400 samples/s)

The graph presented in Figure 5.13 indicates discrete oscillation between two values. This is the result of analogue-to-digital conversion within the Spider Bridge Amplifier. This oscillation has a magnitude of approximately 0.45 kg and hence corresponds to a SNR ≈ 40.

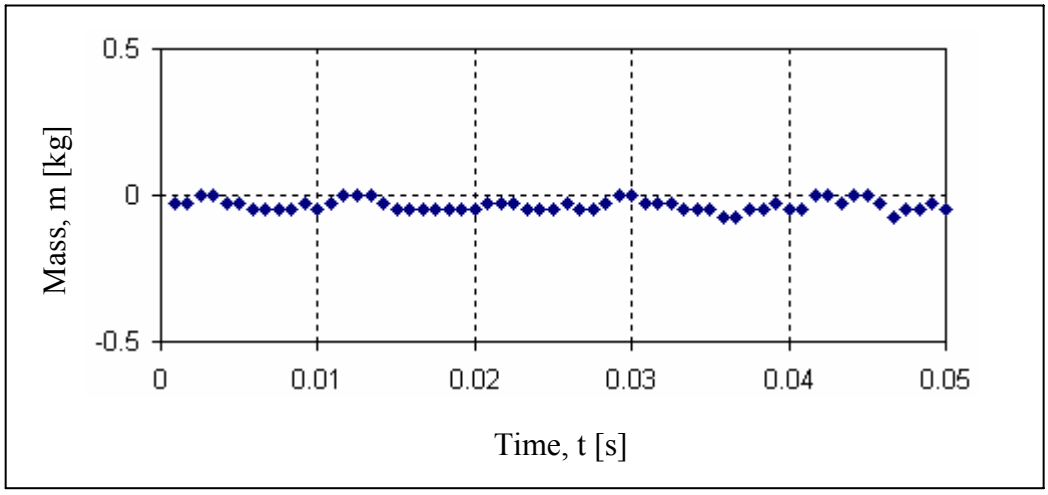

Figure 5.14: Platform LL with no mass supported (Spider at 1 200 samples/s)

The magnitude of the oscillation, present in Figure 5.13, reduces significantly with a decrease in sampling rate – see Figure 5.14. Here the oscillation's magnitude is a mere 0.019 kg, which results in a SNR ≈ 66.5. This is within the specification.

Therefore, it is concluded that set-up 2 is the better of the two set-ups. Reasons are the better SNR, no manual zeroing and no drifting (two other problems associated with the HBM Bridge Amplifiers used in set-up 1).

5.4 Experimental Procedures

This section describes the testing and analysing procedures. The testing subsection describes the computer program used (LabView) to perform the test as well as stating briefly what was expected from the test subjects. The analysing subsection deals with the computer program (visual basic) written for analysing the raw data.

5.4.1 Test Procedure

The LabView program written for testing human subjects is started and the LabView program's "front panel" appears on the screen (Figure 5.15).

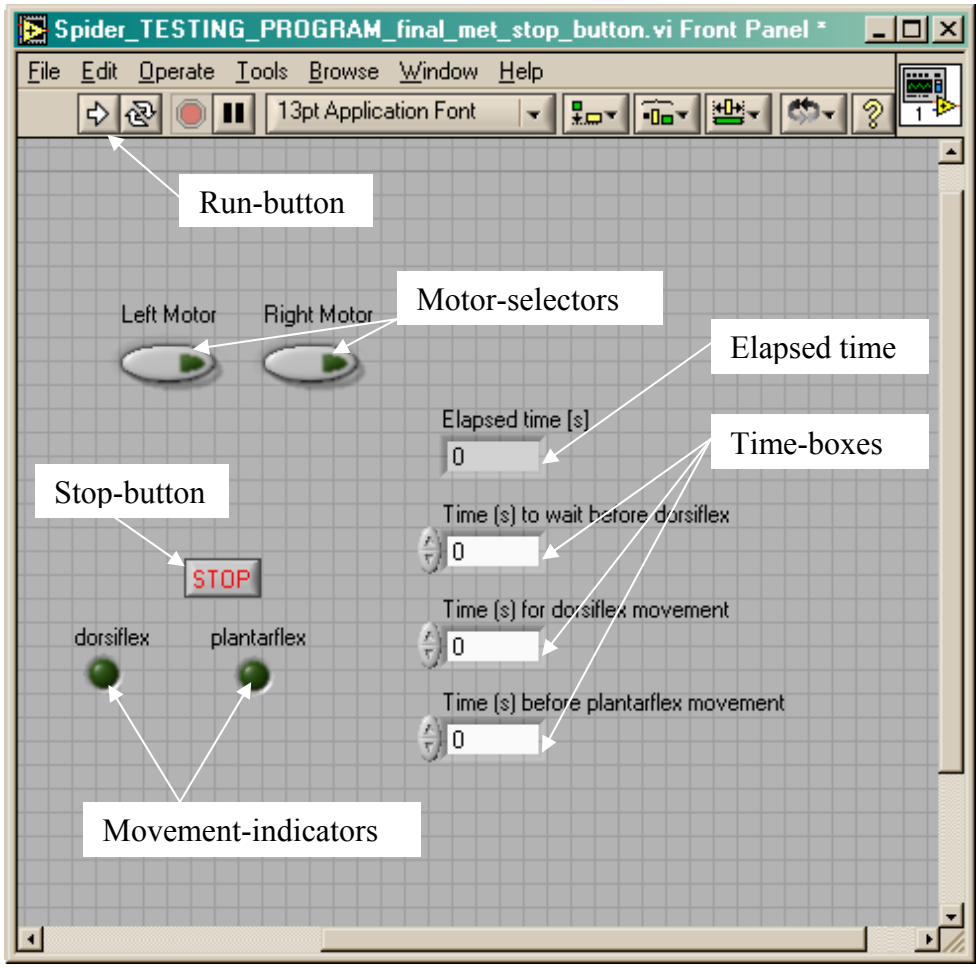

Figure 5.15: LabView program's front panel

The ‘Motor-selector’ (see Figure 5.15) determines whether or not the specified motor will rotate the corresponding platform during the test. For all tests done, both ‘Motor-selectors’ were selected, causing both platforms to rotate simultaneously. The ‘Time-boxes’ determine the execution of the program. All the times are set to two seconds (for both test set 1 and 2). This means that, after the ‘Run’-button is pressed, the platforms remain stationary for two seconds, then tilt (dorsiflex-direction) for two seconds stops tilting and finally remain in the tilted position for another two seconds (after this, the platforms return to the starting position by tilting in the opposite direction – the plantarflex direction). LabView takes a continual 30 000 samples/s per channel for set-up 1 (test set 1), while the Spider logged 1 200 samples/s for set-up 2 (test set 2) for the first six seconds. This six seconds consist of the following movements: two seconds before dorsiflexion (BD), two seconds during dorsiflexion (DD) and two seconds after dorsiflexion (AD).

To start the test sequence, the ‘Run’-button is pressed. However, the time (in seconds) has to be entered for the three time-boxes and both ‘Motor-selectors’ must be selected before pressing the ‘Run’-button. The ‘Movement-indicators’ (Figures 5.15 and 5.16) shine depending on the movement executed by the platforms. The ‘Elapsed time’-box (Figure 5.15) indicates the amount of time, in seconds, elapsed after the Run-button was pressed – see Figure 5.16.

The ‘stop-button’ can be pressed at anytime to stop the program from executing. Figure 5.16 shows the front panel in executing mode (note that the ‘Run’-button indicates that the program is “running”).

The preceding paragraph only discusses the use of the LabView program written to test a human test subject during the experiment and logging the sampled data. Before the ‘Run’-button (see Figure 5.15) is pressed and data acquisition starts, the test subject is asked to stand with the left foot on the left platform, and the right foot on the right platform, with arms relaxed, looking straight ahead. The subject is required to stand still until after the platforms returned to the starting horizontal position. After this, the subject can step off the platforms.

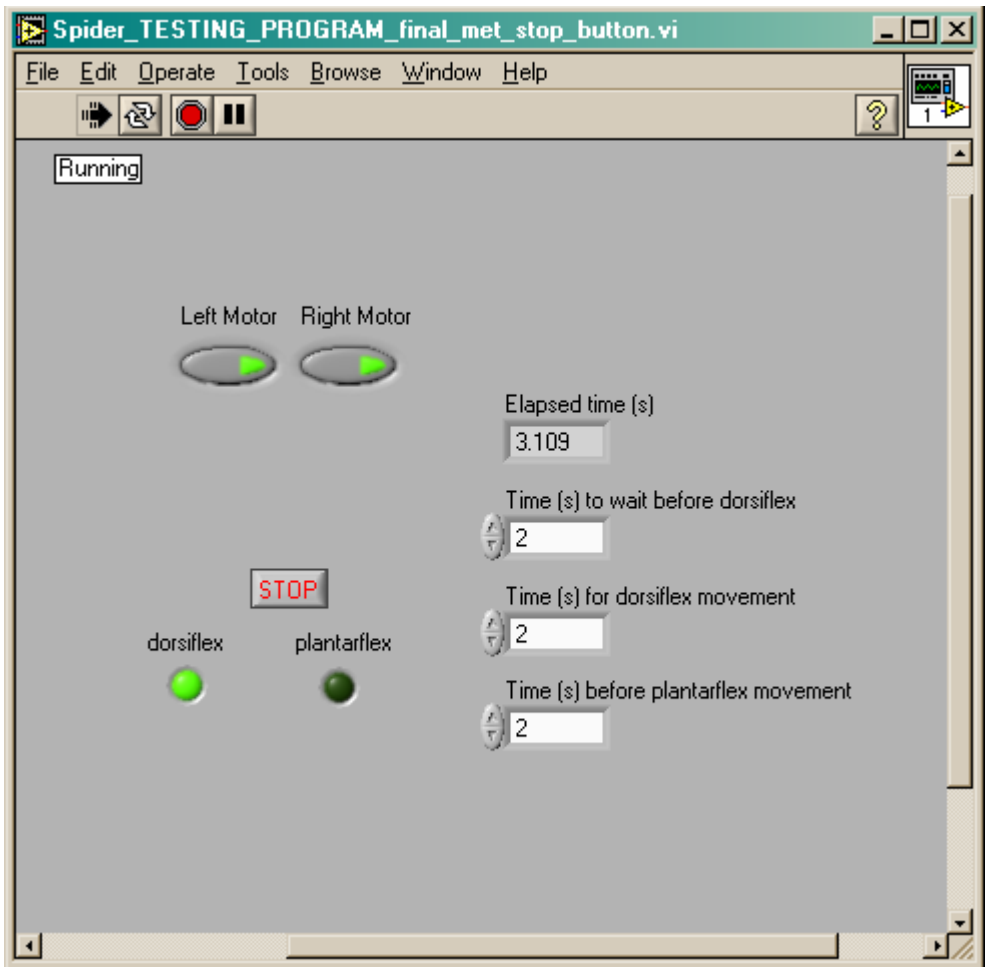

Figure 5.16: LabView program's front panel (executing)

5.4.2 Analyses Procedure

Data captured and stored by the PC during testing, is analysed using a Visual Basic program. In Appendix A the equations used in the computer program is derived (Note that V_{tot}, as defined and used in Appendix A, has magnitude and position on a two-dimensional plane. V_{tot}'s coordinates are that of the position of the normal component of the resultant force created by the subject standing on the platform. Plotting the position of V_{tot} with respect to time therefore yields a graph of the resultant force's normal component's movement during a specified time). Sample calculations are also presented in Appendix A.

The computer program's main window is shown in Figure 5.17 (note that the program has executed already). By pressing the 'START'-button, data analyses start. Detailed use of this program will not be discussed here. The program has a help-file –

accessible by pressing the 'HELP'-button – which explains how one uses the program to analyse captured raw data.

In this section, only some of the graphs that can be produced by this analysing program will be shown and discussed. Various buttons are present on the program's main window, as well as on the window that opens when the 'Press to see SCALED graph for comparative study' is pressed. These buttons are necessary to present different analysed data in an understandable, user-friendly manner.

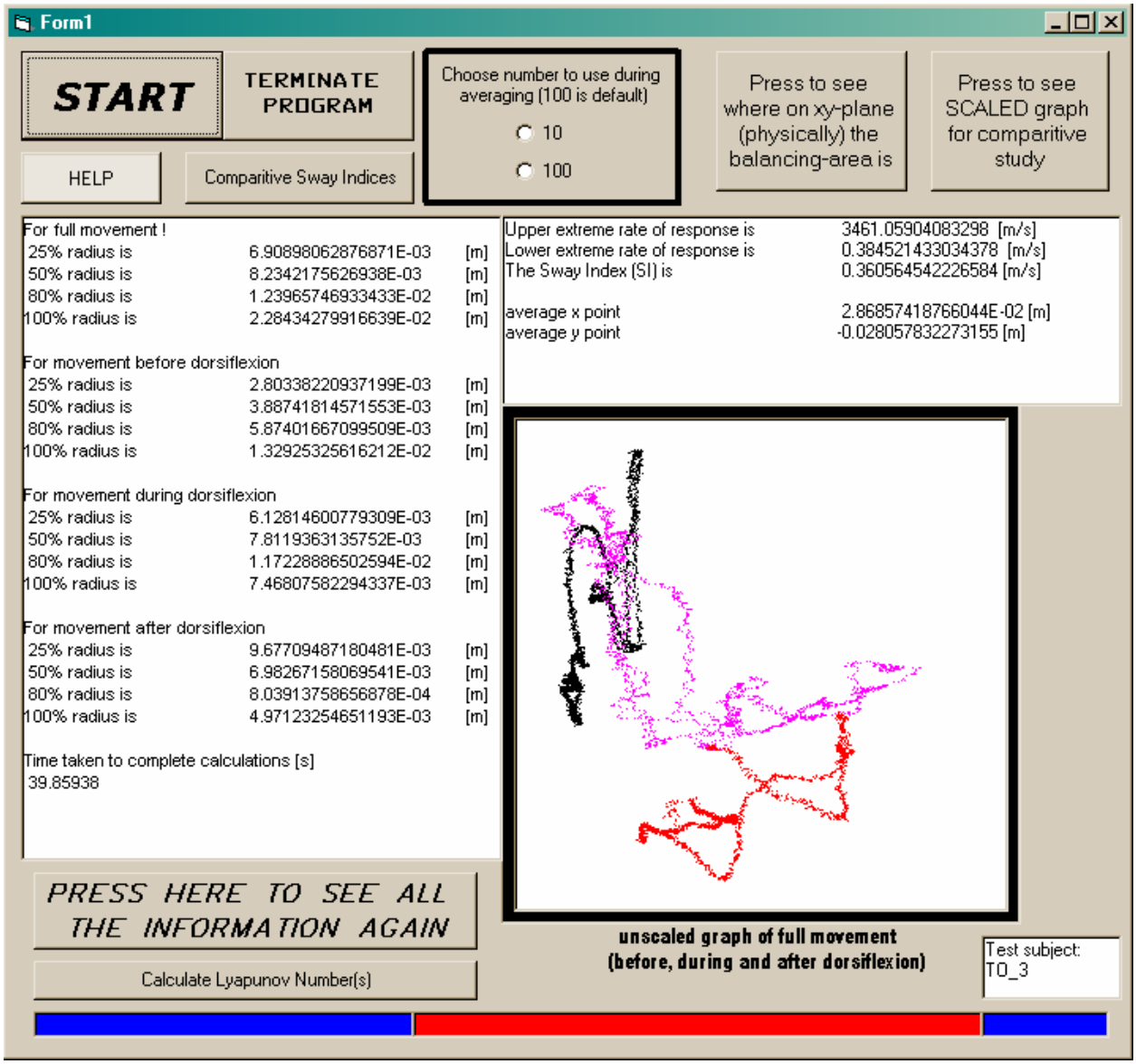

Figure 5.17: The executed Visual Basic program for test subject TO_3

The graph in Figure 5.17 indicates the movement of the normal component of the subject's resultant force as a function of time for the duration of the test (abbreviated TM, for Total Movement). The rest of the information displayed in Figure 5.17 is

explained in Appendix A – which includes how the Lyapunov Numbers and the Sway Index are calculated. The subject tested to obtain the displayed results presented in Figure 5.17 is labelled TO_3. Further analysis of the data is now possible by pressing other buttons on the screen. The 'Press to see SCALED graph for comparative study'-button, for example, opens another window, and when the 'Click to see TOTAL MOVEMENT'-button is pressed on this window the graph shown in Figure 5.18 is presented.

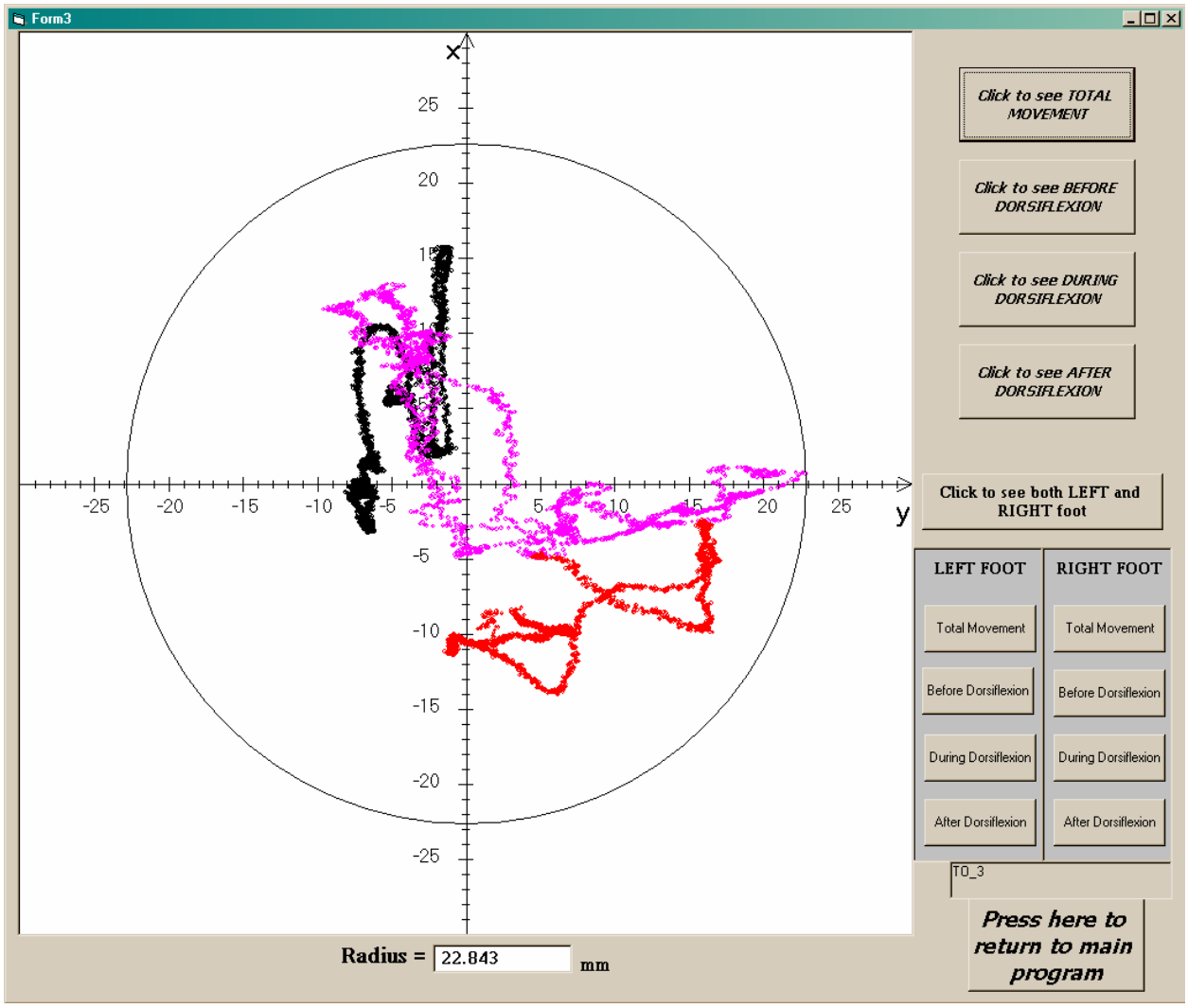

Figure 5.18: Secondary window of the Visual Basic Program displaying the TM of test subject TO_3

Figure 5.18 shows the graph of test subject TO_3 while standing on both platforms for the test's duration. In the graph, the movement of the resultant forces normal component is plotted. Henceforth, all the graphs presented in Section 5 and 6 are for the movement of the normal component of the subject's resultant force on either one or both of the platforms. The only difference being the specified time during testing for

which the movement is plotted. This can be for the full six seconds of the test (TM), as presented in Figure 5.18, or parts of the test – be it before dorsiflexion starts (BD), during dorsiflexion (DD) or after dorsiflexion (AD). These graphs, depicts the different parts of the test sequence presented (including Figure 5.18), and is colour-coded for easy classification. The black plot is the subject's movement during the two seconds before dorsiflexion starts, the magenta plot is the movement during the two seconds the platforms cause dorsiflexion by tilting and the red plot is the movement during the two seconds after the platforms stopped tilting.

The graph shown by Figure 5.18 can be enclosed by a circle. The point of the circle is the average x- and y-point calculated for the movement presented (therefore for the whole six seconds of the test), and the furthest point calculated defines its radius. This is one parameter used to compare different test subjects' analysed results. The circle's radius is displayed in the 'Radius = '-box.

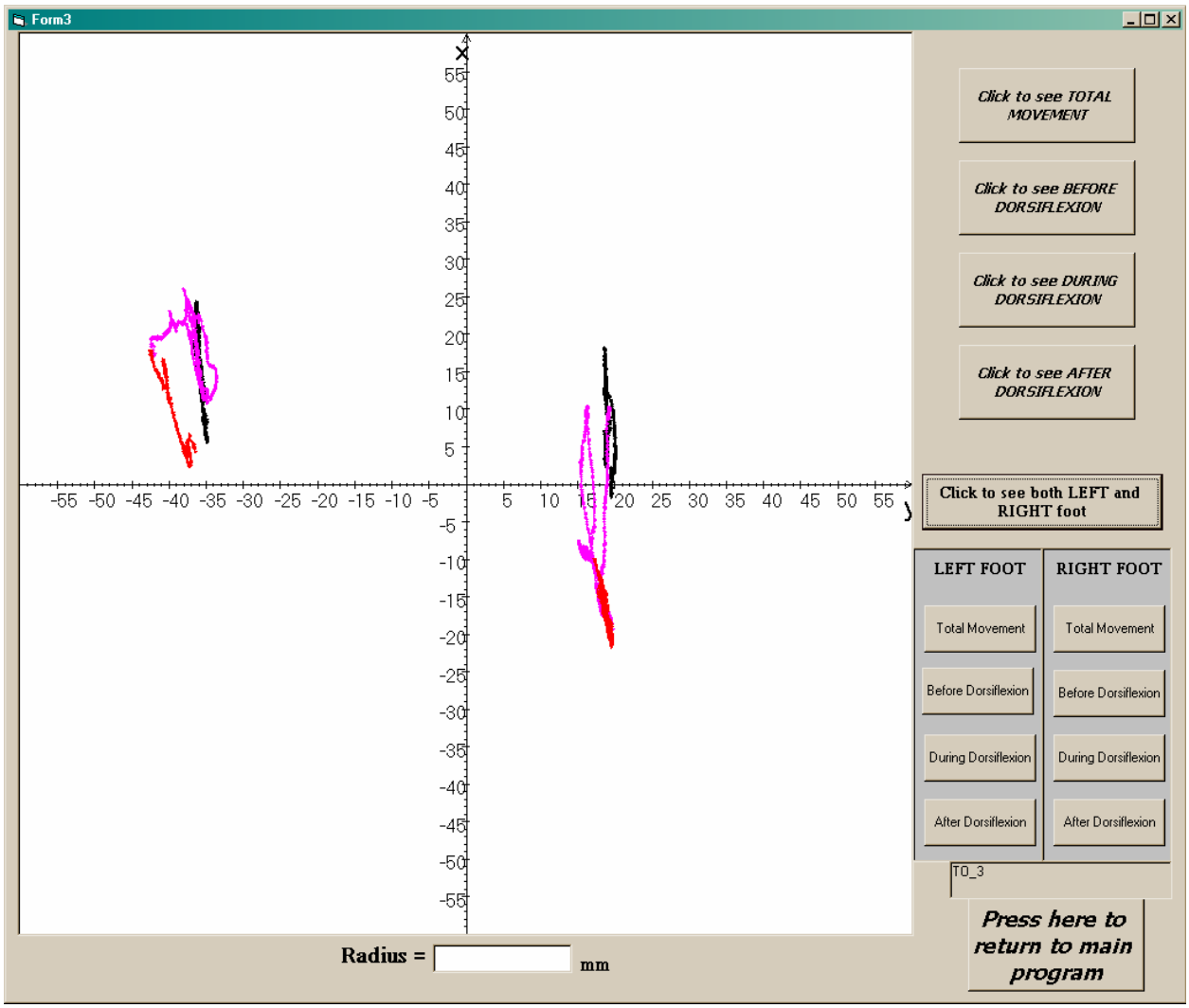

Figure 5.19: TM of the left and right foot of subject TO_3

Figure 5.19 is the graph showing the movement of the resultant force's normal component of the left and right platform respectively. This means that the movement of the left (V_L as defined in Appendix A) and right foot's (V_R as defined in Appendix A) normal component of the respective resultant force, applied to the left and right force platform, is plotted. This graph is obtained by pressing the 'Click to see both LEFT and RIGHT foot'-button. Note that the right foot does more compensating than the left in this particular subject's test. Detailed explanations of the various buttons in Figures 5.17 and 5.19 are explained in Appendix F.

6 Results

In this section, the results for the various tests done on the Dorsiflexometer are presented. Since two experimental set-ups were used, two sets of experiments were done – one on each of the experimental set-ups. These experiments were done explicitly to verify the ability of the Dorsiflexometer to distinguish between good balance and balance impairment. To induce slight balance impairment the two experiments used different methods. The first of the two experiments subjected the test subjects to the intake of alcohol. In the second experiment a close and open eyes test was conducted. The experiments were done according to the experimental procedures explained in Section 5.4.

The tabulated results in Section 6 display the three main calculated parameters. These parameters are the Sway Index (SI), Lyapunov's coefficient/number (LN or λ) and the radius of the circle which confines the movement of the normal component of the subject's resultant force. All these parameters are calculated for the four parts of the movement (as explained in Section 5.4.2 and Appendix A). The subscripts TM (total movement), BD (before dorsiflexion), DD (during dorsiflexion) and AD (after dorsiflexion) are used to identify which part of the test's results is displayed, while the abbreviations TM, BD, DD and AD (not subscripts) are used to denote the calculated radius confining the movement of the normal component of the resultant force for the different parts of the test.

The equations used to calculate these parameters are given in Appendix A on page A-18. The following two equations are presented for convenience:

$$SI = \frac{\sum_{i=1}^{n-1} \frac{\Delta l_i}{\Delta t}}{(n-1)} \tag{6.1}$$

And

$$\lambda = \lim_{n\to\infty}\left[\frac{1}{n}\sum_{i=0}^{n-1} \ln\left| f'(x\ , y_i)\right|\right] \tag{6.2}$$

6.1 Experiment 1: Using Experimental Set-up 1

Experiment 1 was done on 17 November 2004. In this experiment, 15 healthy subjects were tested. Test subjects were between the ages of 18 and 26 and were of mixed gender. This was done in order to obtain a 'normal' balance value for each or any of the said parameters. In Table 6.1, these 17 subject's parameters are presented. The first four columns of Table 6.1 display the Sway Index, while the last four columns contain the calculated radii. The bottom three columns of Table 6.1 denote the average, the standard deviation and the R^2 value respectively.

Table 6.1: Comparing SI and Radius parameters for different test subjects in Experiment 1

Test no.	$SI_{TM} \times 10^{-3}$	$SI_{BD} \times 10^{-3}$	$SI_{DD} \times 10^{-3}$	$SI_{AD} \times 10^{-3}$	TM	BD	DD	AD
#	[m/s]	[m/s]	[m/s]	[m/s]	[mm]	[mm]	[mm]	[mm]
1	3.6	1.0	4.2	0.3	21.0	14.6	1.1	1.3
2	2.0	4.2	1.3	0.4	6.7	4.2	2.6	3.7
3	2.4	4.3	2.3	7.0	47.7	36.7	2.0	1.6
4	4.1	5.2	1.7	5.5	5.7	4.9	1.3	3.7
5	5.6	13.2	1.9	1.5	3.4	0.7	1.6	1.2
6	4.2	5.6	3.5	6.4	43.8	27.3	7.4	1.6
7	11.4	26.4	2.1	1.6	43.8	23.1	23.3	13.3
8	4.3	6.8	2.7	3.3	5.6	1.8	5.2	1.2
9	1.5	1.4	2.2	1.1	47.8	20.0	21.3	8.9
10	16.1	41.1	5.9	1.5	21.1	13.6	6.9	0.2
11	19.9	2.6	20.9	12.4	4.9	2.3	0.6	3.2
12	3.2	3.8	4.8	1.1	18.0	9.3	2.5	12.3
13	17.7	26.9	18.3	7.9	20.1	7.0	8.3	2.2
14	5.1	10.4	4.7	0.1	9.0	5.0	6.2	2.5
15	3.4	5.1	3.1	2.0	7.0	4.8	3.4	2.4
Average	7.0	11.0	5.0	3.0	21.3	12.2	6.5	4.1
St. dev.	6.0	12.0	6.0	4.0	17.3	11.0	7.2	4.2
R^2	0.15	0.07	0.26	0.01	0.04	0.04	0.11	0.01

Table 6.2 contains the Lyapunov exponents calculated for the same tests as presented in Table 6.1. Since the calculated Lyapunov exponents are relatively highly negative, it denotes chaotic behaviour. Chaotic behaviour causes standard statistical methods for analysing to be inconclusive. This implies that every result has to be treated individually.

Table 6.2: Comparing Lyapunov coefficient parameter for Experiment 1

Test no. #	LN_{TM}	LN_{BD}	LN_{DD}	LN_{AD}
1	-7.63	-5.69	-8.32	-8.89
2	-6.80	-5.93	-6.95	-7.81
3	-6.54	-5.77	-6.59	-7.27
4	-5.85	-5.48	-6.61	-5.47
5	-5.96	-4.69	-6.39	-6.78
6	-5.65	-5.31	-5.77	-5.86
7	-5.63	-4.06	-6.30	-6.54
8	-5.84	-5.70	-6.05	-5.77
9	-6.72	-7.09	-6.27	-6.80
10	-5.20	-3.34	-5.76	-6.50
11	-4.08	-3.94	-3.86	-4.40
12	-6.25	-5.98	-5.93	-6.83
13	-4.22	-3.76	-4.05	-4.86
14	-6.68	-5.15	-5.78	-9.12
15	-5.99	-5.78	-5.81	-6.40
Average	-5.94	-5.18	-6.03	-6.62
St. dev.	0.95	1.02	1.07	1.31
R^2	0.23	0.06	0.51	0.07

Tables 6.3 and 6.4 present the parameters of tests done on the same subject. This was the same subject that was tested in position number 15 (in Tables 6.1 and 6.2). The subject was asked to be tested at different times of the day over a two-week period. This was done to try and assign a specific value to either one or more of the parameters indicating 'normal' balance behaviour.

Table 6.3: Comparing SI and Radius parameters for the same test subject in Experiment 1

Test no. #	$SI_{TM} \times 10^{-3}$ [m/s]	$SI_{BD} \times 10^{-3}$ [m/s]	$SI_{DD} \times 10^{-3}$ [m/s]	$SI_{AD} \times 10^{-3}$ [m/s]	TM [mm]	BD [mm]	DD [mm]	AD [mm]
15	3.4	5.1	3.1	2.0	7.0	4.8	3.4	2.4
16	8.0	8.8	6.4	8.8	20.7	6.0	6.5	9.7
17	3.9	5.8	4.6	1.4	11.6	7.2	4.5	1.0
18	3.0	5.4	2.7	1.0	7.4	2.9	3.3	1.3
19	2.4	3.5	0.7	3.2	4.9	2.3	0.6	3.2
20	3.1	4.4	1.5	3.4	3.5	3.8	2.1	2.7
21	5.2	4.1	5.0	6.4	11.7	5.7	5.9	4.5
Average	4.0	6.0	4.0	3.0	9.6	4.7	3.8	3.5
St. dev.	2.0	2.0	2.0	3.0	5.8	1.8	2.1	2.9
R^2	0.09	0.59	0.15	0.11	0.13	0.38	0.47	0.35

Table 6.4: Comparing Lyapunov number parameter for the same test subject for Experiment 1

Test no. #	LN_{TM}	LN_{BD}	LN_{DD}	LN_{AD}
15	-5.99	-5.78	-5.81	-6.40
16	-4.99	-5.00	-5.21	-4.75
17	-6.36	-6.07	-5.88	-7.14
18	-6.46	-5.67	-6.28	-7.42
19	-6.77	-6.55	-7.81	-5.95
20	-6.44	-6.43	-6.98	-5.91
21	-5.56	-5.91	-5.53	-5.26
Average	-6.16	-5.82	-6.16	-6.49
St. dev.	0.61	0.55	0.85	1.38
R^2	0.001	0.46	0.18	0.29

Four of the subjects (of those presented in Tables 6.1 and 6.2) then volunteered to take part in another part of this experiment to see whether or not blood alcohol level alters some of these parameters. These four individuals then set out to increase their blood alcohol level systematically and being tested in three stadia of the alcohol intake procedure. The alcohol level of each subject was calculated using the subject's mass – therefore the amount of alcohol intake is divided by the subjects mass and expressed in the unit ml/kg. Results are tabulated in Tables 6.5 and 6.6. Each of the four subjects was tested three times during the alcohol-intake process. The letters A, B and C are used to distinguish between the relative amounts of alcohol levels present in the subject during testing. Tables 6.7 to 6.9 groups the A-, B- and C-parts of Table 6.5 to establish average, standard deviation and R^2 values.

Table 6.5: Comparing SI and Radius parameters for four sober (A), semi-inebriated (B) and inebriated (C) test subjects in Experiment 1

Test no. #		Alcohol level [ml/kg]	SI_{TM} x 10^{-3} [m/s]	SI_{BD} x 10^{-3} [m/s]	SI_{DD} x 10^{-3} [m/s]	SI_{AD} x 10^{-3} [m/s]	TM [mm]	BD [mm]	DD [mm]	AD [mm]
1	A	0.19	3.6	1.0	0.4	0.3	13.7	12.8	0.7	0.2
	B	0.85	4.7	11.0	1.3	1.5	18.9	14.8	1.7	1.5
	C	1.21	4.3	5.7	3.1	4.2	10.1	7.7	3.4	4.7
2	A	0.00	2.0	4.2	1.3	0.4	5.8	4.2	1.5	0.5
	B	0.64	3.5	4.0	3.8	2.6	6.4	3.6	3.6	2.6
	C	1.54	2.8	4.8	2.1	1.6	10.2	5.5	2.9	1.2
3	A	0.00	2.4	4.3	2.3	7.0	5.3	3.2	3	0.9
	B	0.53	1.2	2.3	0.5	0.8	2.2	1.1	0.5	1.2
	C	1.01	1.5	3.0	0.6	0.9	3.2	1.7	0.5	1.0
4	A	0.00	4.1	5.2	1.7	5.5	6.6	4.2	1.2	6.5
	B	0.44	6.1	5.2	5.5	7.6	16.7	5.2	6.9	10.2
	C	0.89	4.1	5.3	3.9	3.1	12.7	4.8	4.3	3.4

Table 6.6: Comparing Lyapunov numbers for four sober (A), semi-inebriated (B) and inebriated (C) test subjects in Experiment 1

Test no. #	Alcohol level [mL/kg]	LN_{TM}	LN_{BD}	LN_{DD}	LN_{AD}
1	A	0.19	-7.63	-5.69	-8.32	-8.89
	B	0.85	-6.28	-4.94	-7.28	-6.62
	C	1.21	-5.83	-6.13	-5.88	-5.50
2	A	0.00	-6.90	-5.93	-6.95	-7.81
	B	0.64	-5.81	-5.78	-5.68	-5.98
	C	1.54	-6.28	-5.86	-6.40	-6.58
3	A	0.00	-6.54	-5.77	-6.59	-7.27
	B	0.53	-7.44	-6.65	-7.81	-8.07
	C	1.01	-7.03	-6.02	-7.94	-7.13
4	A	0.00	-5.85	-5.48	-6.61	-5.47
	B	0.44	-5.55	-5.82	-5.57	-5.26
	C	0.89	-5.61	-5.45	-5.57	-5.81

Table 6.7: Comparing SI and Radius parameters for four sober test subjects in Experiment 1

Test no. #	$SI_{TM} \times 10^{-3}$ [m/s]	$SI_{BD} \times 10^{-3}$ [m/s]	$SI_{DD} \times 10^{-3}$ [m/s]	$SI_{AD} \times 10^{-3}$ [m/s]	TM [mm]	BD [mm]	DD [mm]	AD [mm]
1 A	3.6	1.0	0.4	0.3	13.7	12.8	0.7	0.2
2 A	2.0	4.2	1.3	0.4	5.8	4.2	1.5	0.5
3 A	2.4	4.3	2.3	7.0	5.3	3.2	3	0.9
4 A	4.1	5.2	1.7	5.5	6.6	4.2	1.2	6.5
Average	3.0	3.7	1.4	3.3	7.9	6.1	1.6	2.0
St. Dev.	1.0	1.8	0.8	3.5	3.9	4.5	1.0	3.0
R^2	0.08	0.79	0.60	0.69	0.22	0.90	0.78	0.24

Table 6.8: Comparing SI and Radius parameters for four semi-inebriated test subjects in Experiment 1

Test no. #	$SI_{TM} \times 10^{-3}$ [m/s]	$SI_{BD} \times 10^{-3}$ [m/s]	$SI_{DD} \times 10^{-3}$ [m/s]	$SI_{AD} \times 10^{-3}$ [m/s]	TM [mm]	BD [mm]	DD [mm]	AD [mm]
1 B	4.7	11.0	1.3	1.5	18.9	14.8	1.7	1.5
2 B	3.5	4.0	3.8	2.6	6.4	3.6	3.6	2.6
3 B	1.2	2.3	0.5	0.8	2.2	1.1	0.5	1.2
4 B	6.1	5.2	5.5	7.6	16.7	5.2	6.9	10.2
Average	3.9	5.6	2.8	3.1	11.05	6.18	3.18	3.88
St. Dev.	2.1	3.8	2.3	3.1	8.03	5.99	2.79	4.26
R^2	0.014	0.43	0.28	0.48	0.80	1.00	0.96	0.99

Table 6.9: Comparing SI and Radius parameters for four inebriated test subjects in Experiment 1

Test no. #		SI_{TM} x 10^{-3} [m/s]	SI_{BD} x 10^{-3} [m/s]	SI_{DD} x 10^{-3} [m/s]	SI_{AD} x 10^{-3} [m/s]	TM [mm]	BD [mm]	DD [mm]	AD [mm]
1	C	4.30	5.70	3.1	4.2	10.1	7.7	3.4	4.7
2	C	2.82	4.82	2.1	1.6	10.2	5.5	2.9	1.2
3	C	1.48	2.97	0.6	0.9	3.2	1.7	0.5	1.0
4	C	4.10	5.33	3.90	3.1	12.7	4.8	4.3	3.4
Average		3.2	4.7	2.4	2.4	9.1	4.9	2.8	2.6
St. Dev.		1.3	1.2	1.4	1.5	4.1	2.5	1.6	1.8
R^2		0.04	0.10	0.01	0.13	0.77	0.86	0.96	0.98

Figure 6.1 presents the movement of the normal component of test subject number 2 (from Table 6.1) during the full 6 seconds of the test procedure. The different colours denote the three different parts of the test as stated in Section 5.4.2 (Black is BD, magenta is DD and red is AD).

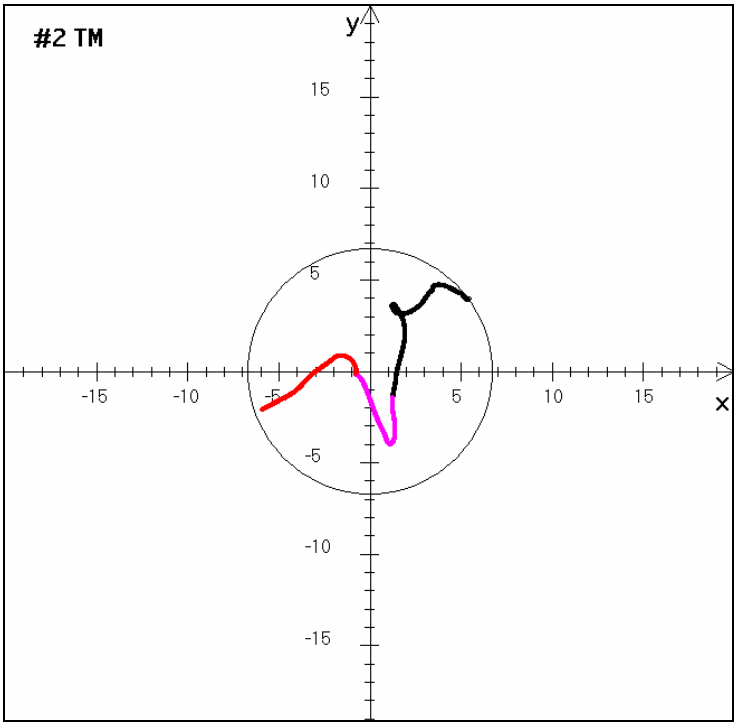

Figure 6.1: TM of subject #6 in Experiment 1

6.2 Experiment 2: Using Experimental Set-up 2

Experiment 2 was conducted on 25 February 2005. This experiment was conducted on experimental set-up 2 and consisted of 10 tests – the first five are of subjects with their eyes open, and the last five are of the same five people but with their eyes closed. This

was done to establish if the Dorsiflexometer can detect slight balance impairment. It has been proven that when standing with closed eyes, a human's sway during quiet stance is a more elaborate than when open (Stephen 2003) – indicating that visual stimuli does play a significant role in balancing. Results are presented in the following two tables.

Table 6.10: Comparing SI and Radius parameters for Experiment 2

	Test #	SI_{TM} x 10^{-3} [m/s]	SI_{BD} x 10^{-3} [m/s]	SI_{DD} x 10^{-3} [m/s]	SI_{AD} x 10^{-3} [m/s]	TM [mm]	BD [mm]	DD [mm]	AD [mm]
Open Eyes	1	361.0	273.6	519.6	377.6	19.2	4.8	16.9	10.1
	2	357.9	274.7	523.7	358.9	23.3	2.9	21.4	9.6
	3	354.5	294.3	504.3	325.2	15.5	5.8	12.2	7.3
	4	358.8	291.3	486.7	366.2	17.1	4.2	14.9	7.1
	5	378.5	316.9	552.7	327.8	19.2	12.2	14.4	10.3
Closed Eyes	1	362.4	295.0	519.7	340.1	25.4	7.6	20.7	18.4
	2	377.0	316.8	516.9	379.2	22.8	8.2	23.6	14.9
	3	360.6	300.2	507.2	335.	22.8	13.3	19.2	11.3
	4	366.5	303.8	512.2	346.8	18.4	6.4	14.8	8.1
	5	388.1	320.2	527.9	384.6	35.2	5.0	13.7	22.2

Table 6.11: Comparing Lyapunov number parameter for Experiment 2

	Test #	LN_{TM}	LN_{BD}	LN_{DD}	LN_{AD}
Open Eyes	1	-2.18	-2.85	-1.15	-1.87
	2	-2.24	-2.81	-1.11	-2.22
	3	-2.28	-2.78	-1.15	-2.43
	4	-2.11	-2.60	-1.27	-1.97
	5	-1.96	-2.39	-0.93	-2.14
Closed Eyes	1	-2.06	-2.58	-1.00	-2.08
	2	-1.93	-2.40	-1.06	-1.85
	3	-2.00	-2.40	-1.05	-2.13
	4	-1.96	-2.40	-1.17	-1.87
	5	-1.77	-2.25	-1.03	-1.55

To present the tabulated results in Tables 6.10 and 6.11 more graphically, a bar chart of the Sway Index calculated during the whole test (TM) is given in Figure 6.2. For each of the test subjects, the SI_{TM} parameter is higher for the open eyes test than the eyes closed test. Five subjects' results are not enough to make definite conclusions concerning the SI-parameter, but it is still a significant result. More subjects need to be tested to verify this finding.

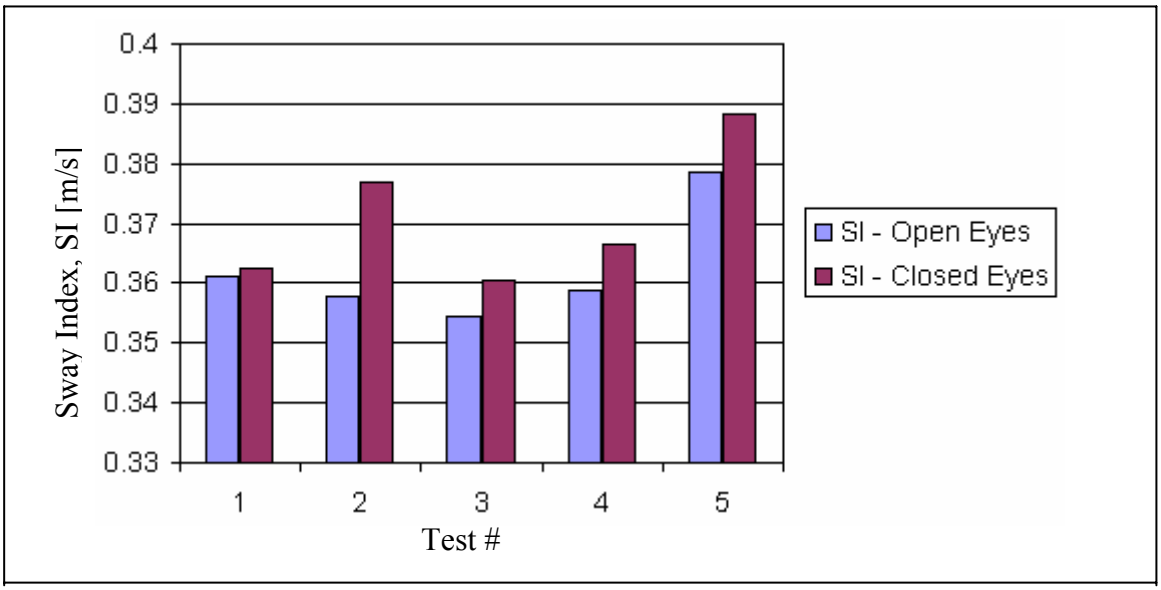

Figure 6.2: Graph indicating SI for both open and closed eyes tests

The following figures (Figures 6.3 to 6.9) show the graphical representation of the obtained data for test subject #4 with eyes closed. These graphs are presented to show how much information can be obtained from these tests. Though it is only graphs that seem meaningless at first glance, much can be said about the person's response to dorsiflexural perturbation relating to the movement of the subject's resultant force on the platform.

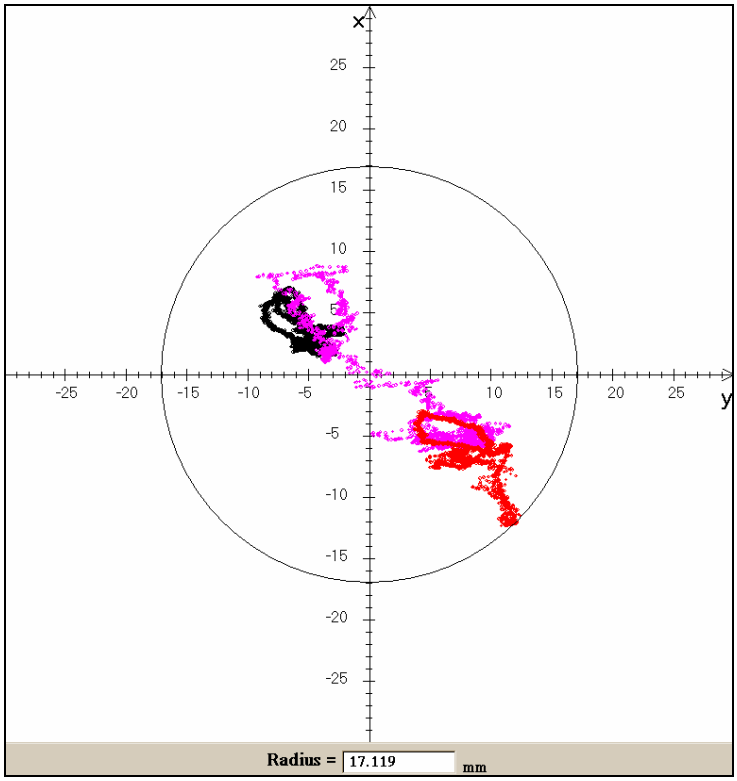

Figure 6.3: TM of test #4 in Experiment 2

From Figure 6.3, it is evident that the subject COP was slightly off-centre in the second quadrant of the two-dimensional plane (defined by the force platform) before the platforms started tilting. In the two seconds while the platforms tilted to cause dorseflexion of the ankle, the subject's COP moved rapidly towards the fourth quadrant where it stayed after perturbation stopped. This movement may be significant to the trained eye of a medical practitioner with some experience in balance impairment and its effect in movement of COP.

Figures 6.4 to 6.6 are presented as a break down of the graph presented in Figure 6.3. This is deemed necessary in order to magnify and clarify the different parts of the movement. These graphs also serve as a means to compare different test subjects to one another. The first of these graphs shows the BD-part of test #4, as presented in Figure 6.4.

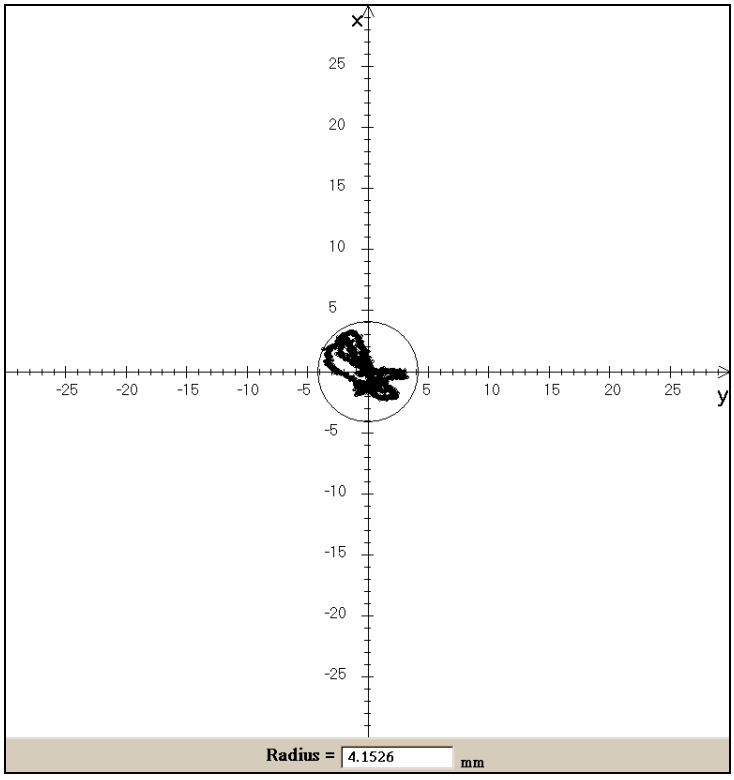

Figure 6.4: BD of test #4 in Experiment 2

Figure 6.4 indicates the BD-movement of the subject in test #4. The centre point of the circle enclosing the movement is calculated using the mean of the x- and y-points calculated for the first part of the test sequence. The whole graph is then moved so that its centre point is the (0,0) point in the graph presented in Figure 6.4. Visible in this

figure, is the subject's sway movement during quiet stance – this is primarily diagonal of nature. The following figure presents the DD-movement of test #4.

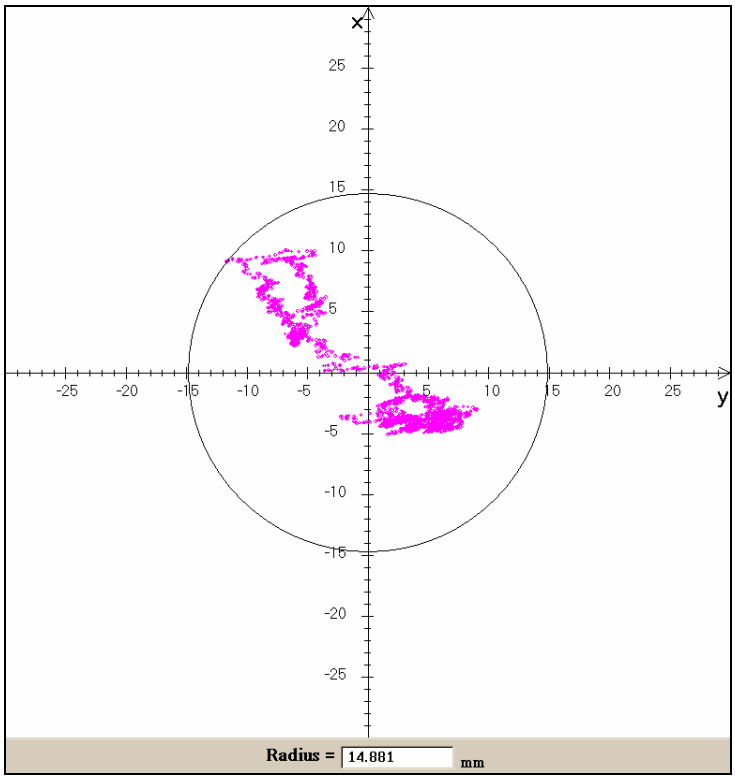

Figure 6.5: DD of test #4 in Experiment 2

The centre point of the circle enclosing the DD-movement presented in Figure 6.5 is calculated in the same manner as that explained in the previous paragraph. This graph indicates the diagonal movement of the position of the normal component of the tested subject towards the fourth quadrant. The movement from left to right may indicate that the subject balances more readily on the right foot and therefore places more weight on the right foot during dorsiflexed perturbation. (This is verified in Figures 6.7 and 6.8). Evident from Figure 6.5, is the noticeably bigger circle than that of Figure 6.4. This is to be expected, since the support platform of the subject is being perturbed and therefore the subject 'searches' for a new balance equilibrium.

Figure 6.6 presents the AD-movement of the same subject during test #4. Noticeable in this figure is the smaller – though still bigger than the BD-movement's circle – circle of confinement than that of the DD-movement presented in Figure 6.5. This may be contributed to the fact that the subject is searching for a new equilibrium point after the platform stopped moving.

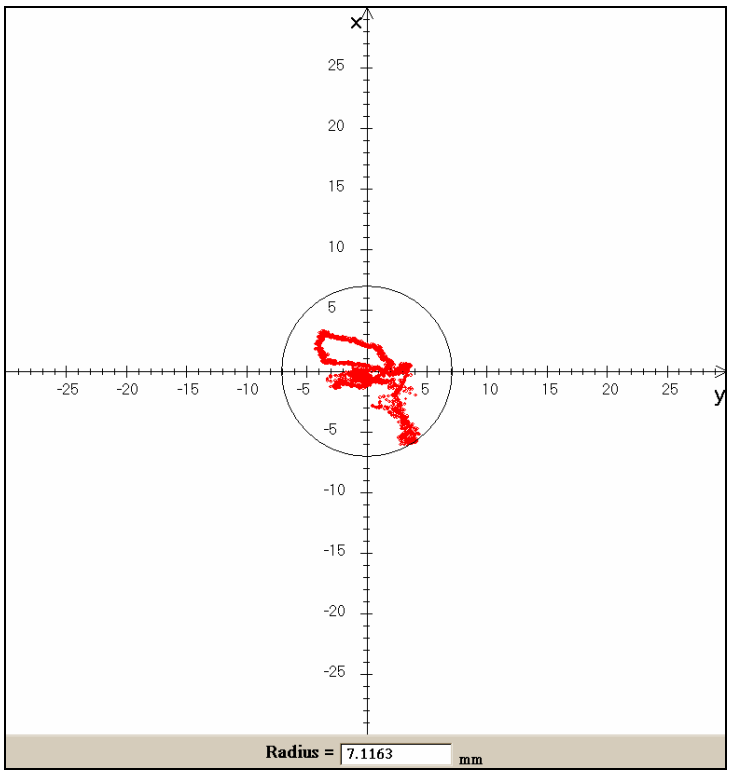

Figure 6.6: AD of test #4 in Experiment 2

Figure 6.7 presents the TM-movement of the left and right foot. Clearly visible is that the right foot does more compensating than the left (the subject tested was right-handed). This graph (as well as the ones in Figure 6.8) facilitates bilateral comparison.

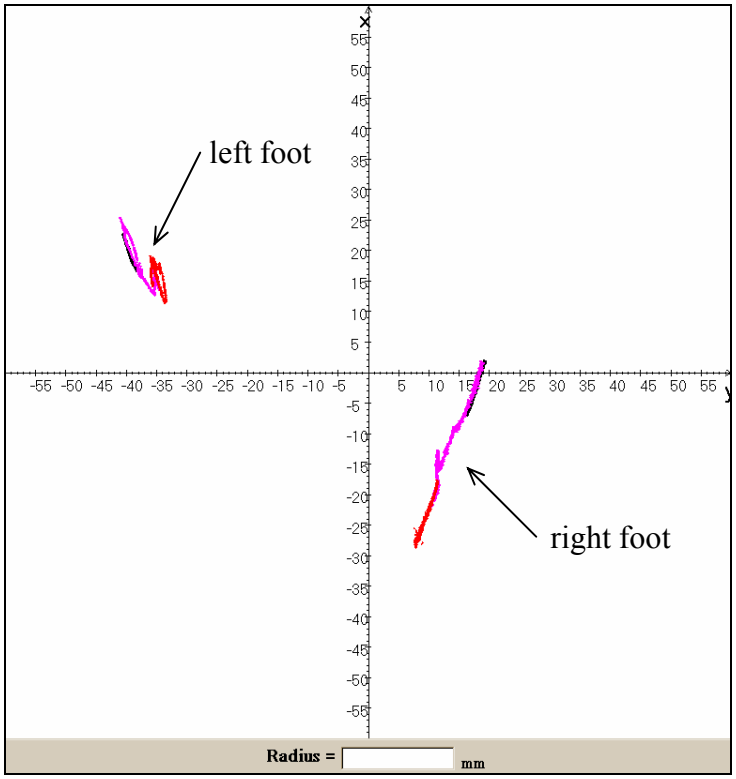

Figure 6.7: Left and right foot's respective TM of test #4 in Experiment 2

The following figure, Figure 6.8, presents the graphs in Figure 6.7 separately. Comparing the left and right foot's respective contribution to maintain balance can be significant in determining pathology relating to balance disorders. The respective circles of confinement in the following figure show the pertinent difference in radius magnitude.

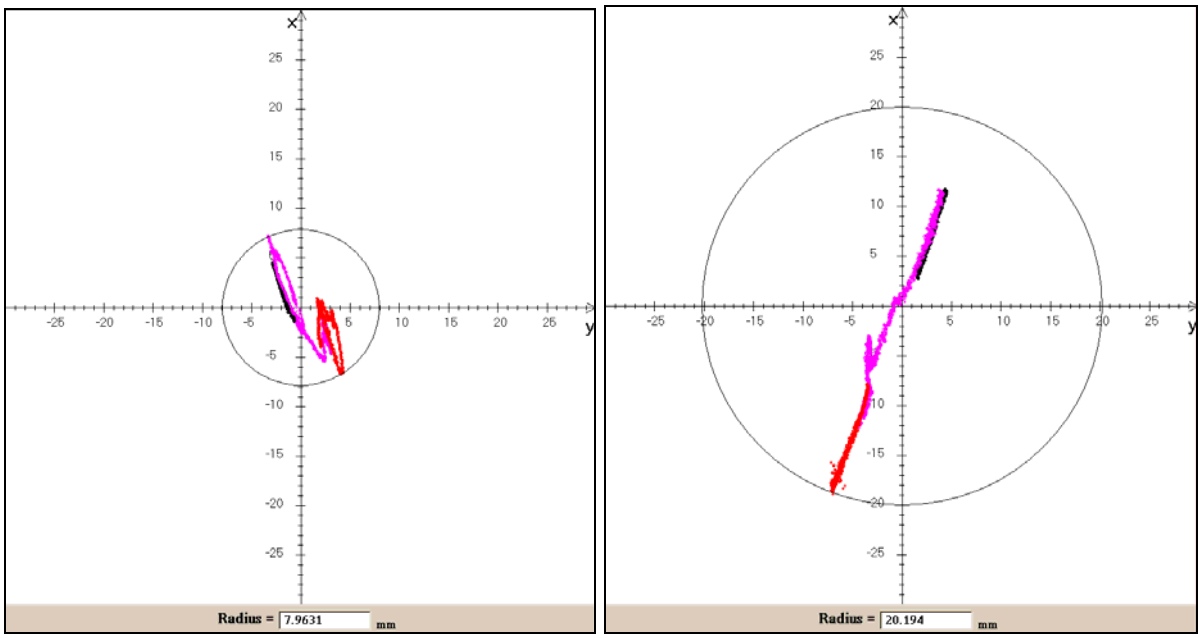

Figure 6.8: Left (left figure) and right (right figure) foot's TM of test #4 in Experiment 2

The short discussions and conclusions made relating to Figures 6.3 to 6.8 are by no means all that can be said. These graphs may assist medical practitioners in the balance disorders field to make a proper diagnosis and suggest the right medication or therapy.

7 Discussions, Conclusions and Recommendations

7.1 Discussions and Conclusions

Section 3 presents a simplified mathematical model for a human balancing on a tiltable platform. This model's intention is not to fully incorporate all the intricacies associated with balance, but to assist in the understanding of the processes involved in keeping a human upright when considering only the torque around the ankles as balance strategy. Results obtained from this model made it clear that the simplifications used are inadequate in that the results obtained from solving the model does not accurately represent that of a human.

Touching on the vast subject of balancing, it has to be mentioned that the model's force, F, represents the brain's response and actions taken to different sensory inputs. Section 2 stipulates all the complex processes involved when a human balances him-/herself. These complex processes include sensory inputs not readily measured by standard equipment. In the mathematical model, all these intricacies were simplified into F, so that the observed reaction of the model's pendulum would be more or less the same as that observed from a human. Sensory inputs (such as the visual and pressure distribution under the feet) are omitted from this model and it is confined to two dimensions only. These two facts add to the model's shortcomings.

The design specification, as stated in Section 4.3.1, was met (cf. Section 5.3). The rest of the Dorsiflexometer's design (including other equipment used in the experimental set-ups) met the device's requirements, as set out on page 4-2. Therefore the constructed device, the Dorsiflexometer, meets the design specifications as proved in Section 5. In this section, the device's sampling and other performances were verified to be within specification. The different procedures and programs written to analyse raw data (of which some are explained in the relevant appendices) were carefully constructed and checked to ensure soundness.

In Section 6 test results produced by the Dorsiflexometer are presented. From the two experimental set-ups used, the second proved to yield better results. It has to be

mentioned that the value of the Lyapunov's exponents should not be underestimated. After analysis of both experiments, these calculated exponents are negative. This implies chaotic behaviour, and brings to pass that ordinary statistical analysis is an invalid basis for making data-related decisions on human balance. Each result should therefore be treated individually, rather than as a statistic. Tables 6.1 to 6.9 present the parameter values obtained for the TM-, BD-, DD- and AD-parts of each test. The incipient thought was that the radius value will be the greatest for DD, lesser for AD and the least for BD. It is evident that this thought is not substantiated by the tabulated values. The SI-parameter proved more useful in experiment 2 and may be an indicator of balance impairment. As presented in Figure 6.7 and 6.8, bilateral comparison is possible when testing a subject on the Dorsiflexometer. This may aid a medical practitioner in making a diagnosis and suggesting appropriate treatment.

In experiment 1, the parameters used in quantifying balance capabilities could not indicate whether or not a test subject was subjected to the intake of alcohol or not. This is illustrated in the tables presented in Section 6.1. Reasons for obtaining these inconclusive results may stem from the fact that experimental set-up 1 was used. The problem lay with the LabView-card, though it was speculated that the HBM Bridge Amplifiers might also have had a slight contribution. This is shown in Section 5 relating to the SNR. The LabView card has a low SNR (the 50 Hz noise is very apparent in Figure 5.6, page 5-8). The LabView software is very powerful and can be used to filter out certain frequencies. This was not the solution though, since the noise that was picked up by the LabView card was distributed over the whole frequency spectrum. Some of the noise was apparently due to digitising (digitising noise), while the rest was said to be because the card used in the computer is not of high enough quality (picking up noise from inside the PC (Naudé 2004).

The readings obtained in experiment 2 were more reliable, since experimental set-up 2 has a better SNR (see Figure 5.12 on page 5-10). Analysed results proved more useful because a distinctive difference can be detected in the SI as well as the BD-, DD- and AD-parameters between open- and closed-eyed tests. There is a definite increase in sway when visual reference is not present (Stephen 2003). This is evident in Table 6.1 – all the radius parameters had higher values when the close-eyed tests were conducted.

Correlation between experimental work and the mathematical model is very poor. There is, in actual fact, no correlation at all. This is evident from comparison between the graphs presented in Sections 3 and 6. The mathematical model was used mainly to gain some understanding as to the main systems at work when subjecting a human to perturbation, as well as during quiet stance. Therefore, trying to draw correlations between the model and the physical tests done is nearly impossible.

A limiting factor of this thesis is that existing equipment and components (such as stepping motors) were used to construct the Dorsiflexometer. Measuring equipment associated with the Dorsiflexometer was needed in other experimental set-ups and therefore a functional Dorsiflexometer was only temporarily in operation.

7.2 Recommendations

It is recommended that, in the event of pursuing a marketable product and taking the Dorsiflexometer into production, a second Dorsiflexometer should be constructed using more appropriate and sophisticated equipment such as better signal conditioning equipment. After a successful second device is constructed, numerous other tests should be done, varying aspects of the testing procedure explained in Section 5 (e.g. tilting speed and duration of test). These tests include the testing and monitoring of patients with known balancing problems, and thereby confirming that the parameters (such as SI-, LN- and radius parameters) can be used with confidence for further monitoring purposes. From this raw data, other parameters may also be ascertained with the help of medical expertise.

The Dorsiflexometer, as it is at present, is not suitable for use by a medical practitioner. It is suggested that the second Dorsiflexometer be an aesthetically enhanced device, and that this prototype should be set up in a medical consultant's room to facilitate further testing. Acorn Industries are interested in funding a continued investigation of the Dorsiflexometer, with the aim of taking the product to market and creating a business.

8 References

An American Physical Therapy Association Anthology. *Gait – basic research.* Vol 1, 1993, APTA publications

Bertec Corporation, *Force Plates Manual,* USA. *Biomechanics.* Vol. 30, No. 4, 1997, pp 347-354

Bronstein A, et al. *Clinical Disorders of Balance Posture and Gait.* First Edition, 1996, Arnold (a division of Hodder Headline PLC)

Brownstein & Bronner, *Functional Movement in orthopeadic and sports physical therapy.* First edition, 1997, Churchill Livingstone

Chen G, Kautz S A and Zajaca FE. Simulation analysis of muscle activity changes with altered body orientations during pedaling. *Biomechanics*. Vol 34, 2001, pp 749-756

Chockalingam N, Giakas G and Iossifidou A. Do strain gauge force platforms need in situ correction? *Gait and Posture.* Vol 16, 2002, pp 233-237

Corazza F, *et al*. Ligament fibre recruitment and forces for the anterior drawer test at the human ankle joint. *Biomechanics*. Vol 33, 2003, pp 363-272

Crosbie J, Green T and Refshauge K. Effects of reduced ankle dorsiflexion following lateral ligament sprain on temporal and spatial gait parameters. *Gait and Posture*. Vol 9, 1999, pp 167-172

Detrembleur C, *et al*. Energy cost, mechanical work, and efficiency of hemiparetic walking. *Gait and Posture*. Vol 00, 2003, pp 1-9

Dimitrov B and Gatev GP. Mechanically evoked cerebral potentials to sudden ankle dorsiflexion in human subjects during standing. *Neuroscience Letters.* Vol 208, 1996, pp 199-202

Ferrarin M, *et al*. Quantitative analysis of gait in Parkinson's disease: a pilot study of the effects of bilateral sub-thalamic stimulation. *Gait and Posture.* Vol 16, 2002, pp 135-148

Freivalds A, *Biomechanics of the upper limbs – mechanics, modeling, and musculoskeletal injuries,* First edition 2004, CRC Press LLC (ISBN 0-7484-0926-2)

Greene PJ and Granat MH. The effects of knee and ankle flexion on ground clearance in paraplegic gait. *Clinical Biomechanics*. Vol 15, 2000, pp 536-540

Helbostad JL and Moe-Nilssen R. The effect of gait speed on lateral balance control during walking in healthy elderly. *Gait and Posture*. Vol 00, 2003, pp 1-10

Helbostad JL and Moe-Nilssen R. The effect of gait speed on lateral balance control during walking in healthy elderly. *Gait and Posture*. Vol 00, 2003, pp 1-10

Hu K, *et al*. Effects of dondylar fibrocartilage on the biomechanical loading of the human temporomandibular joint in a three-dimensional, nonlinear finite element model. *Medical Engineering and Physics*. Vol 25, 2003, pp 107-113

Hunter DG and Spriggs J. Investigation into the relationship between the passive flexibility and active stiffness of the ankle plantar-flexor muscles. *Clinical Biomechanics*. Vol 15, 2000, pp 600-606

Hwang LS and Abraham LD. Quantitative EMG analysis to investigate synergistic coactivation of ankle and knee muscles during isokinetic ankle movement Part I: time amplitude analysis. *Electromyography and Kinesiology*. Vol 11, 2001, pp 319-325

Kasai T, Kawanishi M and Yahagi S. Posture-dependent modulation of reciprocal inhibition upon initiation of ankle dorsiflexion in man. *Brain research*. Vol 792, 1998, pp 159-163

Kejonen P, *Body movements during postural stabilization: Measurements with a motion analysis system,* Department of Physical Medicine and Rehabilitation, University of Oulu, 2002

Kim K-J, *et al*. An in vitro study of individual ankle muscle actions on the centre of pressure. *Gait and Posture.* Vol 00, 2002, pp 1-7

Ku Y-G, Challis JH and Newell KM. Postural coordination patterns as a function of dynamics of the support surface. *Human Movement*. Vol 20, 2001, pp 737-764

Kura H, *et al*. Measurement of surface contact area of the ankle joint. *Clinical Biomechanics*. Vol 13, 1998, pp 365-370

Lamontagne A, et al. Mechanisms of disturbed motor control in ankle weakness during gait after stroke. *Gait and Posture*. Vol 15, 2002, pp 244-255

Leardini A and O'Connor JJ. A model for lever-arm length calculation of the flexor and extensor muscles at the ankle. *Gait and Posture*. Vol 15, 2002, pp 220-229

Lee NKS, *et al*. A flexible encapsulated MEMS pressure sensor system for biomechanical applications. *Microsystem Technologies.* Vol 7, 2001, pp 55-62

Lelas JL, *et al*. Predicting peak kinematic and kinetic parameters from gait speed. *Gait and Posture.* Vol 00, 2002, pp 1-7

Leonard CT *The neuroscience of Human Movement.* First edition, 1998, Mosby-Year Book.

Liu W, *et al*. Three-dimensional, six-degrees-of-freedom kinematics of the human hindfoot during the stance phase of level walking. *Human Movement Science.* Vol 16, 1997, pp 283-298

Lo Monaco EA, Hui-Chan CWY and Paquet N. A spring-activated tilting apparatus for the study of balance control in man. *Neuroscience Methods.* Vol 58, 1995, pp 39-48

MacWilliams BA, Cowley M and Nicholson DE. Foot kinematics and kinetics during adolescent gait. *Gait and Posture.* Vol 00, 2002, pp 1-11

Maganaris CN, Baltzopoulos V and Sargeant AJ. Changes in the tibialis anterior tendon moment arm from rest to maximum isometric dorsiflexion: in vivo observations in man. *Clinical Biomechanics*. Vol 14, 1999, pp 661-666

McLean WG and Nelson EW. *Engineering Mechanics, schaum's outline series*, First Edition 1978, McGraw Hill, New York

Medved V. Measurement of human locomotion. *Biomechanics.* Vol 36, 2003, pp 147-150

Mela P, Veltink PH and Huijing PA. The influence of stimulation frequency and ankle joint angle on the moment exerted by human dorsiflexor muscles. *Electromyography and Kinesiology*. Vol 11, 2001, pp 53-63

Mela P, Veltink PH and Huijing PA. The influence of stimulation frequency and ankle joint angle on the moment exerted by human doriflexor muscles. *Electromyography and Kinesiology*. Vol 11, 2001, pp 53-63

Mills PM and Barett RS. Swing phase mechanics of healthy young and elderly men. *Human Movement Science*. Vol 20, 2001, pp 427-446

Mills PM and Barrett RS. Swing phase mechanics of healthy young and elderly men. *Human Movement Science.* Vol 20, 2001, pp 427-446

Mitoma H, *et al*. Characteristics of parkinsonian and ataxic gaits: a study using surface electromyograms, anular displacements and floor reaction forces. *Neurological Sciences*. Vol 174, 2000, pp 22-39

Moisio KC, *et al*. Normalization of joint moments during gait: a comparison of two techniques. *Biomechanics*. Vol 36, 2003, pp 599-603

Moseley AM, Crosbie J and Adams R. High- and low-ankle flexibility and motor task performance. *Gait and Posture*. Vol 00, 2003, pp 1-8

Moseley AM, Crosbie J and Adams R. Normative data for passive ankle plantarflexion-dorsiflexion flexibility. *Clinical Biomechanics*. Vol 16, 2001, pp 514-521

Nedoma J, *et al*. Numerical simulation of some biomechanical problems. *Mathematics and computers in simulation*. Vol 61, 2003, pp 283-295

Naudé D. National Instruments, private communication, April 2004.

Nester CJ, Van der Linden ML and Bowker P. Effect of foot orthoses on the kinematics and kinetics of normal walking gait. *Gait and Posture*. Vol 17, 2003, pp 180-187

Nester CJ, Van der Linden ML and Bowker P. Effect of foot orthoses on the kinematics and kinetics of normal walking gait. *Gait and Posture.* Vol 17, 2003, pp 180-187

NeuroCom ® International, Inc., *Management of Balance and Mobility Disorders Bibliography* (A compilation of resources)

Pai Y-C and Patton J. Centre of mass velocity-position predictions for balance control. *Biomechanics.* Vol 30, No 4, 1997, pp 347-354

Papa E and Cappozzo A. Sit-to-stand motor strategies investigated in able-bodied young and elderly subjects. *Biomechanics*. Vol 33, 2000, pp 1113-1122

Perry J. *Gait Analysis – normal and pathological function.* Second Edition, 1992, McGraw-Hill

Reinschmidt C, *et al*. Tibiofemoral and tebiocalcaneal motion during walking: external vs. skeletal markers. *Gait and Posture.* Vol 6, 1997, pp 98-109

Rose J and Gamible JG. *Human Walking.* Second edition, 1994, Williams & Wilkins, Baltimore USA

Simmons RW, Richardson C and Deutsch K. Limited joint mobility of the ankle in diabetic patients with cutaneous sensory deficit. *Diabetes Research and Clinical Practice.* Vol 37, 1997, pp 147-143

Singer BJ, *et al*. Velocity dependent passive plantarflexor resistive torque in patients with acquired brain injury. *Clinical Biomechanics*. Vol 18, 2003, pp 157-165

Stephen R, Vision, Balance and Falls in the Elderly. *Geriatric Times*. Vol 4, Issue 6, 2003

Strogatz SH, *Nonlinear Dynamic and Chaos, with applications to physics, biology, chemistry and engineering,* First edition 1993, Addison-Wesley Publishing Company (ISBN 0-201-54344-3)

Sutherland DH. The evolution of clinical gait analysis Part II: kinematics. *Gait and Posture.* Vol 16, 2002, pp 159-179

Van der Kooij, *et al.* A multisensory integration model of human stance control. *Biological Cybernetics.* Vol 80, 1999, pp 299-308

Wang M-Y, *et al*. Lower-extremity biomechanics during forward and lateral stepping activities in older adults. *Clinical Biomechanics*. Vol 12, 2003, pp 53

Ward KA and Soames RW. Contact patterns at the tarsal joints. *Clinical Biomechanics.* Vol 12, No 7,8, 1997, pp 496-507

Weber W and Weber E. *Mechanics of the Human Walking Apparatus.* First edition, 1992, Springer-Verslag, Berlin Heidelberg.

White, M *Gait Analysis – an introduction.* First edition, 1991, Butterworth-Heinemann Ltd.

Williams M and Lissner HR. *Biomechanics of Human Motion*. Third edition, 1992, WB Saunders Company, Philadelphia, PA

Zajac FE, Neptune RR and Kautz SA. Biomechanics and muscle coordination of human walking Part I: Introduction to concepts, power transfer, dynamics and simulations. *Gait and Posture*. Vol 16, 2002, pp 215-232

Zajac FE, Neptune RR and Kautz SA. Biomechanics and muscle coordination of human walking Part II: Lessons from dynamical simulations and clinical implications. *Gait and Posture*. Vol 17, 2003, pp 1-17

Internet websites consulted:
National Instruments (www.nationalinstruments.com)
Online Encyclopedia (www.en.wikipedia.org/wiki/Signal-to-noise_ration)
Online Website (www.ntt.dk/hps_gb_ntt.pdf)
www.medtrakoline.com
www.ntt.dk/hps_gb_ntt.pdf

Appendix A: Computer Program's Sample Calculations

PLATFORM CALCULATIONS

Determining the equations for converting platform measurements into movement of the normal component of the resultant force is a simple task. The derivation of the equations follows Figure A1. The aim of this derivation is to acquire the X- and Y-coordinate ($\overline{X}$ and $\overline{Y}$) of where the normal component of the resultant force (applied to both platforms) works in. It is the movement of this point with respect to time that is of interest to the development of the Dorsiflexometer.

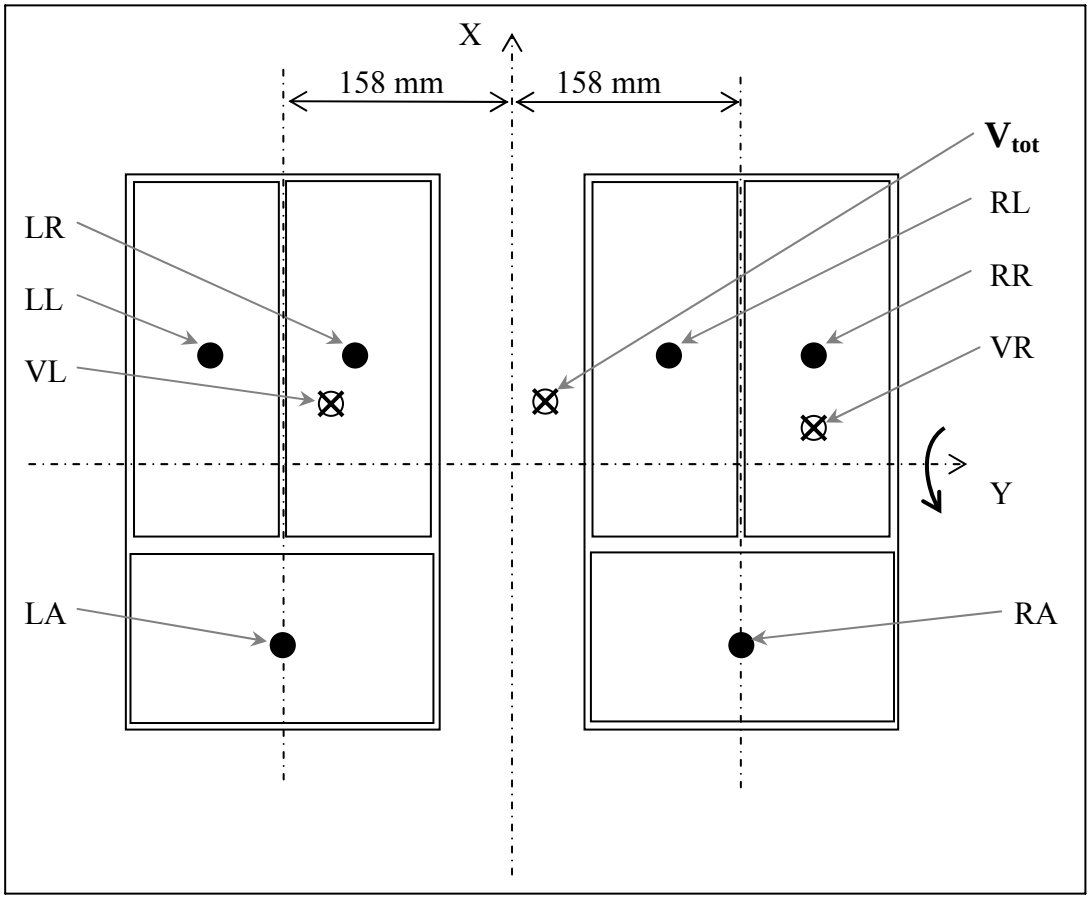

Figure A1: Sketch of the force platforms – indicating the positions of the load cells

The main axis is the X- and Y-axis (please refer to Figure A1). The Y-axis is chosen to be the axis of revolution of the platforms. Each platform has its own axis system (see Figure A2), but this is not of interest just yet. V_{tot} is the normal component of the total resultant force (the force applied to both platforms), while VL and VR are the normal

components of the resultant force of the left and right force platform respectively. LR, LL and LA are the vertical forces measured by each of the corresponding load cells of the left platform – the same applies for the right platform, though here it is RR, RL and RA. Note that the load cells are only capable of measuring the normal component of the force applied to it (this is because of the full-bridge configuration of the load cell plus its corresponding setting for the bridge amplifier). The relations according to which all these variables are linked are as follows:

$$VL = LA + LL + LR \quad [\text{N}] \tag{A.1}$$

and

$$VR = RA + RL + RR \quad [\text{N}] \tag{A.2}$$

and therefore,

$$V_{tot} = VL + VR \quad [\text{N}] \tag{A.3}$$

In these equations, the values of LA, LL, LR, RA, RL, and RR are actually the small change of the resistance of the strain gauge. These values are then amplified by the bridge amplifier (set to the full-bridge configuration), and it is these amplified signals that are samples by the LabView-card and thus fed into the computer. With the computer, these voltage values for each of the mentioned variables are converted to the actual force the specific load cell carries (this is done by calibrating each of the platforms beforehand). What all this boils down to, is the fact that LA, LL, LR, RA, RL, and RR – when used in the equations – are values in Newton. So the physical force on each of the six platforms is known.

Now that the values of VR and VL are known, the actual position where these forces work in can be determined (therefore obtaining $\bar{x}_L$ and $\bar{y}_L$ as well as $\bar{x}_R$ and $\bar{y}_R$). See Figure A2 for the appropriate sketch.

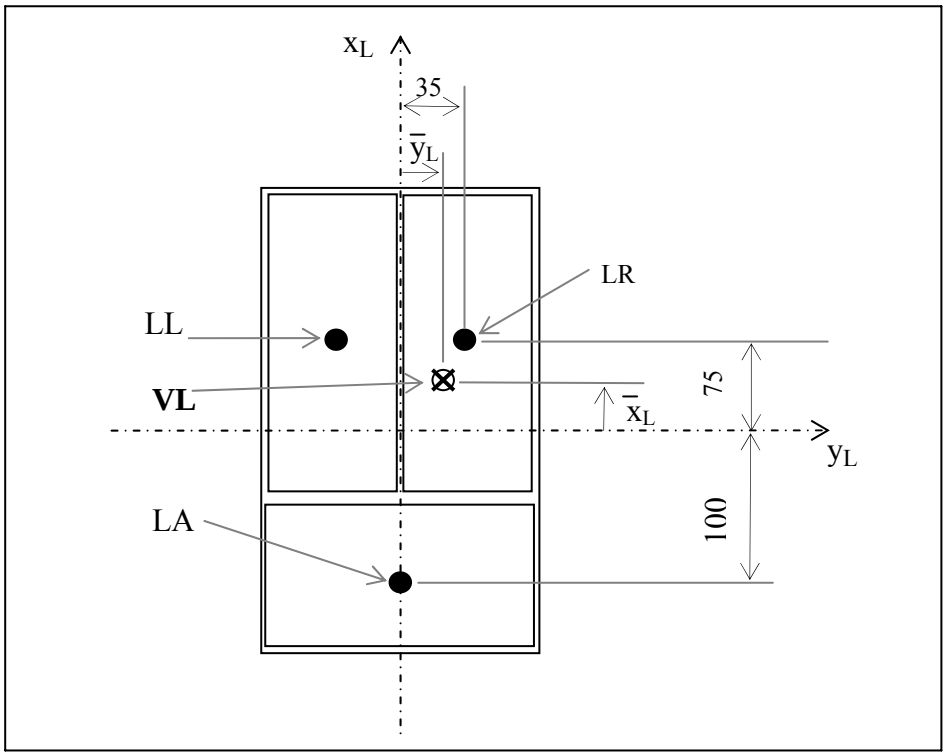

Figure A2: Sketch of the left platform

For the left platform:

To determine the x-coordinate $\bar{x}_L$, the sum of the moments around y_L-axis is taken:

$$\circlearrowleft + \sum M_{y_L} = VL(\bar{x}_L)$$

$$(LR + LL)(0.075) - LA(0.1) - \bar{x}_L(VL) = 0$$

$$\therefore \bar{x}_L(VL) = -LA(0.1) + (LR + LL)(0.075)$$

$$\therefore \bar{x}_L = \frac{-LA(0.1) + (LR + LL)(0.075)}{VL} \qquad \text{[m]} \qquad \text{(A.4)}$$

To determine the y-coordinate $\bar{y}_L$, the sum of the moments around y_L-axis is taken:

$$\circlearrowleft + \sum M_{x_L} = VL(\bar{y}_L)$$

$$(LR - LL)(0.035) - \bar{y}_L(VL) = 0$$

$$\therefore \bar{y}_L(VL) = (LR - LL)(0.035)$$

$$\therefore \bar{y}_L = \frac{(LR - LL)(0.035)}{VL} \quad \text{[m]} \quad \text{(A.5)}$$

For the right platform:

The same applies to the right platform.

$$\therefore \bar{x}_R = \frac{-RA(0.1) + (RR + RL)(0.075)}{VR} \quad \text{[m]} \quad \text{(A.6)}$$

$$\therefore \bar{y}_R = \frac{(RR - RL)(0.035)}{VR} \quad \text{[m]} \quad \text{(A.7)}$$

The above equations are used to determine the movement of the resultant force applied to each of the individual platforms. The total applied force to both platforms' coordinate, is the coordinate of interest ($\bar{X}$, $\bar{Y}$). Therefore, the same rationale is followed with the following sketch (see Figure A3).

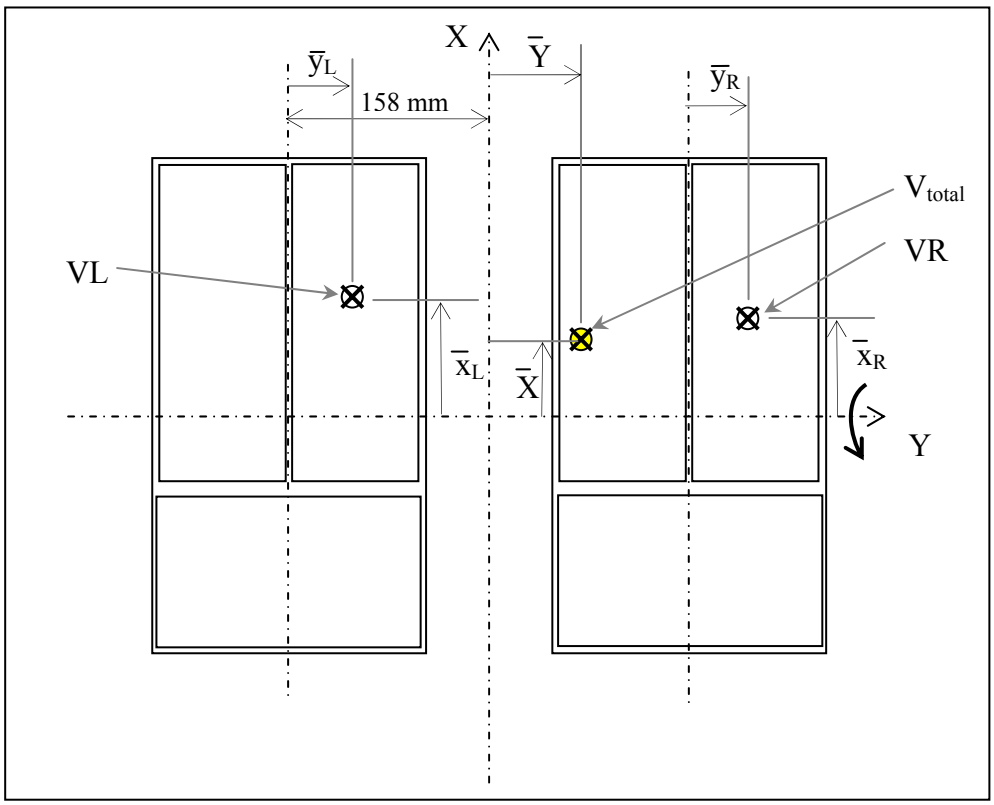

Figure A3: Sketch of both platforms

For both platforms: (from Figure A3)

$$+\circlearrowright \quad \sum M_X = V_{TOT}\left(\overline{Y}\right)$$

$$VR\left(\overline{y}_R + 0.158\right) - V_{TOT}\left(\overline{Y}\right) - VL\left(0.158 - \overline{y}_L\right) = 0$$

$$\therefore V_{TOT}\left(\overline{Y}\right) = VR\left(\overline{y}_R + 0.158\right) - VL\left(0.158 - \overline{y}_L\right)$$

$$\therefore \overline{Y} = \frac{VR\left(\overline{y}_R + 0.158\right) - VL\left(0.158 - \overline{y}_L\right)}{V_{tot}} \quad \text{[m]} \qquad \text{(A.8)}$$

$$+\circlearrowleft \quad \sum M_Y = V_{TOT}\left(\overline{X}\right)$$

$$VL\left(\overline{x}_L\right) - V_{TOT}\left(\overline{X}\right) + VR\left(\overline{x}_R\right) = 0$$

$$\therefore \overline{X} = \frac{VL\left(\overline{x}_L\right) + VR\left(\overline{x}_R\right)}{V_{tot}} \quad \text{[m]} \qquad \text{(A.9)}$$

The above two equations are the ones of interest. Equations A.8 and A.9 give the precise location (i.e. are the coordinates) of the normal component of the resultant force applied to both the force platforms. By plotting the point (indicated by the $\overline{X}$- and $\overline{Y}$-coordinate) for each of the time steps, the movement of the subject's normal component can be observed.

SAMPLE CALCULATIONS

In this section, one complete set of calculations will be done. Starting from the raw data (read by LabView), to the final X-Y plot, the sway index and the calculated Lyapunov number. The first 200 points' data read in by LabView for subject #6 (see Section 6) is displayed in Table A1. The first column displays the point number (in chronological order), while the columns that follow display each of the channels read (corresponding to the applicable platform reading). The first of these columns, for example, is that of the top left footplate of the left platform's (see Figure A1) readings. In the left half of this column, under Time-LL (measured in seconds), is the exact time corresponding to the

reading of that platform – in this instance, LL's measurement taken in volts. After both the 100th and the 200th point, the average of the preceding 100 points of voltage measurements are calculated. The first of these points is then used as a new first point (point A) used to calculate the actual X and Y coordinate (see Table A2). Point A's time stamp is calculated by taking the time point #1 was measured and adding it to time when point #100 was measured, and then dividing by two. This corresponds to the time point #50 was measured. Therefore, the two equations used to 'average' the data, is (for the LL-column):

$$Time - LL = (Point\ \#1_{time} + Point\ \#100_{time}) / 2 \qquad [s] \qquad (A.10)$$

and

$$LL = \frac{\sum_{i=1}^{n} LL_{(100-x*100)+i}}{n} \qquad [V] \qquad (A.11)$$

where n is the number of points used for averaging, in this case n = 100, and x is the number of the averaged point (meaning that A = 1 and B = 2, etc).

Therefore, for point A, from Equation (A.10):

$$\therefore Time - LL = \frac{(0 + 0.003302)}{2} = 0.001651 \qquad [s]$$

and, from Equation (A.11),

$$LL = \frac{\sum_{i=1}^{100} LL_{(100-1*100)+i}}{100} = \frac{\sum_{i=1}^{100} LL_i}{100} = 1.6693 \qquad [V]$$

And the same for point B, from Equation (A.10):

$$\therefore Time - LL = \frac{(0.003335 + 0.00657)}{2} = 0.004953 \qquad [s]$$

and, from Equation (A.11)

$$LL = \frac{\sum_{i=1}^{100} LL_{(100-2*100)+i}}{100} = \frac{\sum_{i=1}^{100} LL_{100+i}}{100} = 1.6716 \qquad [V]$$

The above calculated values are displayed in Table A2, after which the other calculations are discussed (these calculations are done in order to know exactly what the weight is that is supported by both platforms, as well as to calculated the movement of the resultants' normal component as a function of time).

Table A1: First 200 points read for subject #6

Point [#]	Time - LL [s]	LL [V]	Time - LR [s]	LR [V]	Time - LA [s]	LA [V]	Time - RL [s]	RL [V]	Time - RR [s]	RR [V]	Time - RA [s]	RA [V]
1	0	1.6644	0	0.2686	0	2.0117	0	1.3358	0	5.2777	0	0.8524
2	3.34E-05	1.651	3.34E-05	0.2652	3.34E-05	1.9943	3.34E-05	1.3199	3.34E-05	5.3766	3.34E-05	0.8521
3	6.67E-05	1.6937	6.67E-05	0.2881	6.67E-05	2.0059	6.67E-05	1.3266	6.67E-05	5.3732	6.67E-05	0.7492
4	0.0001	1.6809	0.0001	0.2881	0.0001	1.9754	0.0001	1.3367	0.0001	5.3705	0.0001	0.8072
5	0.000133	1.6632	0.000133	0.3271	0.000133	2.0026	0.000133	1.3065	0.000133	5.3674	0.000133	0.9079
6	0.000167	1.6479	0.000167	0.3204	0.000167	1.9907	0.000167	1.2381	0.000167	5.3748	0.000167	0.8994
7	0.0002	1.6333	0.0002	0.3064	0.0002	2.037	0.0002	1.3464	0.0002	5.3445	0.0002	0.8408
8	0.000233	1.665	0.000233	0.2951	0.000233	2.0139	0.000233	1.3062	0.000233	5.289	0.000233	0.8466
9	0.000267	1.6608	0.000267	0.2792	0.000267	1.9977	0.000267	1.3208	0.000267	5.3702	0.000267	0.8539
10	0.0003	1.6922	0.0003	0.311	0.0003	1.9873	0.0003	1.3214	0.0003	5.372	0.0003	0.8359
11	0.000333	1.6769	0.000333	0.3134	0.000333	1.9525	0.000333	1.3333	0.000333	5.3729	0.000333	0.7968
12	0.000367	1.662	0.000367	0.3311	0.000367	1.9977	0.000367	1.3049	0.000367	5.3729	0.000367	0.8853
13	0.0004	1.6443	0.0004	0.3137	0.0004	2.0038	0.0004	1.2518	0.0004	5.3729	0.0004	0.8957
14	0.000434	1.6306	0.000434	0.2997	0.000434	2.037	0.000434	1.3409	0.000434	5.3418	0.000434	0.8389
15	0.000467	1.6702	0.000467	0.2829	0.000467	2.0193	0.000467	1.3354	0.000467	5.2887	0.000467	0.8282
16	0.0005	1.6748	0.0005	0.2588	0.0005	1.9992	0.0005	1.3248	0.0005	5.3568	0.0005	0.8624
17	0.000534	1.6846	0.000534	0.2887	0.000534	1.9824	0.000534	1.3248	0.000534	5.3778	0.000534	0.867
18	0.000567	1.6736	0.000567	0.2963	0.000567	1.9604	0.000567	1.3437	0.000567	5.3775	0.000567	0.7904
19	0.0006	1.669	0.0006	0.2957	0.0006	2.0004	0.0006	1.3046	0.0006	5.3699	0.0006	0.8835
20	0.000634	1.6592	0.000634	0.293	0.000634	2.0117	0.000634	1.2442	0.000634	5.3909	0.000634	0.8746
21	0.000667	1.6467	0.000667	0.296	0.000667	2.0282	0.000667	1.3324	0.000667	5.351	0.000667	0.8411
22	0.0007	1.6745	0.0007	0.2863	0.0007	2.0169	0.0007	1.3403	0.0007	5.304	0.0007	0.8371
23	0.000734	1.68	0.000734	0.2924	0.000734	2.0023	0.000734	1.3342	0.000734	5.347	0.000734	0.8746
24	0.000767	1.6632	0.000767	0.3156	0.000767	1.9971	0.000767	1.3202	0.000767	5.3687	0.000767	0.911
25	0.0008	1.6678	0.0008	0.3174	0.0008	1.9952	0.0008	1.3379	0.0008	5.3839	0.0008	0.787
26	0.000834	1.6699	0.000834	0.3091	0.000834	1.9974	0.000834	1.3028	0.000834	5.3174	0.000834	0.8694
27	0.000867	1.6626	0.000867	0.3076	0.000867	2.0157	0.000867	1.2445	0.000867	5.3705	0.000867	0.8707
28	0.0009	1.6885	0.0009	0.3198	0.0009	2.012	0.0009	1.3165	0.0009	5.34	0.0009	0.845
29	0.000934	1.683	0.000934	0.3235	0.000934	2.0099	0.000934	1.3419	0.000934	5.3006	0.000934	0.8374
30	0.000967	1.6785	0.000967	0.3433	0.000967	2.0157	0.000967	1.3428	0.000967	5.3189	0.000967	0.867
31	0.001	1.6422	0.001	0.3467	0.001	2.0013	0.001	1.3101	0.001	5.3796	0.001	0.9338
32	0.001034	1.6617	0.001034	0.3354	0.001034	2.0169	0.001034	1.3324	0.001034	5.3812	0.001034	0.7495
33	0.001067	1.6803	0.001067	0.2988	0.001067	2.0386	0.001067	1.3068	0.001067	5.3537	0.001067	0.853
34	0.001101	1.6708	0.001101	0.3104	0.001101	2.0145	0.001101	1.2531	0.001101	5.3674	0.001101	0.8578
35	0.001134	1.6949	0.001134	0.3302	0.001134	1.9827	0.001134	1.3181	0.001134	5.3476	0.001134	0.845
36	0.001167	1.6922	0.001167	0.3244	0.001167	1.9989	0.001167	1.3376	0.001167	5.3061	0.001167	0.8371
37	0.001201	1.6821	0.001201	0.3357	0.001201	2.0285	0.001201	1.337	0.001201	5.3336	0.001201	0.8698
38	0.001234	1.64	0.001234	0.3229	0.001234	2.0074	0.001234	1.3217	0.001234	5.3787	0.001234	0.9314
39	0.001267	1.6544	0.001267	0.3165	0.001267	2.0297	0.001267	1.3336	0.001267	5.3812	0.001267	0.7886
40	0.001301	1.6882	0.001301	0.274	0.001301	2.0496	0.001301	1.3153	0.001301	5.3528	0.001301	0.8572
41	0.001334	1.6763	0.001334	0.2777	0.001334	2.0181	0.001334	1.2625	0.001334	5.3757	0.001334	0.8798
42	0.001367	1.6849	0.001367	0.3058	0.001367	1.9775	0.001367	1.3315	0.001367	5.3595	0.001367	0.8047
43	0.001401	1.6809	0.001401	0.2975	0.001401	1.9919	0.001401	1.3321	0.001401	5.2927	0.001401	0.8344
44	0.001434	1.6895	0.001434	0.2869	0.001434	2.0313	0.001434	1.3348	0.001434	5.3534	0.001434	0.8823
45	0.001467	1.6574	0.001467	0.2649	0.001467	2.016	0.001467	1.3211	0.001467	5.3738	0.001467	0.8539
46	0.001501	1.6595	0.001501	0.2963	0.001501	2.0197	0.001501	1.3361	0.001501	5.3751	0.001501	0.8188
47	0.001534	1.6888	0.001534	0.274	0.001534	2.005	0.001534	1.3089	0.001534	5.368	0.001534	0.8636

48	0.001567	1.6858	0.001567	0.2728	0.001567	2.0273	0.001567	1.2479	0.001567	5.3751	0.001567	0.8813
49	0.001601	1.6699	0.001601	0.2982	0.001601	1.9992	0.001601	1.3452	0.001601	5.3442	0.001601	0.8478
50	0.001634	1.6632	0.001634	0.2991	0.001634	1.9928	0.001634	1.3333	0.001634	5.282	0.001634	0.8533
51	0.001667	1.6888	0.001667	0.2753	0.001667	2.0245	0.001667	1.3269	0.001667	5.3748	0.001667	0.8661
52	0.001701	1.6782	0.001701	0.2365	0.001701	2.0258	0.001701	1.3239	0.001701	5.3787	0.001701	0.8301
53	0.001734	1.6629	0.001734	0.3024	0.001734	2.0078	0.001734	1.3217	0.001734	5.3641	0.001734	0.8218
54	0.001768	1.6803	0.001768	0.2997	0.001768	1.9748	0.001768	1.311	0.001768	5.3632	0.001768	0.8737
55	0.001801	1.6873	0.001801	0.2896	0.001801	2.0419	0.001801	1.2402	0.001801	5.3693	0.001801	0.8826
56	0.001834	1.6605	0.001834	0.303	0.001834	2.0068	0.001834	1.3464	0.001834	5.3534	0.001834	0.8514
57	0.001868	1.6296	0.001868	0.311	0.001868	2.0004	0.001868	1.319	0.001868	5.2902	0.001868	0.8578
58	0.001901	1.6867	0.001901	0.2832	0.001901	2.0227	0.001901	1.3184	0.001901	5.3815	0.001901	0.8539
59	0.001934	1.6809	0.001934	0.2332	0.001934	2.027	0.001934	1.3223	0.001934	5.3723	0.001934	0.77
60	0.001968	1.6711	0.001968	0.2994	0.001968	2.0032	0.001968	1.3281	0.001968	5.3604	0.001968	0.8463
61	0.002001	1.6748	0.002001	0.3037	0.002001	1.9412	0.002001	1.3089	0.002001	5.3687	0.002001	0.8716
62	0.002034	1.6843	0.002034	0.2988	0.002034	2.0444	0.002034	1.2628	0.002034	5.3745	0.002034	0.8783
63	0.002068	1.6589	0.002068	0.2917	0.002068	2.0193	0.002068	1.2881	0.002068	5.3607	0.002068	0.8438
64	0.002101	1.6153	0.002101	0.3021	0.002101	2.0166	0.002101	1.3162	0.002101	5.3439	0.002101	0.8655
65	0.002134	1.6727	0.002134	0.282	0.002134	2.0227	0.002134	1.311	0.002134	5.3665	0.002134	0.8636
66	0.002168	1.6806	0.002168	0.2423	0.002168	2.0343	0.002168	1.3297	0.002168	5.3525	0.002168	0.7968
67	0.002201	1.6821	0.002201	0.2942	0.002201	2.0013	0.002201	1.3239	0.002201	5.3546	0.002201	0.8517
68	0.002234	1.6711	0.002234	0.3088	0.002234	1.9427	0.002234	1.3193	0.002234	5.3668	0.002234	0.8905
69	0.002268	1.6867	0.002268	0.3113	0.002268	2.0386	0.002268	1.3428	0.002268	5.3613	0.002268	0.8673
70	0.002301	1.6592	0.002301	0.3055	0.002301	2.0169	0.002301	1.3297	0.002301	5.3589	0.002301	0.8575
71	0.002334	1.6129	0.002334	0.3177	0.002334	2.0117	0.002334	1.2979	0.002334	5.3857	0.002334	0.8688
72	0.002368	1.6702	0.002368	0.2917	0.002368	2.0273	0.002368	1.3123	0.002368	5.3671	0.002368	0.8682
73	0.002401	1.6846	0.002401	0.2457	0.002401	2.0294	0.002401	1.3071	0.002401	5.3491	0.002401	0.8517
74	0.002435	1.6815	0.002435	0.2969	0.002435	1.9995	0.002435	1.3184	0.002435	5.351	0.002435	0.86
75	0.002468	1.6769	0.002468	0.3156	0.002468	1.9357	0.002468	1.3092	0.002468	5.3745	0.002468	0.8679
76	0.002501	1.6824	0.002501	0.3091	0.002501	2.0322	0.002501	1.333	0.002501	5.3586	0.002501	0.8569
77	0.002535	1.6602	0.002535	0.2988	0.002535	2.0236	0.002535	1.3223	0.002535	5.3442	0.002535	0.8585
78	0.002568	1.6141	0.002568	0.2972	0.002568	2.0218	0.002568	1.3135	0.002568	5.3702	0.002568	0.8698
79	0.002601	1.6705	0.002601	0.2798	0.002601	2.023	0.002601	1.3214	0.002601	5.3302	0.002601	0.8649
80	0.002635	1.6922	0.002635	0.2307	0.002635	2.0248	0.002635	1.3214	0.002635	5.3568	0.002635	0.8649
81	0.002668	1.6861	0.002668	0.2841	0.002668	1.9986	0.002668	1.315	0.002668	5.3537	0.002668	0.8725
82	0.002701	1.673	0.002701	0.3	0.002701	1.9559	0.002701	1.3123	0.002701	5.3638	0.002701	0.8591
83	0.002735	1.6779	0.002735	0.2969	0.002735	2.0361	0.002735	1.3184	0.002735	5.354	0.002735	0.8582
84	0.002768	1.6568	0.002768	0.2948	0.002768	2.02	0.002768	1.3174	0.002768	5.3543	0.002768	0.8646
85	0.002801	1.6238	0.002801	0.3046	0.002801	2.0151	0.002801	1.3223	0.002801	5.3613	0.002801	0.8502
86	0.002835	1.6782	0.002835	0.296	0.002835	2.0184	0.002835	1.3226	0.002835	5.3583	0.002835	0.8481
87	0.002868	1.6858	0.002868	0.2692	0.002868	2.0251	0.002868	1.3184	0.002868	5.3659	0.002868	0.8771
88	0.002901	1.676	0.002901	0.318	0.002901	2.009	0.002901	1.319	0.002901	5.3604	0.002901	0.8673
89	0.002935	1.6718	0.002935	0.3308	0.002935	1.9781	0.002935	1.3248	0.002935	5.3632	0.002935	0.8682
90	0.002968	1.6782	0.002968	0.3305	0.002968	2.0267	0.002968	1.3202	0.002968	5.3625	0.002968	0.86
91	0.003001	1.666	0.003001	0.3308	0.003001	2.0221	0.003001	1.3153	0.003001	5.3671	0.003001	0.8627
92	0.003035	1.6425	0.003035	0.3378	0.003035	2.0157	0.003035	1.3226	0.003035	5.3625	0.003035	0.8517
93	0.003068	1.6751	0.003068	0.3308	0.003068	2.0282	0.003068	1.322	0.003068	5.3607	0.003068	0.8435
94	0.003102	1.6797	0.003102	0.3091	0.003102	2.0227	0.003102	1.3187	0.003102	5.3625	0.003102	0.8667
95	0.003135	1.6754	0.003135	0.3363	0.003135	2.0102	0.003135	1.3272	0.003135	5.3534	0.003135	0.8572
96	0.003168	1.6791	0.003168	0.332	0.003168	2.0093	0.003168	1.3269	0.003168	5.3616	0.003168	0.864
97	0.003202	1.6757	0.003202	0.3278	0.003202	2.0267	0.003202	1.3187	0.003202	5.3558	0.003202	0.8722
98	0.003235	1.6656	0.003235	0.3253	0.003235	2.0206	0.003235	1.3187	0.003235	5.369	0.003235	0.8661
99	0.003268	1.6568	0.003268	0.318	0.003268	2.0139	0.003268	1.3217	0.003268	5.3534	0.003268	0.8588
100	0.003302	1.6782	0.003302	0.3104	0.003302	2.0197	0.003302	1.3251	0.003302	5.3568	0.003302	0.8615
	0.001651	**1.6693**	**0.001651**	**0.3004**	**0.001651**	**2.0093**	**0.001651**	**1.3165**	**0.001651**	**5.3562**	**0.001651**	**0.8545**
101	0.003335	1.6782	0.003335	0.2948	0.003335	2.0215	0.003335	1.3193	0.003335	5.361	0.003335	0.8719
102	0.003368	1.6736	0.003368	0.3101	0.003368	2.0193	0.003368	1.3187	0.003368	5.3598	0.003368	0.8563
103	0.003402	1.6736	0.003402	0.3067	0.003402	2.0184	0.003402	1.3257	0.003402	5.3552	0.003402	0.8548
104	0.003435	1.6751	0.003435	0.3018	0.003435	2.0224	0.003435	1.3211	0.003435	5.3629	0.003435	0.8636
105	0.003468	1.673	0.003468	0.3021	0.003468	2.0166	0.003468	1.3214	0.003468	5.3635	0.003468	0.863

106	0.003502	1.6714	0.003502	0.303	0.003502	2.0148	0.003502	1.3309	0.003502	5.3568	0.003502	0.8676
107	0.003535	1.6757	0.003535	0.3061	0.003535	2.0187	0.003535	1.3208	0.003535	5.3595	0.003535	0.856
108	0.003568	1.6736	0.003568	0.3046	0.003568	2.0203	0.003568	1.3174	0.003568	5.3598	0.003568	0.8606
109	0.003602	1.6736	0.003602	0.3116	0.003602	2.0242	0.003602	1.3245	0.003602	5.358	0.003602	0.8585
110	0.003635	1.6748	0.003635	0.3116	0.003635	2.0209	0.003635	1.3242	0.003635	5.3564	0.003635	0.8688
111	0.003668	1.6748	0.003668	0.3119	0.003668	2.0187	0.003668	1.3205	0.003668	5.3622	0.003668	0.8643
114	0.003702	1.6754	0.003702	0.3156	0.003702	2.0142	0.003702	1.3272	0.003702	5.3629	0.003702	0.856
115	0.003735	1.6748	0.003735	0.3159	0.003735	2.0139	0.003735	1.3199	0.003735	5.3601	0.003735	0.8722
116	0.003769	1.6748	0.003769	0.3201	0.003769	2.0184	0.003769	1.3095	0.003769	5.3616	0.003769	0.8633
117	0.003802	1.6708	0.003802	0.322	0.003802	2.0181	0.003802	1.3208	0.003802	5.361	0.003802	0.8615
118	0.003835	1.6736	0.003835	0.3235	0.003835	2.019	0.003835	1.3043	0.003835	5.3598	0.003835	0.8585
119	0.003869	1.6736	0.003869	0.3195	0.003869	2.0215	0.003869	1.3174	0.003869	5.3589	0.003869	0.8759
120	0.003902	1.6733	0.003902	0.318	0.003902	2.019	0.003902	1.3049	0.003902	5.3577	0.003902	0.8664
121	0.003935	1.6708	0.003935	0.321	0.003935	2.0126	0.003935	1.3217	0.003935	5.3558	0.003935	0.8627
122	0.003969	1.676	0.003969	0.3195	0.003969	2.0132	0.003969	1.3239	0.003969	5.3558	0.003969	0.8691
123	0.004002	1.6745	0.004002	0.3204	0.004002	2.0184	0.004002	1.3193	0.004002	5.3607	0.004002	0.8633
124	0.004035	1.6696	0.004035	0.3229	0.004035	2.0178	0.004035	1.322	0.004035	5.3571	0.004035	0.8566
125	0.004069	1.6702	0.004069	0.3207	0.004069	2.0175	0.004069	1.3165	0.004069	5.358	0.004069	0.8649
126	0.004102	1.6721	0.004102	0.3156	0.004102	2.0184	0.004102	1.3177	0.004102	5.3845	0.004102	0.8691
127	0.004135	1.673	0.004135	0.314	0.004135	2.0175	0.004135	1.3242	0.004135	5.3534	0.004135	0.8664
128	0.004169	1.6714	0.004169	0.3174	0.004169	2.0136	0.004169	1.3138	0.004169	5.3589	0.004169	0.8514
129	0.004202	1.6751	0.004202	0.3165	0.004202	2.0154	0.004202	1.3181	0.004202	5.3622	0.004202	0.8636
130	0.004235	1.6745	0.004235	0.3174	0.004235	2.0187	0.004235	1.3116	0.004235	5.3619	0.004235	0.8612
131	0.004269	1.6687	0.004269	0.3192	0.004269	2.0169	0.004269	1.3278	0.004269	5.3598	0.004269	0.8621
132	0.004302	1.6705	0.004302	0.3165	0.004302	2.0145	0.004302	1.304	0.004302	5.3546	0.004302	0.863
133	0.004335	1.673	0.004335	0.3131	0.004335	2.0163	0.004335	1.3177	0.004335	5.3683	0.004335	0.8667
134	0.004369	1.6724	0.004369	0.3091	0.004369	2.0209	0.004369	1.3214	0.004369	5.3503	0.004369	0.86
135	0.004402	1.669	0.004402	0.3104	0.004402	2.0169	0.004402	1.3174	0.004402	5.3568	0.004402	0.8563
136	0.004436	1.673	0.004436	0.3061	0.004436	2.0169	0.004436	1.322	0.004436	5.3552	0.004436	0.8585
137	0.004469	1.6736	0.004469	0.304	0.004469	2.0178	0.004469	1.322	0.004469	5.3601	0.004469	0.863
138	0.004502	1.6687	0.004502	0.3061	0.004502	2.0172	0.004502	1.33	0.004502	5.3293	0.004502	0.8633
139	0.004536	1.6684	0.004536	0.3067	0.004536	2.0129	0.004536	1.3232	0.004536	5.3589	0.004536	0.8624
140	0.004569	1.6711	0.004569	0.3064	0.004569	2.0203	0.004569	1.3226	0.004569	5.3662	0.004569	0.8734
141	0.004602	1.6705	0.004602	0.3067	0.004602	2.023	0.004602	1.3226	0.004602	5.3534	0.004602	0.8578
142	0.004636	1.6669	0.004636	0.3125	0.004636	2.0187	0.004636	1.3196	0.004636	5.3546	0.004636	0.8569
143	0.004669	1.6718	0.004669	0.3137	0.004669	2.0172	0.004669	1.3196	0.004669	5.3564	0.004669	0.8606
144	0.004702	1.6736	0.004702	0.3156	0.004702	2.0184	0.004702	1.322	0.004702	5.3568	0.004702	0.8542
145	0.004736	1.6699	0.004736	0.3223	0.004736	2.0163	0.004736	1.3242	0.004736	5.3555	0.004736	0.8643
146	0.004769	1.6708	0.004769	0.3259	0.004769	2.0132	0.004769	1.3165	0.004769	5.3586	0.004769	0.867
147	0.004802	1.6739	0.004802	0.3271	0.004802	2.019	0.004802	1.3196	0.004802	5.3574	0.004802	0.8624
148	0.004836	1.6739	0.004836	0.3253	0.004836	2.0218	0.004836	1.3062	0.004836	5.3571	0.004836	0.8569
149	0.004869	1.6678	0.004869	0.3271	0.004869	2.0212	0.004869	1.3171	0.004869	5.3543	0.004869	0.874
150	0.004902	1.6721	0.004902	0.3214	0.004902	2.0203	0.004902	1.3098	0.004902	5.3549	0.004902	0.8496
151	0.004936	1.6754	0.004936	0.3174	0.004936	2.0175	0.004936	1.3242	0.004936	5.3558	0.004936	0.8606
152	0.004969	1.6736	0.004969	0.3198	0.004969	2.0181	0.004969	1.3174	0.004969	5.3522	0.004969	0.8804
153	0.005002	1.6739	0.005002	0.3204	0.005002	2.0145	0.005002	1.3226	0.005002	5.3564	0.005002	0.864
154	0.005036	1.6736	0.005036	0.3177	0.005036	2.0197	0.005036	1.3187	0.005036	5.3461	0.005036	0.8884
155	0.005069	1.6711	0.005069	0.3131	0.005069	2.023	0.005069	1.315	0.005069	5.3549	0.005069	0.8667
156	0.005103	1.6666	0.005103	0.3125	0.005103	2.0221	0.005103	1.3174	0.005103	5.3372	0.005103	0.7993
157	0.005136	1.6708	0.005136	0.307	0.005136	2.02	0.005136	1.3248	0.005136	5.3497	0.005136	0.8603
158	0.005169	1.6721	0.005169	0.3061	0.005169	2.0209	0.005169	1.3232	0.005169	5.3543	0.005169	0.8585
159	0.005203	1.6721	0.005203	0.3107	0.005203	2.0203	0.005203	1.3129	0.005203	5.3555	0.005203	0.8643
160	0.005236	1.6705	0.005236	0.3116	0.005236	2.019	0.005236	1.3235	0.005236	5.3564	0.005236	0.8621
161	0.005269	1.6702	0.005269	0.3137	0.005269	2.0218	0.005269	1.3147	0.005269	5.3479	0.005269	0.8643
162	0.005303	1.6699	0.005303	0.3098	0.005303	2.0203	0.005303	1.3181	0.005303	5.3546	0.005303	0.8719
163	0.005336	1.6669	0.005336	0.3104	0.005336	2.0212	0.005336	1.3165	0.005336	5.3571	0.005336	0.8621
164	0.005369	1.6699	0.005369	0.3052	0.005369	2.0236	0.005369	1.3229	0.005369	5.3564	0.005369	0.8591
165	0.005403	1.6699	0.005403	0.303	0.005403	2.0209	0.005403	1.319	0.005403	5.3506	0.005403	0.8548
166	0.005436	1.6718	0.005436	0.3021	0.005436	2.0233	0.005436	1.3159	0.005436	5.3549	0.005436	0.8582
167	0.005469	1.6708	0.005469	0.2969	0.005469	2.0242	0.005469	1.3223	0.005469	5.347	0.005469	0.8621

168	0.005503	1.6699	0.005503	0.2957	0.005503	2.0206	0.005503	1.326	0.005503	5.3564	0.005503	0.8691
169	0.005536	1.6699	0.005536	0.2902	0.005536	2.0184	0.005536	1.3159	0.005536	5.3586	0.005536	0.8542
170	0.005569	1.6696	0.005569	0.2856	0.005569	2.0233	0.005569	1.3174	0.005569	5.3528	0.005569	0.8563
171	0.005603	1.6702	0.005603	0.2826	0.005603	2.0218	0.005603	1.319	0.005603	5.3528	0.005603	0.8591
172	0.005636	1.6666	0.005636	0.2811	0.005636	2.0169	0.005636	1.3126	0.005636	5.3433	0.005636	0.867
173	0.005669	1.6711	0.005669	0.278	0.005669	2.0239	0.005669	1.3235	0.005669	5.3552	0.005669	0.863
174	0.005703	1.669	0.005703	0.2753	0.005703	2.0258	0.005703	1.3248	0.005703	5.343	0.005703	0.8615
175	0.005736	1.6669	0.005736	0.2808	0.005736	2.0193	0.005736	1.2958	0.005736	5.3656	0.005736	0.8594
176	0.00577	1.6711	0.00577	0.2814	0.00577	2.0209	0.00577	1.3214	0.00577	5.3568	0.00577	0.863
177	0.005803	1.6739	0.005803	0.282	0.005803	2.0233	0.005803	1.319	0.005803	5.3629	0.005803	0.8591
178	0.005836	1.6696	0.005836	0.2884	0.005836	2.0233	0.005836	1.3208	0.005836	5.3546	0.005836	0.864
179	0.00587	1.6666	0.00587	0.2905	0.00587	2.0197	0.00587	1.3272	0.00587	5.343	0.00587	0.8682
180	0.005903	1.6705	0.005903	0.2872	0.005903	2.0279	0.005903	1.3248	0.005903	5.3577	0.005903	0.8594
181	0.005936	1.669	0.005936	0.2884	0.005936	2.0279	0.005936	1.3205	0.005936	5.3616	0.005936	0.8554
182	0.00597	1.6711	0.00597	0.2951	0.00597	2.0218	0.00597	1.319	0.00597	5.3656	0.00597	0.8545
183	0.006003	1.676	0.006003	0.2975	0.006003	2.0227	0.006003	1.3226	0.006003	5.3589	0.006003	0.8578
184	0.006036	1.6769	0.006036	0.2982	0.006036	2.0242	0.006036	1.3226	0.006036	5.3571	0.006036	0.8606
185	0.00607	1.6711	0.00607	0.3021	0.00607	2.0267	0.00607	1.322	0.00607	5.3522	0.00607	0.8664
186	0.006103	1.6693	0.006103	0.3018	0.006103	2.0209	0.006103	1.3275	0.006103	5.3619	0.006103	0.8716
187	0.006136	1.6705	0.006136	0.2963	0.006136	2.0261	0.006136	1.3251	0.006136	5.3552	0.006136	0.8588
188	0.00617	1.6718	0.00617	0.2969	0.00617	2.0282	0.00617	1.3187	0.00617	5.3668	0.00617	0.8676
189	0.006203	1.6708	0.006203	0.2994	0.006203	2.0236	0.006203	1.3156	0.006203	5.3705	0.006203	0.8676
190	0.006236	1.6727	0.006236	0.3	0.006236	2.027	0.006236	1.3232	0.006236	5.3555	0.006236	0.8655
191	0.00627	1.6754	0.00627	0.2972	0.00627	2.0251	0.00627	1.3232	0.00627	5.3653	0.00627	0.8609
192	0.006303	1.6705	0.006303	0.3018	0.006303	2.0239	0.006303	1.322	0.006303	5.3583	0.006303	0.8737
193	0.006336	1.6693	0.006336	0.3064	0.006336	2.019	0.006336	1.3229	0.006336	5.3174	0.006336	0.8615
194	0.00637	1.6705	0.00637	0.3049	0.00637	2.0221	0.00637	1.3239	0.00637	5.3577	0.00637	0.8728
195	0.006403	1.6699	0.006403	0.3079	0.006403	2.0251	0.006403	1.3214	0.006403	5.3574	0.006403	0.8765
196	0.006437	1.6666	0.006437	0.3088	0.006437	2.0258	0.006437	1.3184	0.006437	5.3595	0.006437	0.8728
197	0.00647	1.6696	0.00647	0.3107	0.00647	2.027	0.00647	1.319	0.00647	5.3549	0.00647	0.853
198	0.006503	1.673	0.006503	0.3073	0.006503	2.0218	0.006503	1.3177	0.006503	5.3525	0.006503	0.86
199	0.006537	1.6699	0.006537	0.311	0.006537	2.0227	0.006537	1.3181	0.006537	5.3525	0.006537	0.8514
200	0.00657	1.6714	0.00657	0.3119	0.00657	2.0209	0.00657	1.3211	0.00657	5.3543	0.00657	0.8649
	0.004953	**1.6716**	**0.004953**	**0.3071**	**0.004953**	**2.0202**	**0.004953**	**1.3196**	**0.004953**	**5.3564**	**0.004953**	**0.8624**

Table A2 presents the averaged data calculated from Table A1.

Table A2: Averaged data

Point [#]	Time - LL [s]	LL [V]	Time - LR [s]	LR [V]	Time - LA [s]	LA [V]	Time - RL [s]	RL [V]	Time - RR [s]	RR [V]	Time - RA [s]	RA [V]
A	0.001651	1.66935	0.001651	0.30042	0.001651	2.00932	0.001651	1.31653	0.001651	5.35625	0.001651	0.8545
B	0.004953	1.67163	0.004953	0.30713	0.004953	2.02021	0.004953	1.31964	0.004953	5.35642	0.004953	0.8624

The next step is to know what force these values represent. This can be calculated by using the calibrating values (obtained by using known masses – see Section 5). One of these calibration curves, the one for the LL-platform, is presented in Figure A4.

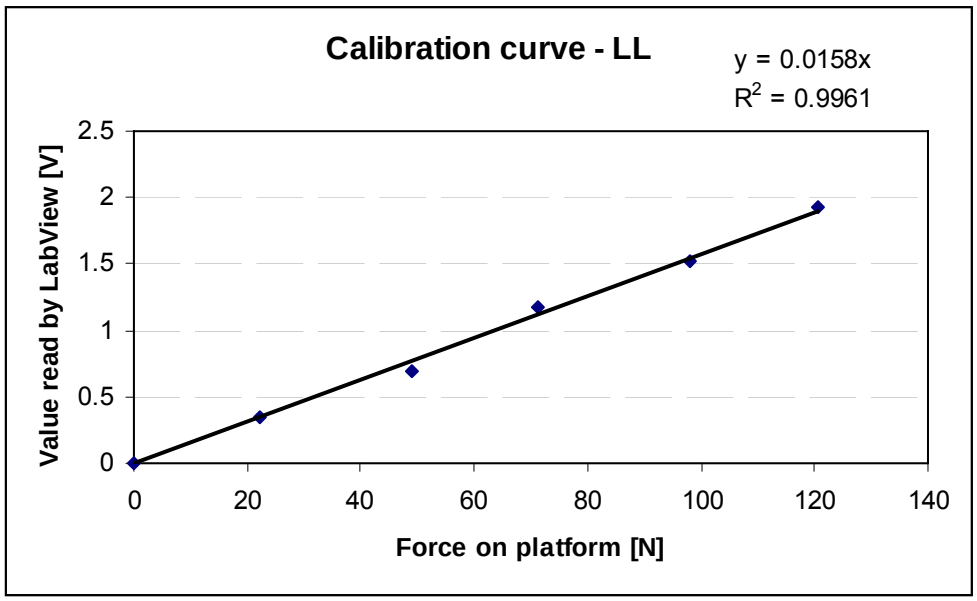

Figure A4: Calibration curve for Platform LL

Therefore, the calibration value for platform LL – to know the force present, with only the voltage measurements known – is the reciprocal of the given trend line in the Figure A4. Therefore:

Calibration value for platform LL, LL_{calib}, $= (0.01577)^{-1} = 63.43$ (A.12 A)

Thus, continuing from Table A2 to Table A3, the calibration values are used to calculate the force present on the each of the six platforms. Only that of platform LL will be done here:

For point A, from Table A2 and Equation (A.12 A):

$LL = 63.43 * 1.66935 = 105.887$ [N]

For point B, from Table A2 and Equation (A.12 A):

$LL = 63.43 * 1.67163 = 106.032$ [N]

Other calibration values are:

LR_{calib} = 94.34 (A.12 B)

LA_{calib} = 110.31 (A.12 C)

RL_{calib} = 55.94 (A.12 D)

RR_{calib} = 58.36 (A.12 E)

RA_{calib} = 240.77 (A.12 F)

Table A3: Calibrated values

Point [#]	Time - LL [s]	LL [N]	Time - LR [s]	LR [N]	Time - LA [s]	LA [N]	Time - RL [s]	RL [N]	Time - RR [s]	RR [N]	Time - RA [s]	RA [N]
A	0.001651	105.887	0.001651	28.3414	0.001651	221.648	0.001651	73.6468	0.001651	312.591	0.001651	205.75
B	0.004953	106.032	0.004953	28.9751	0.004953	222.85	0.004953	73.8206	0.004953	312.601	0.004953	207.64

It is interesting to note that, at this point, the mass of the person can be determined:

$$Mass = \frac{LL + LR + LA + RL + RR + RA}{g} \quad \text{[kg]} \qquad \text{(A.13)}$$

Therefore, the subject's mass at point A is, calculated from Equation (A.13):

$$Mass = \frac{105.887 + 28.3414 + 221.648 + 73.6468 + 312.591 + 205.75}{9.81}$$

$$= 96.623 \quad \text{[kg]}$$

The next step is to use the derived equations to acquire the exact location of the normal component of the total resultant force applied to both the platforms – see Table A4.

Table A4: Calculating the exact XY-coordinate for each point

Point [#]	VL [N]	VR [N]	V_{tot} [N]	$\bar{x}_L$ [m]	$\bar{y}_L$ [m]	$\bar{x}_R$ [m]	$\bar{y}_R$ [m]	X [m]	Y [m]
A	355.87663	591.98315	947.85978	-0.033994	-0.007626	0.0141782	0.0141272	-0.003908	0.0453166
B	357.85665	594.05786	951.91451	-0.033979	-0.007536	0.0138335	0.0140682	-0.004141	0.0451512

The following calculations show how the values in Table A4 are obtained. Note that only the values for point A will be calculated – the values for point B follows in exactly the same manner. Please note that the numbers worked with in the following calculations are rounded to two or three significant numbers, thus they may differ a little due to rounding errors.

From Equation (A.1):

$$VL = LL + LR + LA = 105.887 + 28.3414 + 221.648 = 355.87 \quad \text{[N]}$$

From Equation (A.2):

$$VR = RL + RR + RA = 73.648 + 312.591 + 205.75 = 591.98 \quad \text{[N]}$$

From Equation (A.3):

$$V_{tot} = VL + VR = 355.87 + 591.98 = 947.86 \quad \text{[N]}$$

From Equation (A.4):

$$\therefore \bar{x}_L = \frac{-(221.648)(0.1) + (28.3414 + 105.887)(0.075)}{355.87} = -0.03399 \quad \text{[m]}$$

From Equation (A.5):

$$\therefore \bar{y}_L = \frac{(28.3414 - 105.887)(0.035)}{355.8766} = -0.007626 \quad \text{[m]}$$

From Equation (A.6):

$$\therefore \bar{x}_R = \frac{-205.75(0.1) + (312.591 + 73.6468)(0.075)}{591.983} = 0.0142 \quad \text{[m]}$$

From Equation (A.7):

$$\therefore \bar{y}_R = \frac{(312.591 - 73.6468)(0.035)}{591.983} = 0.0141 \quad \text{[m]}$$

From Equation (A.9):

$$\therefore \bar{X} = \frac{355.877(-0.03399) + 591.983(0.0142)}{947.860} = -0.0039 \quad \text{[m]}$$

From Equation (A.8):

$$\therefore \bar{Y} = \frac{591.983(0.0141 + 0.158) - 355.877(0.158 - (-0.007626))}{947.860} = 0.0453 \quad \text{[m]}$$

The values calculated above are required to plot the XY-coordinates. The resulting plot for subject #6's movement of his/her resultant's normal component can then be plotted. However, this plot's location on the XY-plane differs from subject to subject. Therefore, the algebraic mean is calculated for both the X- and Y-coordinates and that point is then made to be the point (0,0) of a new graph. A recalculation of all calculated XY-coordinates is necessary in order to plot the new graph which can then be used for

comparative purposes. The equations used to calculate this new zero-point, is as follows:

$$X_{mean} = \frac{\sum_{i=1}^{n} X_i}{n} \quad \text{[m]} \tag{A.14}$$

and

$$Y_{mean} = \frac{\sum_{i=1}^{n} Y_i}{n} \quad \text{[m]} \tag{A.15}$$

This point (X_{mean}, Y_{mean}) becomes the new centre point for the graph shown in Figure A5. For subject #6, Equations (A.14) and (A.15) yield the following value:

$$X_{mean} = \frac{\sum_{i=1}^{n} X_i}{n} = 0.03203 \quad \text{[m]}$$

$$Y_{mean} = \frac{\sum_{i=1}^{n} Y_i}{n} = 0.01877 \quad \text{[m]}$$

Now, the physical point (X_{mean} = 32.03, Y_{mean} = 18.77) in millimeters becomes the point (0,0) in the new graph (presented in Figure A5). It is necessary to acquire such a new graph in order to make a comparative study of all the subjects tested. Only the centre point (0,0) is known at this stage. The whole array of data (the X- and Y-coordinates with its corresponding time values) needs to be recalculated to ensure the graph is plotted 'around' this new centre point.

But first, the physical length from the point to the centre point needs to be calculated – called the radius. This is done in order to know, later on, how 'big' the 'circle' is within which this normal component moved during the test. Calculating the radius of this circle is done by the following equation:

$$radius_i = \sqrt{(X_i - X_{mean})^2 + (Y_i - Y_{mean})^2} \quad \text{[m]} \tag{A.16}$$

Thus, the distance towards the centre point (X_{mean}, Y_{mean}) from the first point calculated (point A in Table A4) is (using Equation A.16):

$$\begin{aligned} radius_1 &= \sqrt{(X_1 - 0.03203)^2 + (Y_1 - 0.01877)^2} \\ &= \sqrt{(-0.0039 - 0.03203)^2 + (0.0153 - 0.01877)^2} \\ &= 0.03706 \qquad [m] \\ &= 37.06 \qquad [mm] \end{aligned}$$

An array is set up with these radii – for the total of the movement as well as for the three distinct parts of the experimental procedure. These parts are the two seconds before dorsiflex starts, then it is the part during the dorsiflexion movement (also two seconds) and lastly it is the part of the two seconds after the dorsiflexion motion stopped. Here is the first set of parameters to be calculated. The maximum radius for each of the parts of the test is calculated, and is an indication of stability. For subject #6, these three maximum radii are calculated to be (using Equation (A.16)):

$$radius\_\max_{BD} = 4.2 \ [mm]$$

$$radius\_\max_{DD} = 2.6 \ [mm]$$

$$radius\_\max_{AD} = 3.7 \ [mm]$$

$$radius\_\max_{TM} = 6.7 [mm]$$

Now, from these calculated radii, the actual X- and Y-coordinates, taken as (X_{mean}, Y_{mean}) is now the centre point and have to be calculated. This is done by the following relations/equations (where $X_{new\text{-}i}$ is the new X value calculated from the old X-values as well as the array of radii – the same applies to Y).

First, whilst the radiuses are being calculated, the following two arrays are also set up (where the subscript i is always the indication that the equation is used for each value – from 1 to n – where n is the total number of points after averaging):

$$\sin\_theta_i = \frac{Y_i - Y_{mean}}{radius_i} \qquad \text{(A.17)}$$

and

$$\cos\_theta_i = \frac{X_i - X_{mean}}{radius_i} \tag{A.18}$$

For the point concerned with (point A in Table A4), the above two equations yield the following results:

From Equation (A.17):

$$\begin{aligned} \sin\_theta_1 &= \frac{Y_1 - Y_{mean}}{radius_1} \\ &= \frac{0.0153 - 0.01877}{0.03706} \\ &= -0.09363 \end{aligned}$$

and

From Equation (A.18):

$$\begin{aligned} \cos\_theta_1 &= \frac{X_1 - X_{mean}}{radius_1} \\ &= \frac{-0.0039 - 0.03203}{0.03706} \\ &= -0.9703 \end{aligned}$$

Now that these three arrays are set up ($radius_i$, sin_theta_i, cos_theta_i), the desired graph can be plotted as presented in Figure A5. The coordinates (X_{new-i}, Y_{new-i}) are calculated with the following two equations:

$$X_{new-i} = (\cos\_theta_i \times rad_i) \times 1000 \quad \text{[mm]} \tag{A.19}$$

and

$$Y_{new-i} = (\sin\_theta_i \times rad_i) \times 1000 \quad \text{[mm]} \tag{A.20}$$

Finally, the first point (point A in table A4) can be plot with the above equations. From Equation (A.19):

$$\begin{aligned} X_{new-1} &= (\cos\_theta_1 \times rad_1) \times 1000 \\ &= (-0.9703 \times 0.03706) \times 1000 \\ &= 5.95 \quad \text{[mm]} \end{aligned}$$

From Equation (A.20):

$$Y_{new-1} = (\sin\_theta_1 \times rad_1) \times 1000$$
$$= (-0.09363 \times 0.03706) \times 1000$$
$$= -3.47 \quad \text{[mm]}$$

The above procedure is carried out for each of the points (after it has been averaged). These points (X_{new-i}, Y_{new-i}) are then all plotted on a fixed scale. The result for subject #6 is then the following graph (see Figure A5):

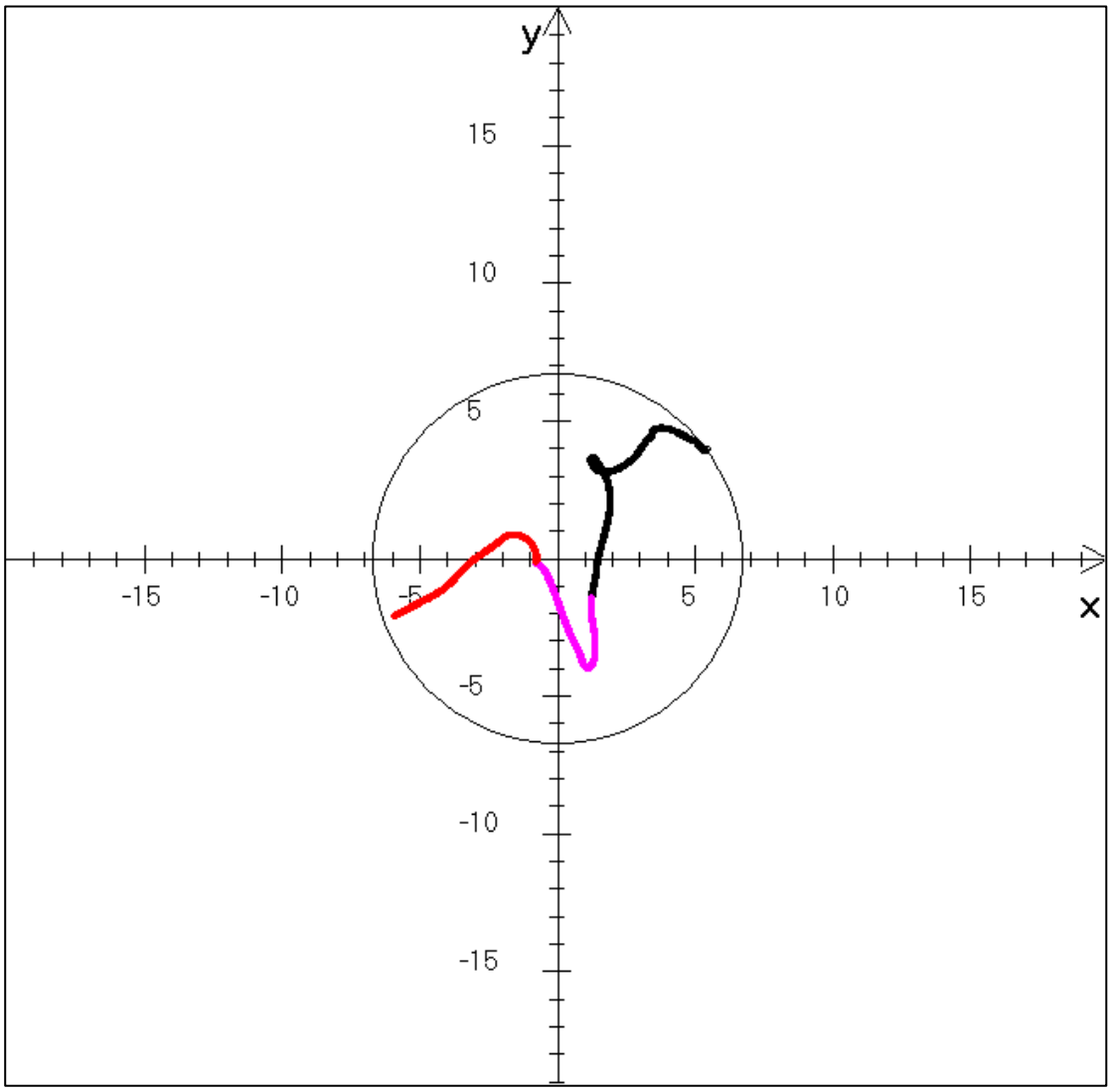

Figure A5: Resulting graph for subject #6

From Figure A5, it is clear that the radius of the outermost point from X_{mean}, Y_{mean} as the centre, is almost 7 mm. The black line is the resultant's movement for the first part of the test (before dorsiflex), the magenta line is the movement during the two seconds of dorsiflex movement (during dorsiflex) and the red line is that of the last two seconds

(after dorsiflex). The scale of this graph is kept the same, in order to do a comparing study between subjects.

Other outcomes of the computer program include a calculation of a Sway Index (SI) as well as calculating the Lyapunov exponent/number (this exponent indicates whether or not the movement is chaotic). The SI is calculated for the total movement (TM) as well as for the three parts of the movement (BD, DD and AD) using Equation (A.21).

$$SI = \frac{\sum_{i=1}^{n-1} \frac{\Delta l_i}{\Delta t}}{(n-1)} \qquad \text{[m/s]} \qquad \text{(A.21)}$$

SI_{BD}, SI_{DD}, and SI_{AD} are calculated for the three parts of the movement, while SI in Equation (A.21) is used for the whole of the movement. For subject #6, these four parameters were calculated to be:

From Equation (A.21):

$$SI_{BD} = 0.00555 \quad \text{[m/s]}$$

$$SI_{DD} = 0.00351 \quad \text{[m/s]}$$

$$SI_{AD} = 0.00641 \quad \text{[m/s]}$$

$$SI = 0.00415 \quad \text{[m/s]}$$

The equation used to calculate the Lyapunov number, where λ is called the Lyapunov exponent, (also done for the three different parts of the test – before, during and after dorsiflexion) is as follows (Strogatz, 1993):

$$\lambda = \lim_{n\to\infty}\left[\frac{1}{n}\sum_{i=0}^{n-1} \ln\left| f'(x\ , y_i)\right|\right] \qquad \text{(A.22)}$$

Because of the seeming chaotic behaviour of the movement of the normal component of the resultant force applied to the platforms during testing, these Lyapunov exponents are calculated. For stable, fixed points, λ is positive and for chaotic behaviour, λ is negative. Since n = 18000, it is considered being large enough for the infinity limit as stated in Equation (A.22). So, again, there are four parameters calculated for the

subject with regard to the Lyapunov number/exponent. Using Equation (A.22), the results for subject #6, is calculated as:

$$\lambda_{BD} = -5.31$$
$$\lambda_{DD} = -5.77$$
$$\lambda_{AD} = -5.86$$
$$\lambda = -5.65$$

Note that the relatively highly negative values for the subject imply that the movement is chaotic in nature and hence not readily amenable to statistical analysis.

This concludes all the calculations done for this experiment and test. Every subject's data is analysed using the above method, so that their different parameters could be compared and analysed.

Appendix B: Market and IP Positioning

The Dorsiflexometer

Adopted from "Pinki" (2004) in conjunction with Acorn Industries

Industry and Marketplace analysis

In 2000, the global medical device market was valued at over US$100 billion. A major portion of which (approximately 43%) was generated from the U.S. market. Today, the USA contributes to approximately 50% of the global medical devices market, followed by Europe (27%) and Japan (11%). The rest of the world only contributes 14% of the global medical devices market[1].

Firms engaged in medical devices production reported net revenues of US$2.6 billion in 2000, according to the results of the Medical Devices Industry Survey. The orthopaedic device industry accounts for 15% of the medical device industry internationally, and was valued at US$22 million in 2002[2].

The medical rehabilitation industry, reducing physical impairments and restoring lost abilities, was estimated to be worth more than US$12 billion to US$15 billion in 2001[3].

Customer Analysis

The human population is aging worldwide, and this is one of the driving forces for growth of the orthopaedic device industry. The target market for this device will be the aged population. The Dorsiflexometer will be used as a measuring tool to determine the success or failure of a medical procedure or medication intended to cure posture and gait-related problems. The device is constructed to objectively measure an individual's balance and dorsiflexion range.

The key customers for the device will be physicians, physiotherapists and hospitals as well as medical clinics.

The estimated selling price per unit of the Dorsiflexometer is R 250,000. The tables below illustrate the sales figures derived from different market penetrations percentages.

International

[1] estimated from Frost&Sullivan + ReNeuron + MedTech Insight + EpiGenesis + Alcavis + Mediligence, 2003.

[2] World medical report

[3] www.bizjournals.com

Country	Number of Hospitals	Number of Physicians	Number of Physiotherapists
USA	6,600	811,440	132,000
Germany	2,000	292,050	85,000
France	3,830	182,103	55,000
Switzerland	420	24,192	10,000
South Africa	808	199,350	4,000
Total	13,658	1,509,135	286,000

Market penetration	Hospitals	Sales (R)	Physicians	Sales (R)	Physiotherapists	Sales (R)
0.5%	68	17,072,500	7,546	1,886,418,750	1,430	357,500,000
1%	137	34,145,000	15,091	3,772,837,500	2,860	715,000,000
2%	273	68,290,000	30,183	7,545,675,000	5,720	1,430,000,000
5%	683	170,725,000	75,457	18,864,187,500	14,300	3,575,000,000
10%	1366	341,450,000	150,914	37,728,375,000	28,600	7,150,000,000
15%	2049	512,175,000	226,370	56,592,562,500	42,900	10,725,000,000

South Africa

Market penetration	Hospitals	Sales (R)	Physicians	Sales (R)	Physiotherapists	Sales (R)
0.5%	4	1,010,000	997	249,187,500	20	5,000,000
1%	8	2,020,000	1,994	498,375,000	40	10,000,000
2%	16	4,040,000	3,987	996,750,000	80	20,000,000
5%	40	10,100,000	9,968	2,491,875,000	200	50,000,000
10%	81	20,200,000	19,935	4,983,750,000	400	100,000,000
15%	121	30,300,000	29,903	7,475,625,000	600	150,000,000

South Africa

2% Market Penetration	2005	2006	2007	2008	2009	2010
Number of Units	16	32	64	128	256	312
Price per unit (R)	250,000	250,000	250,000	250,000	250,000	250,000
Unit Revenue (R)	4,000,000	8,000,000	16,000,000	32,000,000	64,000,000	78,000,000
COGS (R)	1,400,000	2,400,000	4,800,000	9,600,000	19,200,000	23,400,000
Gross Profit (R)	2,600,000	5,600,000	11,200,000	22,400,000	44,800,000	54,600,000
Distributor's margin	0.30	0.30	0.30	0.30	0.30	0.30
Net Profit (R)	**1,820,000**	**3,920,000**	**7,840,000**	**15,680,000**	**31,360,000**	**38,220,000**

Assumptions: R 200,000 required in Year 1 to put a prototype in place; COGS R 75,000 per unit.

Competitor Analysis

NeuroCom® International, Inc.

NeuroCom® International, Inc. is involved in the development of computerised tools for the assessment and rehabilitation of patients with balance and mobility disorders.
There are more than one thousand medical and academic institutions utilizing NeuroCom technology in the United States and abroad.

Products

Prices of the equipment for gait analysis range from US$100,000 to US$500,0004. The price of the Dorsiflexometer is estimated at R 250,000 per unit. The Balance Master® (NeuroCom® International, Inc.) consists of a computer and a force platform with 4 transducers beneath each of the 4 corners of the platform.

Alternatives

An example of a balance board/moving platform available on the market is the “Wobble Board”. It is used to improve a person balance response by measuring how long a person can keep their balance. It is manufactured by Fitter International and sells for US$59.95 per unit.

[4] The Interdisciplinary Journal of Rehabilitation. Gait Analysis comes out ahead.

Intellectual property

128-774 SR
10/22/85 OR 4,548,289

United States Patent [19]
Mechling

[11] **Patent Number: 4,548,289**
[45] **Date of Patent: Oct. 22, 1985**

[54] **VARIABLE RESISTANCE TILTBOARD FOR EVALUATION OF BALANCE REACTIONS**

[76] Inventor: **Richard W. Mechling,** 830 Vedado Way, NE., Atlanta, Ga. 30308

[21] Appl. No.: **551,061**

[22] Filed: **Nov. 14, 1983**

[51] **Int. Cl.**[4] **A61B 5/10**
[52] **U.S. Cl.** **128/774;** 128/782
[58] **Field of Search** 128/774, 782; 272/146, 272/DIG. 6

[56] **References Cited**

U.S. PATENT DOCUMENTS

3,416,792	12/1968	Morgan et al. .	
3,605,732	9/1971	Rapoza .	
3,702,188	11/1972	Phillips et al.	272/146 X
3,890,958	6/1975	Fisker et al.	128/774 X
3,984,100	10/1976	Firster .	
4,183,521	1/1980	Kroeker .	
4,270,749	6/1981	Hebern .	
4,306,714	12/1981	Loomis et al. .	

FOREIGN PATENT DOCUMENTS

825000	4/1981	U.S.S.R.	128/774

OTHER PUBLICATIONS

Terekhov, "Measuring Mans Stability of Stance", Jrnl. Clin. Eng., vol. 4, No. 1, Jan.-May, 1979, pp. 61-65.
"Construction of a Stabilometer Capable of Indicating the Variability of Non-Level Performance", *Perceptual and Motor Skills,* Dec., 1982.
"Specificity vs. Generality in Learning and Performing Two Large Muscle Tasks", *The Research Quarterly,* vol. 32, No. 1, 1961.
"Body Oscillations in Balancing Due to Segmental Stretch Reflex Activity", *Experimental Brain Research,* 1980.

Primary Examiner—Edward M. Coven
Attorney, Agent, or Firm—Jones & Askew

[57] **ABSTRACT**

A method and apparatus for the objective analysis of human balance reactions involving a pivotable platform and a variably positionable viscuous damping device which provides a known resistance to angular displacement of the platform. Parameters of movement of the platform such as differential weight and angular velocity for varying resistances are recorded as a measure of the subject's balance and motor skills.

22 Claims, 5 Drawing Figures

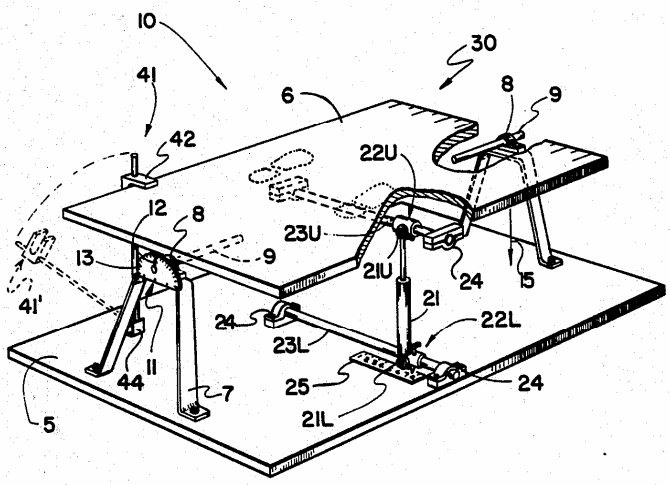

United States Patent 4,548,289
Mechling October 22, 1985

Variable resistance tiltboard for evaluation of balance reactions

Abstract

A method and apparatus for the objective analysis of human balance reactions involving a pivotable platform and a variably positionable viscous damping device which provides a known resistance to angular displacement of the platform. Parameters of movement of the platform such as differential weight and angular velocity for varying resistances are recorded as a measure of the subject's balance and motor skills.

I claim:

1. An apparatus for the objective analysis and quantification of human balance reactions, comprising:

- a base; a platform pivotably supported above said base for supporting a person whose balance reactions are to be analysed;

- variable resistance means operatively associated with said platform and said base for providing a selectively variable predetermined resistance to the movement of said platform relative to said base; and

- measuring means operatively associated with said platform and said base for measurement of a parameter of the movement of said platform relative to said base so as to obtain an objective quantification of a person's balancing ability.

2. The apparatus as described in claim 1, wherein said variable resistance means comprises viscous damping means.

3. The apparatus as described in claim 1, wherein the resistance to movement of said platform relative to said base is directly proportional to and in the opposite direction of the instantaneous velocity of said platform relative to said base.

4. The apparatus as described in claim 3, wherein the proportionality of resistance to movement of said platform relative to said base is variable.

5. The apparatus as described in claim 1, wherein said variable resistance means comprises a conventional automotive shock absorber having a longitudinal axis oriented substantially perpendicular to an axis of rotation of said platform relative to said base, said shock absorber being mounted between and having opposite ends attached to said platform and said base.

6. The apparatus as decribed in claim 5, wherein said shock absorber is variably positionable with respect to said axis of rotation of said platform relative to said base.

7. The apparatus as described in claim 5, further comprising a second conventional automotive shock absorber having a longitudinal axis oriented substantially perpendicular to a second axis of rotation of said platform relative to said base, said shock absorber being mounted between and having opposite ends attached to said platform and said base.

8. The apparatus as described in claim 1, further comprising means for immobilizing said platform at a predetermined angular position relative to said base.

9. The apparatus as described in claim 8, wherein said immobilizing means is operative to release said platform from said predetermined position to allow movement.

10. The apparatus as described in claim 1, wherein said variable resistance means comprises means for resisting angular movement of said platform relative to said base.

11. The apparatus as described in claim 1, wherein said variable resistance means comprises resisting means selectively positionable with respect to an axis of rotation of said platform relative to said base.

12. A method of objectively evaluating the balance reactions of a subject, comprising the steps of:

- selecting a predetermined resistance to displacement of a movable platform to match;
- the subject's level of balance skill;

- situating the subject on the platform;

- allowing the subject to attempt to maintain balance on the platform; and

- recording a movement parameter of the platform produced by the subject's reactions to the platform so as to obtain an objective quantification of the subject's balancing ability.

13. The method of claim 12, wherein the person is situated in a standing position.

14. The method of claim 13, further comprising the step of situating the feet of the person on the platform at predetermined positions with respect to an axis of angular displacement of the platform.

15. The method of claim 12, wherein the person is situated on hands and knees.

16. The method of claim 12, further comprising the steps of:

providing a second predetermined resistance to the displacement of the platform; and

recording a second movement parameter of the platform produced by the person's reactions to the platform.

17. The method of claim 12, further comprising the steps of providing a predetermined displacement for the platform prior to the step of situating the person on the platform, and releasing the platform from the predetermined displacement prior to recording the movement parameter.

18. The method of claim 12, wherein the step of recording a movement parameter of the platform comprises determining the relative displacement of the platform, and recording the determined relative displacement.

19. The method of claim 12, wherein the step of recording a movement parameter of the platform comprises determining the angular velocity of the platform, and recording the determined angular velocity.

20. The method of claim 12, wherein the step of recording a movement parameter of the platform comprises determining the differential weight shifted by the person over a given body limb in response to movement of the platform, and recording the differential weight.

21. The method of claim 11, wherein said predetermined resistance is an initial predetermined resistance, and further comprising the step of decreasing said initial predetermined resistance to provide a lower, second predetermined resistance for a subject demonstrating improved or progressive balance skills relative to said initial predetermined resistance.

22. The method of claim 11, wherein said predetermined resistance is an initial predetermined resistance, and further comprising the step of increasing said initial predetermined resistance to provide a higher, second predetermined resistance for a subject demonstrating handicapped or regressive balance skills relative to said initial predetermined resistance.

US005820096A

United States Patent [19]

Lynch et al.

[11] Patent Number: 5,820,096

[45] Date of Patent: Oct. 13, 1998

[54] **ADJUSTABLE KINETIC STABILIZATION INSTRUMENT**

[76] Inventors: **James M. Lynch**, 10200 Breckenridge Ave., St. Ann, Mo. 63074; **Teresa A. Lynch**, P.O. Box 10457, Jackson, Wyo. 83001; **James R. Moe**, 2419 Mayer Dr., St. Charles, Mo. 63301

[21] Appl. No.: **959,186**

[22] Filed: **Oct. 28, 1997**

[51] **Int. Cl.**[6] **A47B 91/00**

[52] **U.S. Cl.** **248/346.01**; 601/27

[58] **Field of Search** 248/143, 144, 248/318, 346.01, 346.06; 601/23, 31

[56] **References Cited**

U.S. PATENT DOCUMENTS

3,136,522	6/1964	Calderone	248/318
4,183,521	1/1980	Kroeker .	
4,505,477	3/1985	Wilkinson .	
4,613,131	9/1986	Anderson .	
4,618,145	10/1986	Inada .	
4,619,462	10/1986	Shaffer et al.	280/242.1
4,736,205	4/1988	Dodge	340/985
4,801,140	1/1989	Bergeron .	
5,048,823	9/1991	Bean .	
5,112,045	5/1992	Mason et al. .	
5,512,912	4/1996	Ross et al.	343/765
5,536,226	7/1996	Gordon .	
5,547,460	8/1996	Ishikawa .	
5,549,536	8/1996	Clark .	
5,582,567	12/1996	Chang .	
5,671,990	9/1997	Teasdale	248/318

Primary Examiner—Ramon O. Ramirez
Assistant Examiner—Robert Lipcsik
Attorney, Agent, or Firm—Kevin L. Klug

[57] **ABSTRACT**

An adjustable kinetic stabilization instrument having a balance platform which provides rotational and linear movement in two axis versus a shift in center of gravity relative to its geometric center. The adjustable kinetic stabilization instrument is used by physical therapists and physical trainers to help improve or revive a person's sense of kinesthesia when a person stands on the platform. The adjustable kinetic stabilization instrument has a plurality of eyelets into which the pivotable pedestal supports may be placed in order to make the platform more or less sensitive to the center of gravity offset caused by the person using the instrument.

8 Claims, 7 Drawing Sheets

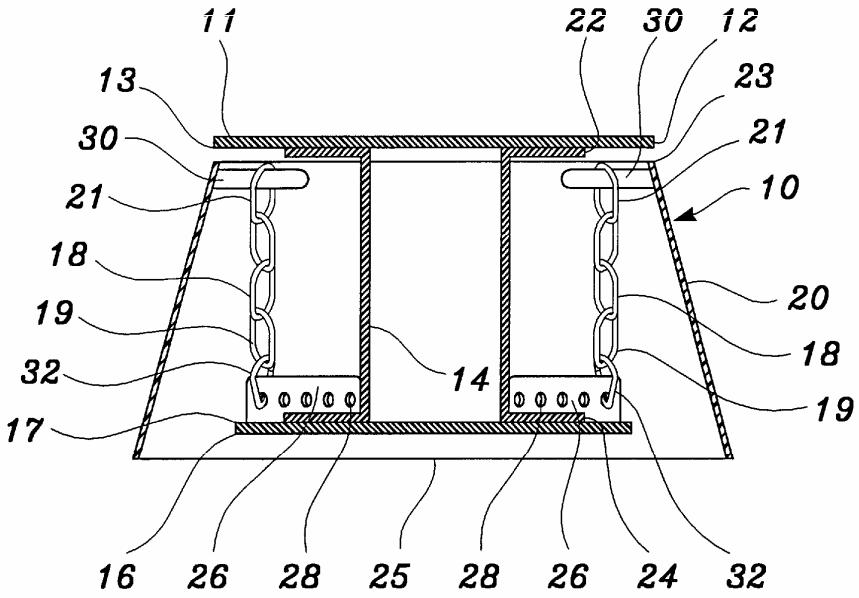

Adjustable kinetic stabilization instrument

Abstract

An adjustable kinetic stabilization instrument having a balance platform which provides rotational and linear movement in two axis versus a shift in center of gravity relative to its geometric centre. The adjustable kinetic stabilization instrument is used by physical therapists and physical trainers to help improve or revive a person's sense of kinesthesia when a person stands on the platform. The adjustable kinetic stabilization instrument has a plurality of eyelets into which the pivotable pedestal supports may be placed in order to make the platform more or less sensitive to the center of gravity offset caused by the person using the instrument.

What is claimed is:

1. An adjustable kinetic stabilization instrument for improving a person's sense of kinesthesia, comprising:

- a platform of substantially flat shape, having an upper side and a lower side; and

- a platform support pedestal, having a topside and a bottomside, said topside mounted onto said lower side of said platform; and

- a pedestal base plate of substantially flat shape and having a mounting surface, said mounting surface of said pedestal base plate mounted onto said bottomside of said platform support pedestal, said pedestal base plate having four or more support attachment brackets mounted onto said pedestal base plate substantially equidistant from the geometric center of said pedestal base plate; and

- said four or more support attachment brackets each having one or more support structure eyelets; and

- a frame with sidewalls, having a bottom, a top and four or more frame support pins

removably attached substantially equidistant from the geometric center of said top of said frame with sidewalls and near said top; and

- four or more pivotable pedestal supports each having a first end and a second end, said second end pivotally attached to a distinct said frame support pin and each of said first ends having an attached snap link; and

- each of said snap links removably and pivotally attached to a distinct said support attachment bracket through said one or more support structure eyelets, whereby rotation and linear movement of said platform may occur as the centre of gravity is shifted away from the geometric center of said platform.

2. The adjustable kinetic stabilization instrument as set forth in claim 1 whereby: said pivotable pedestal supports comprise chains.

3. The adjustable kinetic stabilization instrument as set forth in claim 1 whereby: said pivotable pedestal supports comprise cables.

4. The adjustable kinetic stabilization instrument as set forth in claim 1 further comprising:

- a sealing material placed onto and across said bottom of said frame with sidewalls, thereby forming a cavity within said frame with sidewalls; and

- a dampening fluid placed into said cavity thereby helping to dampen the linear and rotational movement of said platform.

5. An adjustable kinetic stabilization instrument for improving a person's sense of kinesthesia, comprising:

- a platform of substantially flat shape, having an upper side and a lower side; and

- a platform support pedestal, having a topside and a bottomside, said topside mounted onto said lower side of said platform; and

- a pedestal base plate having a mounting surface, said mounting surface of said pedestal base plate mounted onto said bottomside of said platform support pedestal, said pedestal base plate having four or more support attachment brackets mounted onto said pedestal base plate substantially equidistant from the geometric center of said pedestal base plate; and

- four or more pivotable pedestal supports each having a first end and a second end, said first end having means to removably attach said pivotable pedestal support to a distinct said support attachment bracket and;

- said four or more support attachment brackets each having means for removably and adjustably attaching said first end of said pivotable pedestal support; and

- a frame with sidewalls, having a bottom, a top and means for attaching to said second ends of said pivotable pedestal supports, substantially equidistant from the geometric center of said top of said frame with sidewalls and near said top, whereby rotation and linear movement of said platform may occur when the centre of gravity of said platform is shifted from its geometric center.

6. The adjustable kinetic stabilization instrument as set forth in claim 5 further comprising:

- a means for dampening the linear and rotational movement of said platform.

7. An adjustable kinetic stabilization instrument for improving a person's sense of kinesthesia, comprising:

- a platform of substantially flat shape, having an upper side and a lower side; and

- a platform support pedestal, having a topside and a bottomside, said topside mounted onto said lower side of said platform; and

- a pedestal base plate of substantially flat shape and having a mounting surface, said mounting surface of said pedestal base plate mounted onto said bottomside of said platform support pedestal, said pedestal base plate having four or more support

attachment brackets mounted onto said pedestal base plate substantially equidistant from the geometric centre of said pedestal base plate; and

- said four or more support attachment brackets each having a plurality of support structure eyelets; and

- a frame with sidewalls, having a bottom, a top and four or more frame support pins removably attached substantially equidistant from the geometric center of said top of said frame with sidewalls and near said top; and

- four or more pivotable pedestal supports each having a first end and a second end, said second end pivotally attached to a distinct said frame support pin and each of said first ends having a means for removably and pivotally attaching to one of said plurality of eyelets; and

- each of said first ends of said pivotable pedestal supports, attached via said means for removably and pivotally attaching, to a distinct said support attachment bracket through one of said plurality of support structure eyelets, whereby rotation and linear movement of said platform may occur as the centre of gravity is shifted away from the geometric center of said platform and said movement is adjustable by moving said first ends of said pivotable pedestal supports to another of said plurality of support structure eyelets.

8. The adjustable kinetic stabilization instrument as set forth in claim 7 further comprising:

- a sealing material placed onto and across said bottom of said frame with sidewalls, thereby forming a cavity within said frame with sidewalls; and

- a dampening fluid placed into said cavity thereby helping to dampen the linear and rotational movement of said platform.

Funding

Technology and Human Resource for Industry Programme (THRIP)

The Programme aims to improve the competitiveness of South African industry, by

supporting research and technology development activities and enhancing the quantity and quality of appropriately skilled people.

THRIP is managed by the National Research Foundation (NRF) and the Department of Trade and Industry (DTI). Grants that match contributions by industry to project activities that qualify for THRIP support, are provided by the DTI/NRF.

CRITERIA FOR THRIP SUPPORT

- The project must be a high quality science, engineering and/or technology research project whose outputs could make a significant contribution towards improving the industry partner's competitive edge.
- At least one registered South African student (at 4th level or higher) must be involved in and trained through the researcher per R150 000 of THRIP investment.
- The project must have clearly defined scientific and/or technology outputs, plus human resource outputs expected for each year of support.
- In the case of "first-time applicants" (project leaders) who are based in either a technikon or HBU, the absence of clearly defined technology outputs in the first year of support, may be overlooked.
- The project leader must have an employment contract with the HEI or Engineering and Technology Institutions (SETI).
- Where the project leader is based at a SETI the project proposal must clearly demonstrate the participation and training of students enrolled at the HEI/s.
- At least one HEI and one industrial partner must be involved.
- The industrial partner must give a clear indication that the project will directly benefit the specific company.
- Commitment from the industrial partner must be clearly shown in terms of investment in the project.
- In the case of a foreign industrial partner there must be an indication of how South Africa stands to benefit from the technology outcomes resulting from the collaboration.
- Arrangement for the ownership and exploitation of intellectual property arising from a project must be agreed upon between the HEI/SETI and industrial partner/s prior to commencement of the project. Such an agreement may not restrict publication of any research results for more than two years after the agreed scheduled completion date of the project.
- Receipt of a complete and satisfactory project proposal.

- Where the application is for continuation of support for a project, the application must be accompanied by:

- a complete and satisfactory progress/annual report
- An evaluation of the reported progress, by the industry partner/s, as being satisfactory.

Appendix C: Theoretical Time of Response of a Patellar Tap Reflex Example

This appendix is necessary in order to know how fast humans can react (Refer to Section 2.2). An autonomic reaction requires no higher brain function, and therefore is the fastest reaction a human can perform.

The timing sequence of a patellar tap reflex can be calculated as follows (Freivalds, 2004). The annulospiral, synapse, neuromuscular junction, and en plate all have approximately 1 ms delays. The large α neurons conduct action potentials at a minimum of 100 m/s. Assuming a knee tap and the neuron stretching is 0.5 m to the L_5/S_1 level of the spinal cord, nerve conduction in either direction requires 5 ms. In addition the extrafusal fibers need a minimum of 20+ [ms] to generate enough force to contract and move the muscle. As a result there is a minimum of a 34 ms delay before any muscle contraction would be apparent. Table C1 tabulate the different elements involved and the corresponding times taken to perform the relation of impulses.

Table C1: Depicting times taken for different actions

Element	Time *[ms]*
Annulospiral	*1.0*
α_{aff}	5.0
Synapse	1.0
α_{eff}	5.0
Neuromuscular junction	1.0
End plate potential	1.0
Force build-up	20.0
Total	**34.0**

Appendix D: Motor Operating Procedure

One of the programming 'problems' that had to be overcome was to operate the motors with the appropriate controls. Since the signal to the drivers (from the LabView-card) is a digital high or low, the programming had to be done accordingly. There is, on the user interface of the LabView program, written for the purpose of driving the motors, a control to switch both platforms on or off and then there are two for the left and right platforms respectively. A flow diagram of this subsection problem is as follows (see Figure D1):

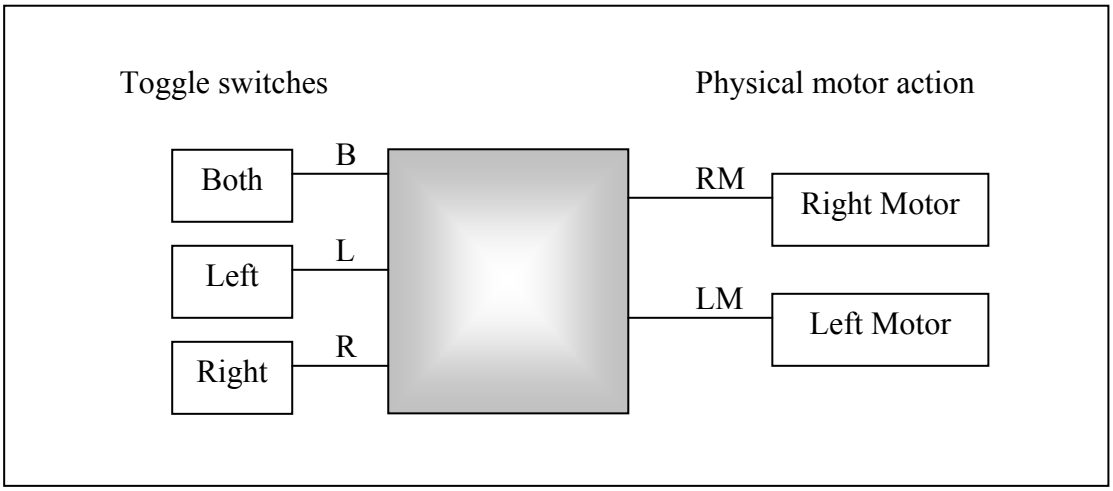

Figure D1: Diagram depicting motor operating problem addressed

The problem – put into simple terms – is what to put in the shaded box of Figure D1. The only way to address this problem is to use Boolean algebra. Therefore, the truth table corresponding to the problem is the following (see Table D1).

Table D1: Truth Table

	Input parameters			*Output*	
	B	L	R	LM	RM
1	0	0	0	0	0
2	0	0	1	0	1
3	0	1	0	1	0
4	0	1	1	1	1
5	1	0	0	1	1
6	1	0	1	1	1
7	1	1	0	1	1
8	1	1	1	1	1

From the truth table, the following equation can be formulated:

LM = (B+L+R)(B+L+R') and RM = (B+L+R)(B+L'+R)

= BB + LB + BR' + LB + LL + LR' + RB + RL + RR'

= B + LB + BR' + LB + L + LR + RB + RL

= B + L + LB + L(R'+R)' + B(R'+R)'

= B + L + L + B + LB

= L + B + LB

= L(1+B) + B

= L + B

therefore,

RM = R + B

Thus, the grey box in Figure D1 can be replaced by the following (see Figure D2):

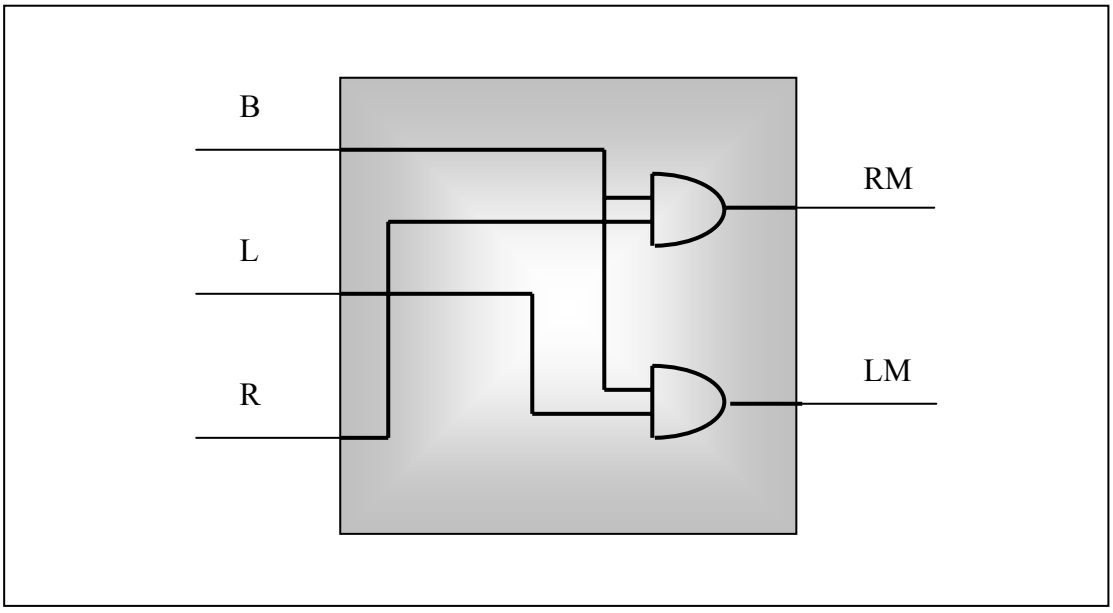

Figure D2: Solution to the motor operating problem

Appendix E: Dorsiflexometer Patent (provisional)

South African Patent **78-5568-879**
Botha **October 13, 2004**

A Device for the Investigation of Dorsiflexion range of the Foot with a Capacity to Measure Pathology, Recovery and Pharmaceutical benefit

Abstract

A device has been constructed to objectively measure an individual's balanced dorsiflexion range. This is beneficial for biomedical mesuration with pharmaceutical efficacy assessment. The device consists of two independently controlled platforms each of which incorporates a force platform. By tilting a platform (or both) to a specific new (known) position, the individual's reaction to this perturbation can be measured. The time it takes for the human to 'find' its balance position is the parameter measured and this is then correlated with a 'normal' value to give an indication of how adaptable the individual is. Dorsiflexion range can also be measured by simply tilting both the platforms until the person cannot sustain balance and becomes unstable. Dorsiflexion range is an important parameter of gait since hypertonia creates difficulties with gait. Another test may be to evaluate the 'cross talk' between the two lower limbs of a subject and therefore document differences in the performance of one lower limb relative to the other. This last test may be useful in determining, by bilateral comparison, physiological and neurological problems associated with a specific individual – and thereafter monitoring therapeutic improvement.

Inventors: Botha, J, Dobson, R T & Driver-Jowitt, J P
Appl. No.: 5586996
Filed: November 2004

Currnet U.S. Class:
Intern'l Class:
Field of Search:

References Cited [Referenced By]

4,548,289	Nov., 1983	Mechling
5,052,406	Jan., 1987	Nashner

Claims

What is claimed is:

1. A device with the object of measuring and thus quantifying the dorsiflexion range of a human and its relation to gait efficiency, as well as resistance to perturbation. The device consists of:

   two independent platforms;

   these platforms are supported on an axis which is above the base of the device. Both platforms can be rotated (individually) to plus and minus 20 degrees from horizontal. This rotation is the effect of two stepper motors attached to each of the platforms. The stepper motor and platform of each subassembly is connected via a worm gear configuration to give a known pivot angle for a specific number of rotations of the stepper motor.

   two force platforms mounted on each platform;

   the purpose of the mounted force platform on each independent platform is to measure the vector of the individual's (standing with one foot on each of the platforms) centre of gravity. This is being deduced form the centre of pressure, which is actually being measured.

   a computer;

   the computer with its associated software is necessary to read the output of both said force platforms, as well as giving each of the platforms the predestined angle of rotation. The computer also relates the measured data to a norm and

from this quantifies the individual's balance (capability). The software is also being written to activate a random selection of protocol possibilities so as to ensure that the specific human present on the device cannot anticipate the movement of either of the platforms and therefore ensure a trustworthy balance test.

2. A method of objectively evaluating the balance reaction of a individual, comprises of the following steps:

   - selecting the appropriate balance measuring scale proportional to an assumed range of dorsiflexion of the individual on the user-friendly computer interface
   - situating the individual on both platforms – one foot on each of the platforms
   - asking the person to keep balance as the device starts its protocol
   - recording all relevant information (gathered by the computer) of the whole protocol sequence and the information from each of the two platforms.
   - the computer then quantifies the individuals balance and/or performance of each of the two lower limbs separately (depending on which test protocol has been chosen at the start of the test). This can then be compared to previous tests run on the same individual to see improvement or deterioration of balance or 'cross-talk' or performance of each individual lower limb.

3. The apparatus described in claim 1, starts off at with both platforms parallel to the horizontal axis.

4. The platforms described in claim 1, moves relative to the said base.

5. The balance test procedure described in claim 2 works on the basis that the subject should not be assisted in balancing (e.g. a stationary handle) except the position when balance can no longer be accommodated by their dorsiflexion range.

6. The method of claim 2 implies that the only way the subject could adjust to a non-horizontal platform is via plantar- and dorsiflexion actions, and without compensation by flexion of the hip or flexion of the knees or hyperextension or head movement relative to the body in the sagittal plane.

7. As in claim 6, hip flexion and flexion of the knee can be monitored visually by the person controlling the test.

8. As in claim 5, hyperextension and head movement relative to the body in the saggital plane can be monitored visually by the person controlling the test.

9. Claims 7 and 8 can also be done (more objectively) by placing markers/reflectors on the subjects head, hip, knee, and ankle to be monitored during the test by a high-speed video camera.

10. Claim 9 would be applicable if visual monitoring as described in claims 7 and 8 is found inaccurate.

11. Claim 1, further comprising the step of situating the feet of the person on both platforms at predetermined positions with respect to an axis of angular displacement of the platform.

12. The method of claim 2, further comprising the step of having appropriate assistance to ensure the security of the subject if balance is lost.

13. This fills the demand for a quick, easy way to quantify a subjects balance capabilities in the sagittal plane.

14. Claim 13 includes that the test (being done in the sagittal plane) provides an easy way (without the problem of incorporating more degrees of freedom) to interpret results.

15. In claim 14, the said results refer to the final outcome of the test that is displayed on the computer screen.

16. In claim 15 the way in which results can be attained is also through a print-out that can be made of the displayed results.

17. Though this invention falls in the broad category of posturography, it provides more information regarding an individual's ability to maintain balance because it is comprised of two independently movable platforms.

18. Claim 17 suggests with posturography that its uniqueness lies in the fact that it assesses capacity for musculo-skeletal adaptations at the level of the ankle rather than attempting to assess peripheral neurological control or central vestibular function more directly.

19. Posturography as in claim 18 is not intended to provide any information regarding aetiology; it does provide functional information regarding how well an individual can use their musculo-skeletal adaptivity and an indication of the importance of a patient's adaptive disturbance on activities of daily living.

Description

FIELD OF THE INVENTION

The discussed invention fits into the musculo-skeletal field of assessing an individual's ground adaptive balance abilities. It can be characterized into the smaller group of posturography, though it differs quite significantly from prior inventions in this field as it consists of two independently tiltable platforms. The purpose of which is to quantify how 'good' or 'bad' is an individual's adaptive capacity.

DESCRIPTION OF PRIOR ART

The capacity of fundamental importance in human function is that of a "balancing machine". The human has to cope with the forces of gravity in the three dimensions of his space, within time constraints. This is done by constantly using sensor mechanisms to send the relevant information to the brain with a frequent re sampling of the position of the body in space. An important source of that information derives from the feet. The brain then makes the relevant decisions and this is translated into calculated, highly refined muscle movements on a micro-second to micro-second basis. In general, the act of balancing for a biped such as a human involves the movement of one's centre of gravity away from a base of support. As this movement of the centre of gravity occurs, skin pressure receptors and proprioceptive muscle tension receptors in the support limbs sense the mass transfer in a particular direction. Additionally, the visual sensors detect the tilting of the visual field and the semicircular canals detect movement of the

head. All this sensory input is integrated by the central nervous system which sends the appropriate instructions to the relevant muscles to sustain balance. Skillfulness and speed of balance depends on the accuracy of these sensory inputs (among other things), and therefore the efficacy of postural control.

A variety of brain disorders exists that impair the ability to perform posture and motor acts such as walking and standing still. Some of the examples include:

- Parkinson's disease,
- Cerebellar degeneration,
- Multiple sclerosis
- Cerebro-vascular damage
- Cerebral palsy
- Certain forms of developmental learning disorders that impair these motor functions.

In all of the above instances, the nature and degree of impairment can vary widely, depending on the localization or extent of the brain injury. In some instances, the impairment can be unequally distributed between sensory and motor aspects of posture and movement control, while in other cases it can be bilaterally unequal.

Treating individuals with defects of muscular skeletal adaptive control is common practice. Therefore objective measurement of treatment efficacy is important. It seems that current measurement techniques are insufficient. This device fills that gap.

Three devices available will be discussed, along with their associated shortcomings.

The stabilometer:

This apparatus has been used to evaluate muscle coordination or skill and motor learning ability and is described in Bachman, "Specificity vs. Generality in Learning and Performing Two Large Muscle Motor Tasks," The Research Quarterly, Vol. 32, No. 1, 1961. The apparatus consists of a subject standing erect on a horizontal platform (a pivotable board), with the feet about 30 [cm] apart from one another. The centre of rotation in this apparatus is placed approximately 25 [cm] above the board upon which the individual stands. Ease of the conducted balance test is attained by the low position of the board relative to the axis of rotation. The motion of the stabilometer is measured

with a work adder. Any movement of the board is recorded on a flat disk which carriers a calibrated deal scaled in arbitrary units, each unit generally representing about twelve degrees of platform tiling. Microswitches fastened under each end of the tilting board and wired in series with an electric clock ensure that all movement is recorded only when the subject has the board completely out of balance as opposed to at rest against a baseboard and can thereby rest without movement.

The problem with this stabilometer is that it approaches the evaluation of balance skills with free movement of the board. This means that subjects with severe balance disorders are unable to perform this test. One needs a device that is adjustable to various degrees of balance disorders – as the proposed invention does – to incorporate subjects across the whole spectrum for testing (except of course persons that are unable to stand in the first place).

Variable resistance tiltboard for evaluation of balance reactions:

This device, (US patent no. 4,548,289) invented by R. W. Mechling, overcomes the above-stated problem by having different resistance settings which can be set so that virtually any balance disorder patient can perform the test. This device also consists of a platform (only one, though) that is tiltable in the saggital plane with one degree of freedom. The resistance being referred to here is attained through viscous damping. On each of the two loose ends of the platform, a damper is situated. Thus, the device involves a pivotable platform and a variably positionable viscous damping device which provides a known resistance to angular displacement of the platform. Parameters of movement of the platform such as differential weight and angular velocity for varying resistances are recorded as a measure of the subject's balance and motor skills.

This device omits the advantage of having two independently movable platforms (as the proposed device does) – thus it cannot 'measure' the 'cross-talk' ability of an individual. Also it cannot measure the relative difference of the two lower limbs performances. The proposed device also makes use of slowly pivoting platforms, and therefore the apparatus is accessible for testing various degrees of balance impairment.

An apparatus and method for movement coordination analysis:

These devices (and methods) are provided for evaluating among the trunk and limbs of the body the distribution of impairments of two types of abilities necessary for posture

and equilibrium control. Firstly, the ability to receive and correctly interpret somatosensory orientation and movement information derived from those body and limb parts in contact with supporting surfaces and secondly the ability to coordinate the muscular contractions in those body and limb parts in contact with a supporting surface to execute functionally effective postural movements. Individuals may be classified in accordance with their performance of a Sense Test Procedure and a Motor Test Procedure, which may be implemented using an appropriate displaceable support surface arrangement. This device works the basis of having two platforms on top of one another. The bottom one is able to translate linearly on wheels parallel to the horizontal plane as viewed in the saggital plane. This platform has its own actuator. The second platform also has its own actuator, but this induces pivoting of the topmost platform. The single platform is not split into two independently moveable platforms (one for each foot). Various tests can be run with this machine, but this will not be discussed here (refer to US patent no. 5,052,406 invented by L. M. Nashner if more information is longed). Some include giving the subject a handle to grasp while both actuators run a certain cycle. Sensors are also placed on the subjects lower limbs to monitor muscle activity.

Two independently movable platforms (one per foot) have advantages. Controlled dorsiflexion range can also not be tested on this machine. This device is impressive in that much of the information can be recorded and assembled evaluate the subjects balance in different ways. The proposed invention (by Botha) is much simpler in concept – and therefore easier to use by any practitioner – it still gives answers to the desired quantification problems stated in the claims-section.

SUMMARY OF THIS INVENTION

This device falls under the broad category of posturography. It consists of a base with two pivotable platforms mounted on it. Each of the platforms is individually driven from its own stepper motor and each is equipped with a force platform. The aim of these force platforms is to deduce a centre of gravity vector from the measured data from each of the platforms. A computer runs certain protocols, chosen by the operator of the instrument, which can include movement of one or both platforms simultaneously. The effect is that the measured COG (centre of gravity) vector will invariably move around. How fast this COG vector finds the balance position after the platforms have been halted is the measure which can objectively quantify a individual's adaptive abilities.

The device can also be used to test dorsiflexion range alone. Dorsiflexion range can be a strong indicator of muscle tone (specifically hypertonia).

Another important measurement, readily made, is the amount of 'cross-talk' between the two lower limbs of the subject and also the relative difference between the performances of one lower limb in relation to the other during the test.

This device is expected to aid in the rehabilitation process of individuals with musculo-skeletal adaptive problems. Measurement of pharmaceutical benefits are expected. Having an accurate way to quantify adapture control is advantageous in various divisions of medicine (for example: neurology, orthopaedic surgery, paediatrics).

BRIEF DESCRIPTION OF DRAWINGS

The only available drawing is a schematic of the device – denoted as Figure E1. In this schematic, the two independently movable platforms are visible, as well as the computer used to operate the device. The side view is that of the saggital plane. Both platforms can be tilted as shown which constitutes to a one degree of freedom per platform (since we have two platforms in this device, the two gets added and therefore the system as a whole is a two degree of freedom dynamic system).

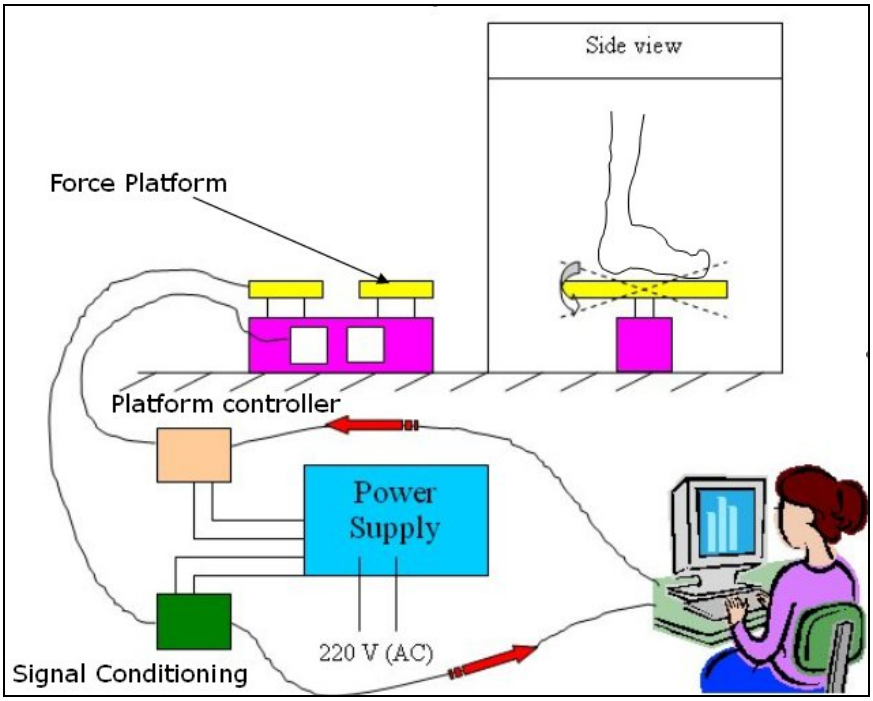

Figure E1: A schematic of the invention

Appendix F: Visual Basic Program for Analysing Raw Data

An explanation of each of the buttons of this Visual Basic program is presented in this appendix. Starting with the main window (Figure F1):

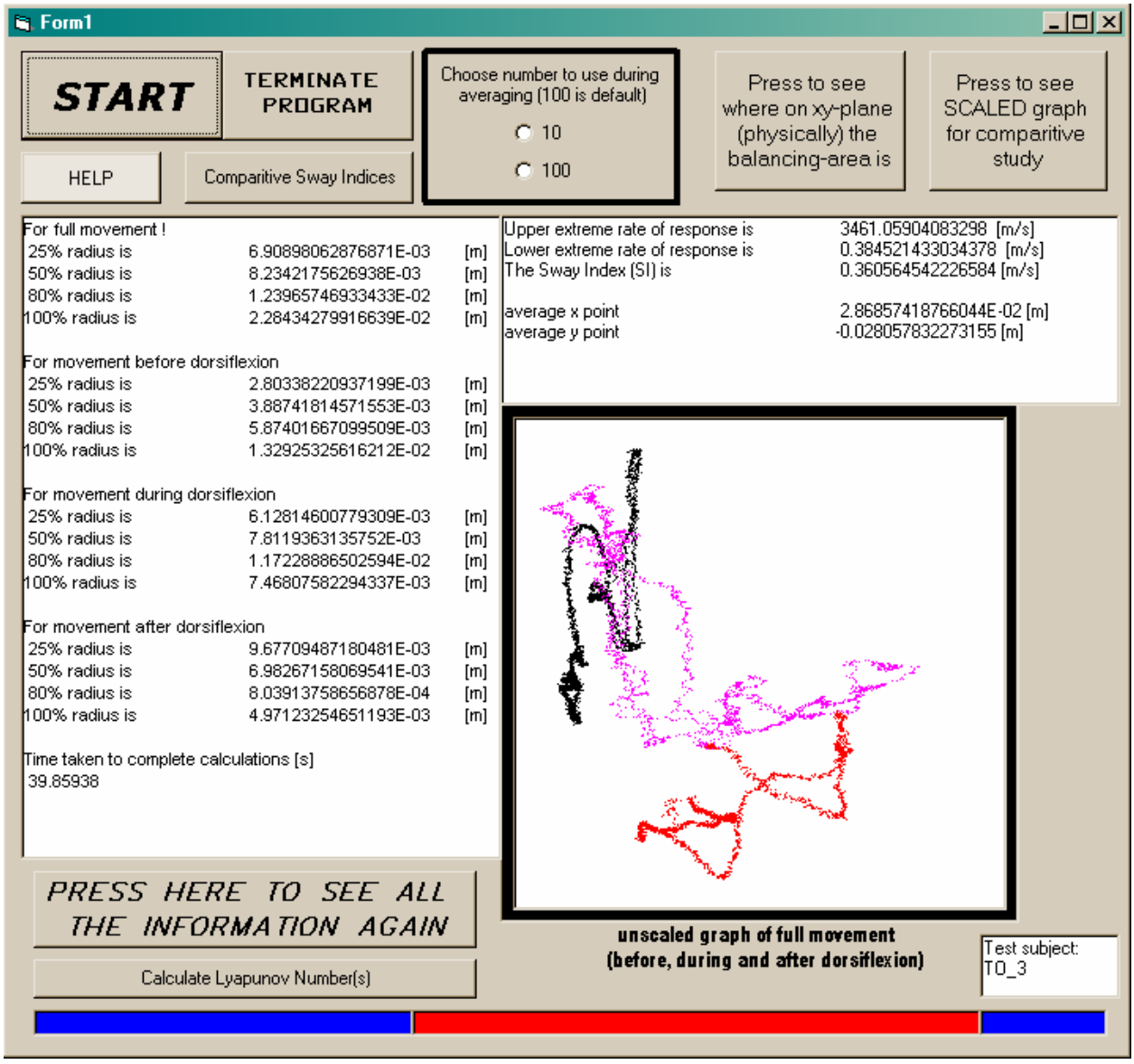

Figure F1: The executed Visual Basic program for test subject TO_3 (Figure 5.17 repeated for convenience).

'Run'-button

Starts the analysing process. Immediately after this button is pressed, a pop-up box appear requesting the file name where the relevant subject's data have been stored during testing. After entering the name, and pressing the 'OK'-button, analysing

commence. When text and a graph are displayed in the windows – looking like Figure 5.17 and F1 – the analysis is complete. Now other buttons may be pressed to see different ways to present the analysed data.

'Terminate Program'-button

This button is pressed to exit the program completely.

'Help'-button

After pressing this button, a help-file is presented on the screen. This file explains, among other things, the more intricate usage of the buttons.

'Comparative Sway Indices'-button

By pressing this button, one of the main window's windows will display text containing the Sway Index before, -during and -after dorsiflexion.

'Choose number to use during averaging (100 is default)'-button

Checking either the 10 or 100 check box is only applicable to set-up 1 (therefore only to be used when analysing the first set of tests done).

'Press to see where on xy-plane (physically) the balancing-area is'-button

Yields a graph showing the platforms and a circle indicating where on the platforms the subject's normal component moved during the test.

'Press to see SCALED graph for comparative study'-button

Yields Figure F2 with its associated buttons – to be explained after Figure F2.

'Press here to see all the information again'-button

When a window is opened in front of the main window, the text and graph are erased. Thus, without having to repeat the analysis, this button presents the data as it was after analysing.

'Calculate Lyapunov Number(s)'-button

By pressing this button, one of the main window's windows will display text containing the Lyapunov Numbers for before, -during and -after dorsiflexion.

The secondary-window's buttons (Figure F2):

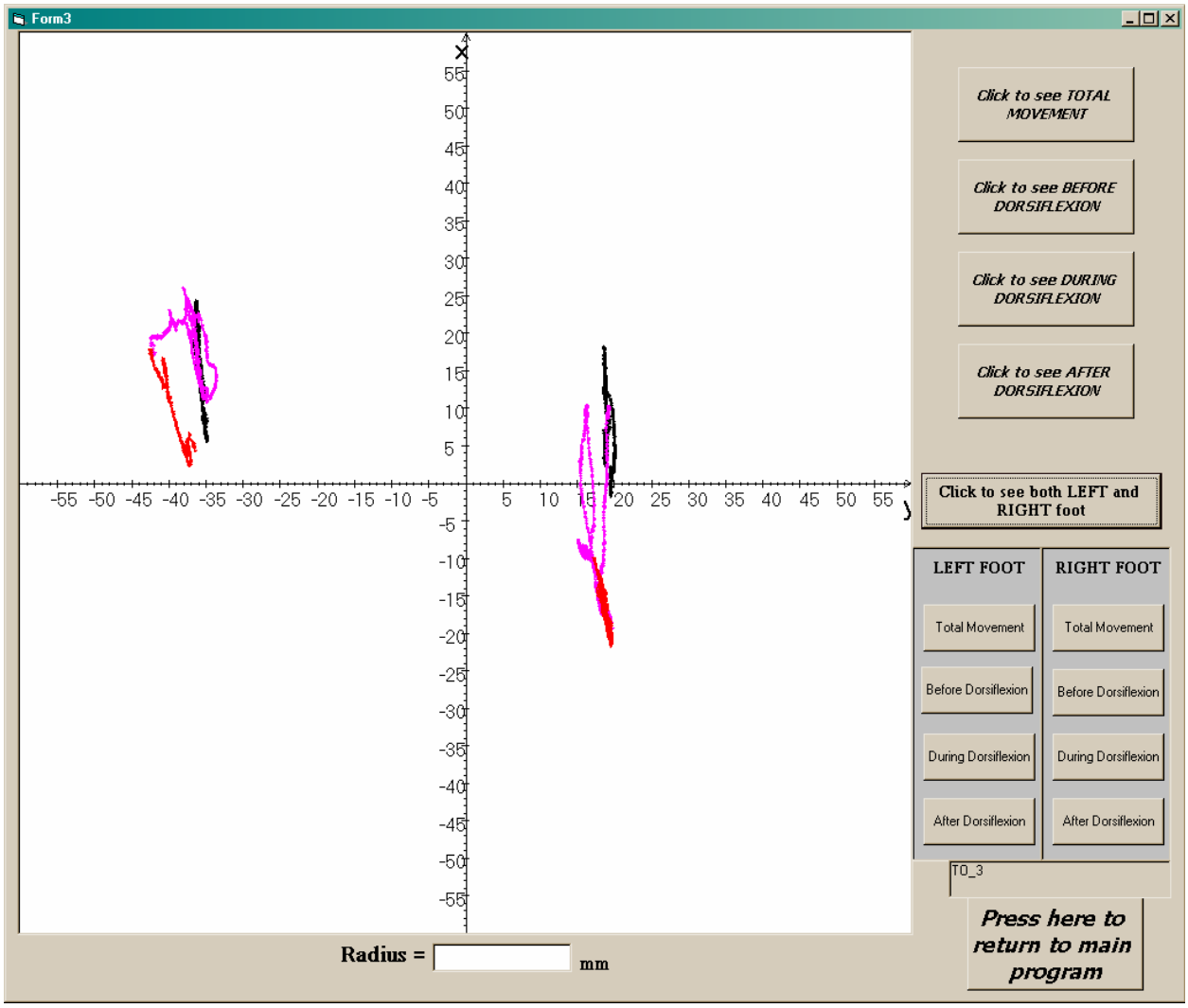

Figure F2: Total Movement of the separate feet of subject TO_3 - repeated for convenience

'Click to see TOTAL movement'-button

By pressing this button, the movement of the normal component of the subject's resultant force for the duration of the test is plotted, using the colour-code associated with each of the movements (before, during and after dorsiflexion). The centre point of this plot is the average x- and y-point calculated for the whole movement. In the 'Radius ='-box, the radius that encloses the movement are given. The circle it implies, are also drawn around the plot. The corresponding radii are presented after any of the buttons (except the 'Click to see both LEFT and RIGHT foot'-button) on this window is pressed.

'Click to see BEFORE DORSIFLEXION'-button

This results in a plot of the movement of the normal component of the subject's resultant force for the first two seconds of the test. Implying that only the 'before dorsiflexion' graph is plotted. The graph is d about the calculated centre point (the average x- and average y-point) during the specified time.

'Click to see DURING DORSIFLEXION'-button

This results in a plot of the movement of the normal component of the subject's resultant force for between two and four seconds of the test. Implying that only the 'during dorsiflexion' graph is plotted. The graph is d about the calculated centre point (the average x- and average y-point) during the specified time.

'Click to see AFTER DORSIFLEXION'-button

This results in a plot of the movement of the normal component of the subject's resultant force for the last two seconds of the test. Implying that only the 'after dorsiflexion' graph is plotted. The graph is d about the calculated centre point (the average x- and average y-point) during the specified time.

'Click to see BOTH LEFT and RIGHT foot'-button

This button results in the graph presented in Figure F2. Both the left and right foot's respective graphs are plotted for the duration of the test. Each of these graphs is colour-coded for identification of which part of the movement it belongs to.

The rest of the buttons (in the LEFT FOOT and RIGHT FOOT divisions), follow the same pattern. Each of the buttons yields the graph explained on the button. For example, the 'Total Movement'-button in the RIGHT FOOT division will result in a graph of the right foot's normal component of its resultants force being plotted – colour coded once again.

'Press here to return to main program'-button

By pressing this button, you close this (Figure F2) window and open the main window (Figure F1) once more.

Appendix G: Solving Equations 3.14 – 3.16 simultaneously

The three equations with the three unknowns (F_{fric}, R_B and R_C) are:

$$(\uparrow)\sum F_y = -O_y + R_B\cos\delta + R_C\cos\delta + F_{fric}\sin\delta + F_1\cos\delta - F_2\sin\delta = 0$$

$$(\rightarrow)\sum F_x = -O_x - R_B\sin\delta - R_C\sin\delta + F_{fric}\cos\delta - F_1\sin\delta - F_2\cos\delta = 0$$

$$(\curvearrowleft)\sum M_O = (0.1)R_B - (0.075)R_C - (0.08)F_{fric} - (X)F_x\sin\xi = 0$$

Simplifying the above three equations

$$R_B\cos\delta + R_C\cos\delta + F_{fric}\sin\delta = O_y - F_1\cos\delta + F_2\sin\delta$$

$$R_B\sin\delta + R_C\sin\delta - F_{fric}\cos\delta = -O_x - F_1\sin\delta - F_2\cos\delta$$

$$(0.1)R_B - (0.075)R_C - (0.08)F_{fric} = (X)F_x\sin\xi$$

and using the following substitutions,

$$O_y - F_1\cos\delta + F_2\sin\delta = AA$$
$$-O_x - F_1\sin\delta - F_2\cos\delta = BB$$
$$(X)F_x\sin\xi = BB$$

The following three equations are obtained:

$$R_B\cos\delta + R_C\cos\delta + F_{fric}\sin\delta = AA \qquad \text{(G.1)}$$

$$R_B\sin\delta + R_C\sin\delta - F_{fric}\cos\delta = BB \qquad \text{(G.2)}$$

$$R_B(0.1) - R_C(0.075) - F_{fric}(0.08) = CC \qquad \text{(G.3)}$$

From (G.1):

$$R_B = \frac{1}{\cos\delta}\left[AA - R_C\cos\delta - F_{fric}\sin\delta\right] \qquad \text{(G.4)}$$

Substitute (G.4) in (G.2):

$$\frac{\sin\delta}{\cos\delta}\left[AA - R_C\cos\delta - F_{fric}\sin\delta\right] + R_C\sin\delta - F_{fric}\cos\delta = BB \qquad \text{(G.5)}$$

Substitute (G.4) in (G.3):

$$\frac{1}{\cos\delta}\left[AA - R_C\cos\delta - F_{fric}\sin\delta\right](0.1) - R_C(0.075) - F_{fric}(0.08) = CC$$

$$\frac{AA(0.1)}{\cos\delta} - (0.1)R_C - (0.1)F_{fric}\tan\delta - R_C(0.075) - F_{fric}(0.08) = CC$$

$$R_C = \left(\frac{1}{-0.175}\right)\left[CC - \frac{(0.1)AA}{\cos\delta} + F_{fric}\left((0.1)\tan\delta + 0.08\right)\right] \qquad \text{(G.6)}$$

Substitute (G.6) in (G.5):

$$\frac{1}{\cos\delta}\left[AA - \left(\frac{1}{-0.175}\right)\left(CC - \frac{(0.1)AA}{\cos\delta} + F_{fric}\left((0.1)\tan\delta + 0.08\right)\right)\cos\delta - F_{fric}\sin\delta\right]\sin\delta$$
$$= F_{fric}\cos\delta - BB - \left(\frac{1}{-0.175}\right)\left(CC - \frac{(0.1)AA}{\cos\delta} + F_{fric}\left((0.1)\tan\delta + 0.08\right)\right)\sin\delta$$

Simplifying:

$$F_{fric} = \frac{1}{DD}\left[BB - AA\tan\delta - \frac{CC\sin\delta}{0.175} + \frac{AA\tan\delta(0.1)}{0.175} + \frac{CC\sin\delta}{0.175} - \frac{AA\tan\delta(0.1)}{0.175}\right] \qquad \text{(G.7)}$$

where,

$$DD = \left[\left(\frac{\sin\delta}{0.175}\right)(0.1\tan\delta + 0.08) - \sin\delta\tan\delta - \frac{\sin\delta}{0.175}\left((0.1)\tan\delta + 0.08\right) - \cos\delta\right] \qquad \text{(G.8)}$$

Now substitute F_{fric} in (G-6) to obtain R_C and then substitute both F_{fric} and R_C in Equation (G-4) to obtain R_B.

Appendix H: Program Logic of the Mathematical Model

In this appendix, the logic of the program written for solving the mathematical model is presented in more detail than in Section 3. The actual program used is given as "Pendulum" in the addendum.

Starting off with the inputs to the system, the following block depicts all the inputs used in the 'Inputs' in Figure H2.

Inputs changeable on main program window:

$\dot{\phi}_{start}$

ϕ_{start}

Δt

TIMESTOP (time at which simulation is terminated)

ϕ_d (detect angle – angle at which person detects sway-angle)

ϕ_s (sway angle – normal sway angle – measured from vertical axis)

A (force representing 'spring'-action causing rectifying movements by ankle)

B (force representing 'damping'-action during excessive sway)

R (length from ankle-joint to concentrated mass)

M (mass of subject concentrated at distance R from ankle-joint)

Inputs not changeable on main program window:

$\phi_{mxs} = 0$ (maximum angle during oscillation)

$\phi_{min} = 0$ (minimum angle during oscillation)

Y (distance from ankle joint to attachment of 'tendon'/force on leg)

X (distance from ankle joint to attachment of 'tendon'/force on foot)

Indicate = 0 (states whether movement of pendulum is one way or the other)

Figure H1: Inputs to the model

Continuing to Figure H2 and thereafter, each of the blocks in Figure H2 having a dashed outline, are presented in subsequent Figures in order to show detail. Figure H2 is the main structure of the program. The code for the program is presented on the CD that accompanies this thesis.

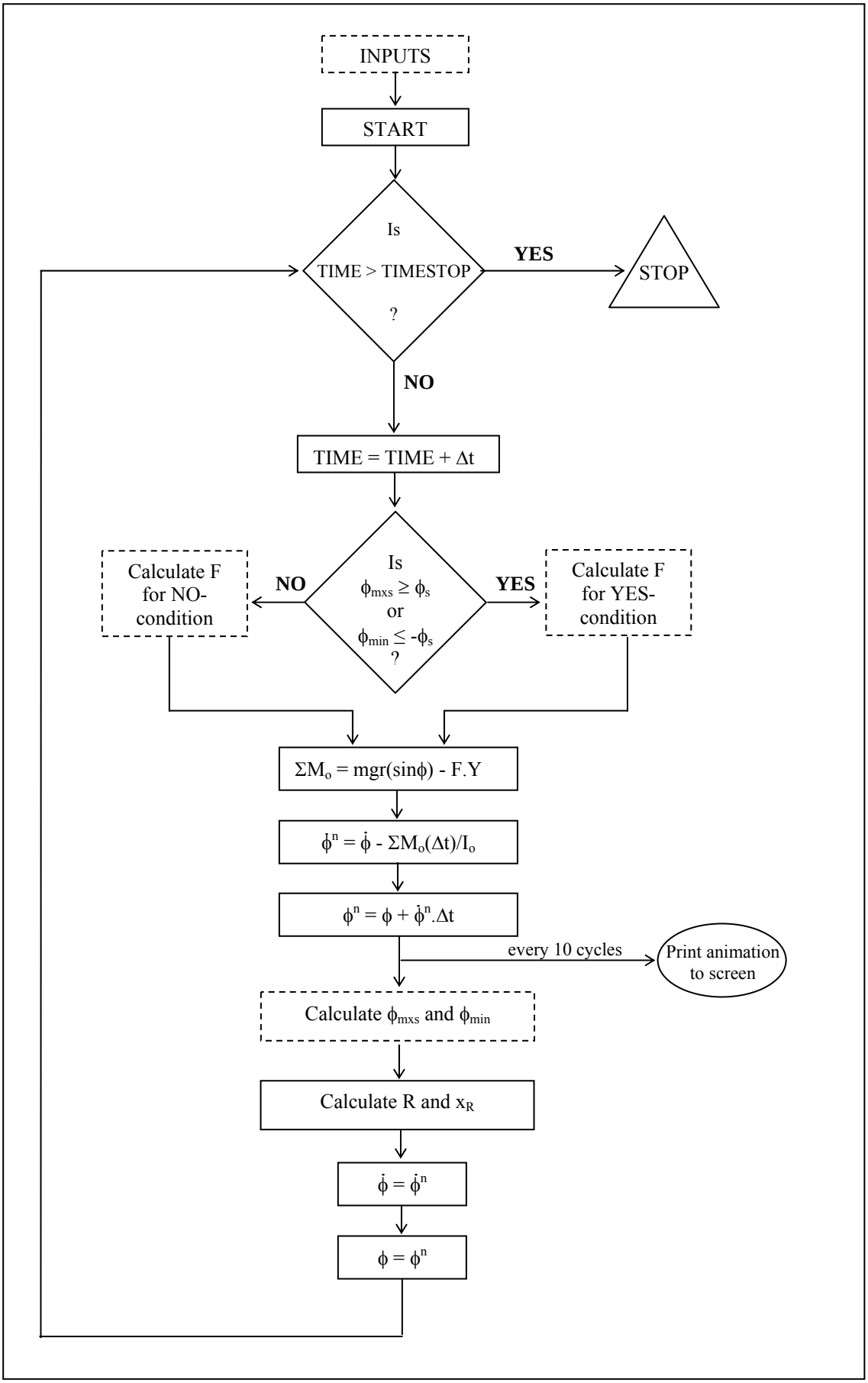

Figure H2: Logic of the Mathematical Model's numerical solution

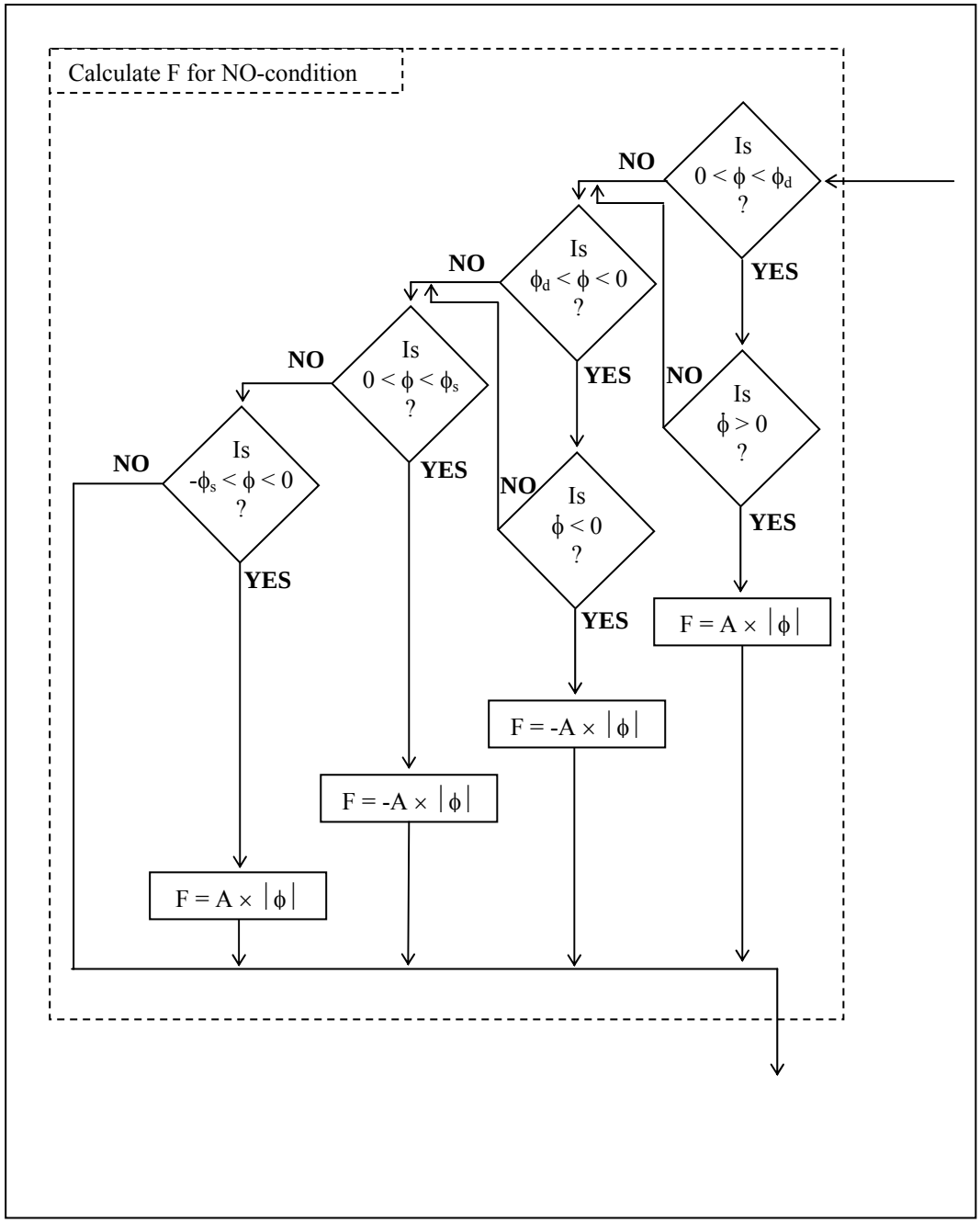

Figure H3: Calculation of F for the NO-condition

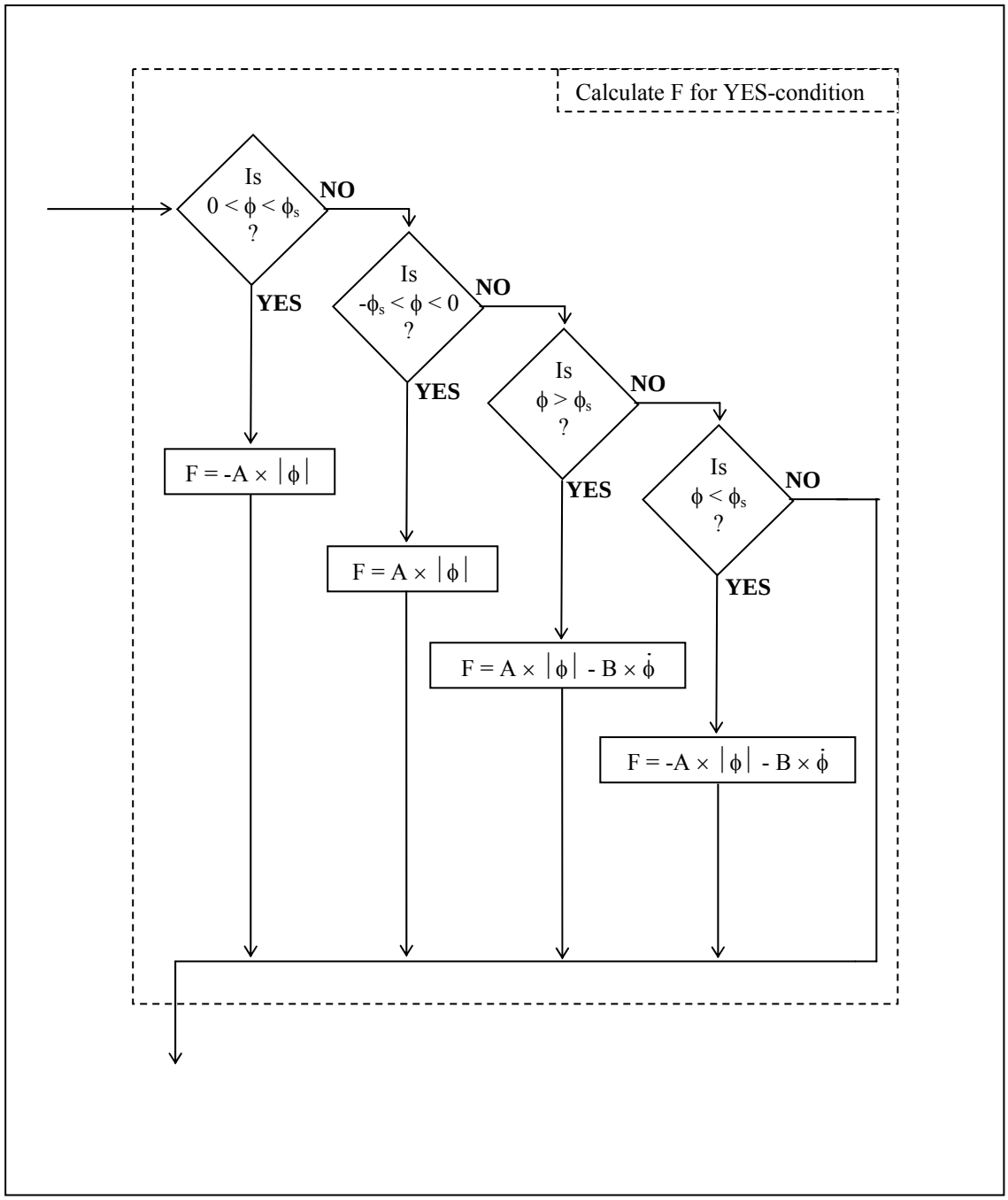

Figure H4: Calculation of F for the YES-condition

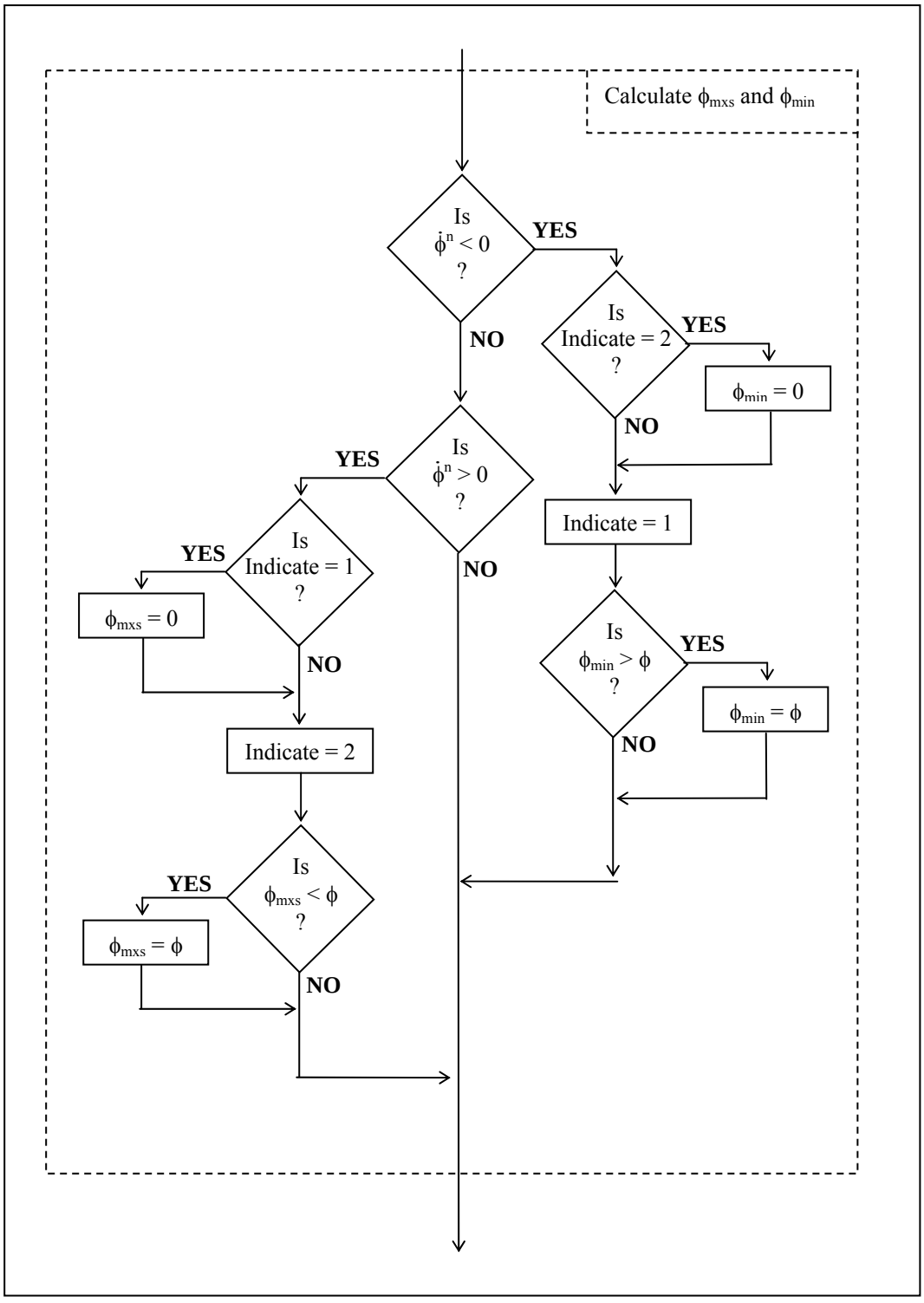

Figure H5: The 'Calculate minimum and maximum sway-angles' box